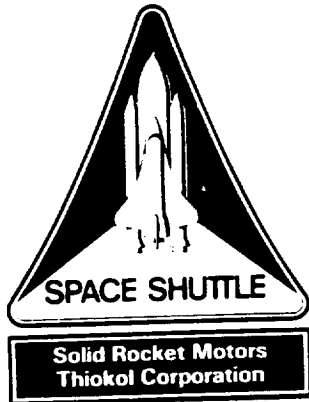TWR-63941

SPACE SHUTTLE

Solid Rocket Motors
Thiokol Corporation

Flight 20 (STS-45) Polysulfide Gas Path Investigation Final Report

NAS8- 38100

July 1992

(NASA-CR-193861) FLIGHT 20 (STS-45) POLYSULFIDE GAS PATH INVESTIGATION Final Report (Thiokol Corp.) 162 p
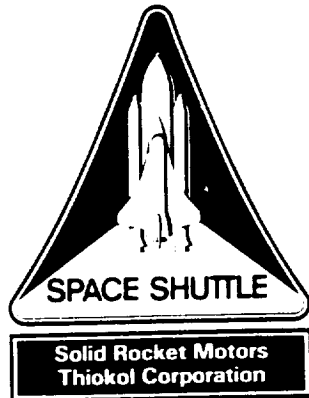
N94-17213

Unclas

G3/20   0193058

Thiokol *CORPORATION*

SPACE OPERATIONS

PO Box 707, Brigham City, UT 84302-0707   (801) 863-3511

Flight 20 (STS-45)
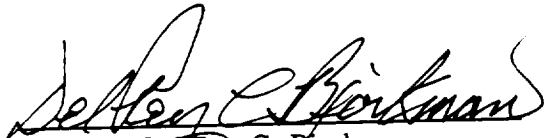# Polysulfide Gas Path Investigation
Final Report
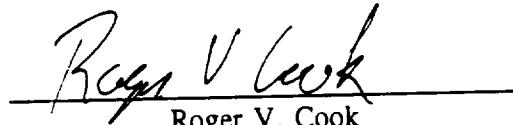
July 1992

Thiokol CORPORATION

SPACE OPERATIONS
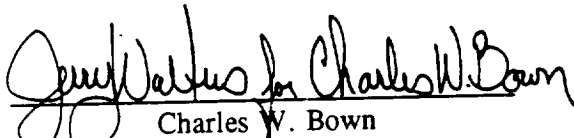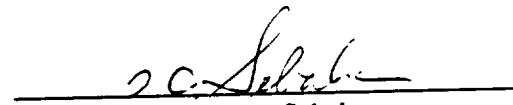
Flight 20 (STS-45)
Polysulfide Gas Path Investigation
Final Report
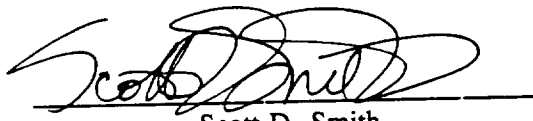
Prepared by:
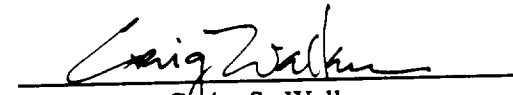
Del Rey C. Bjorkman
Chairman, Investigation Board
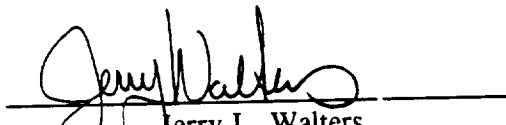
Roger V. Cook
Engineering Board Member
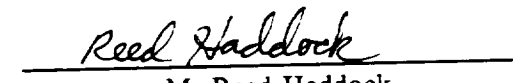
Charles W. Bown
Materials Assessment Board Member

David A. Sebahar
Production Board Member

Scott D. Smith
Quality Assurance Board Member

Craig S. Walker
Reliability Board Member

Jerry L. Walters
Program Support Board Member

M. Reed Haddock
Laboratory Testing Board Member

Suresh B. Kulkarni
Vice President, Space Engineering

Robert E. Lindstrom
Senior Vice President
and General Manager

Data Management/Release   11-16-92

Thiokol CORPORATION
SPACE OPERATIONS

CONTENTS

FIGURES

FIGURES (cont)

Tables

1

INTRODUCTION

This report documents the results of the investigation into causes of gas paths on the 20A and 20B case-to-nozzle joints on STS-42. The investigation was conducted by the Investigation Board appointed by the senior vice president and general manager of Space Operations, Mr. R. E. Lindstrom, on 7 Feb 1992.

The probability of gas path occurrence in the nozzle-to-case-joint polysulfide had been identified during joint redesign. However, actual flight gas path incidence has been limited to RSRM-11 and the 20A and 20B segments. The blow-by condition on the 20A segment was a first time occurrence which was a special concern.

The investigation covered all technical aspects associated with the gas path and blow-by conditions: materials and processing history, design requirements and as-built compliance to the design, thermal and structural analyses, computer modeling, and laboratory experimentation with the materials involved. The investigation was coordinated with Mr. Ken Jones at NASA Marshall in bi-weekly teleconferences. The Board also supported Dr. James C. Blair's 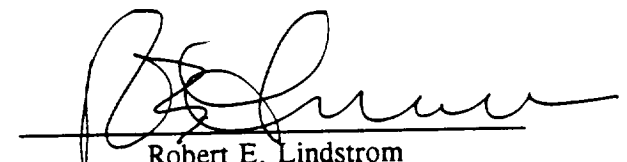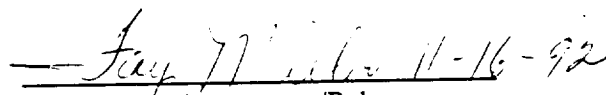independent NASA investigation team by providing copies of collected data, conducting requested analyses, and supporting several all-day teleconferences to provide understanding and resolve issues. The Dr. Blair support requirement was successfully concluded on 4 Mar 1992.

2

SUMMARY AND CONCLUSIONS

2.1 PERFORMANCE CONCLUSIONS

The Investigation Board concluded the following:

2.1.1 The nozzle-to-case wiper O-ring and insulation system performed as designed. Polysuflide did not reach the primary O-ring and the primary O-ring did not experience heat effect or blow-by.

2.1.1.1 The gas paths on the 20A and 20B motors resulted from joint air being preferentially expelled through the polysulfide rather than venting out of the bleed port. The probable cause of this condition was out-of-roundness of the mating parts, which caused the planned air bleed path to be blocked by local contact of mating surfaces.

2.1.1.2 Physical inspection of 20A and 20B gas paths identified areas characteristic of a pristine void which confirmed gas path formation during nozzle installation.

2.1.1.3 A comprehensive review of void history determined a high frequency of long void (1-in. length or more axial) alignment with vent slots which supports the scenario of air being expelled from the joint by reverse venting.

2.1.1.4 Occasional gas path formation appears to be inherent in the present joint design.

2.1.2 Contributing causes of gas path formation included the following factors:

2.1.2.1 Polysulfide Lot 037 (used on the 20B) has been demonstrated to have anomalous rheological and slow cure rate characteristics, which would not have afforded normal resistance to gas path formation.

2.1.2.2 Polysulfide Lot 036 (used on the 20A) likely had similar characteristics. Although no residual material was available for test, acceptance data indicate a similarity between Lots 036 and 037.

2.1.2.3 The low absolute humidity (< 0.002 lb. H_2O/lb dry air) in the processing area during nozzle installation on both 20A and 20B could have further retarded the polysulfide cure, thus contributing to propensity for gas path formation.

2.1.2.4 During assembly of the nozzle, a 90°F hot zone on the 20B fixed housing at the location that the gas path developed could also have contributed to gas path formation. Laboratory testing demonstrated a short term viscosity drop with local heating of polysulfide with resistance to gas path formation dropping as temperature increases.

2.1.3 The wiper O-ring is not designed to be a seal and pressure application via a gas path may cause blow-by.

2.1.3.1 Stress relaxation of NBR insulation at the wiper O-ring causes a local depression at the point of contact on the order of 0.038-inch.

2.1.3.2 Cure shrinkage of NBR insulation (1.5 percent) due to autoclave vulcanization would also reduce theoretical contact with wiper O-ring.

2.1.3.3 Dynamic gap opening under pressure (0.021-in.) increases risk of blow-by.

2.1.3.4 Presence of cured polysulfide under and around the wiper O-ring could also inhibit ideal O-ring response to pressure and interfere with sealing.

2.1.3.5 Thermal analysis using the RSRM-20A nozzle-to-case joint configuration predicted that primary O-ring erosion could have initiated if the wiper O-ring blow-by lasted longer than 0.25 seconds. Using worst case joint volumes, maximum primary O-ring erosion from a single gas path was predicted to be 18.8 mil.

2.1.4 The risk of gas path formation on the RSRM-21 which used Lot 037 polysulfide was considered to be higher than previous flights due to the unique characteristics of this lot.

2.2 DESIGN ASSESSMENT CONCLUSIONS

2.2.1 The possibility of gas path formation was previously identified as a risk which if experienced would not jeopardize flight due to a fail safe joint design.

2.2.2 Elimination of gas path risk will require limited redesign of the nozzle to case joint and fixed housing bleed provisions. Additional bleed ports and/or a bleed groove in the fixed housing to accommodate joint venting would be needed.

2.2.3 The wiper O-ring has been serving its intended function of keeping polysulfide away from the primary O-ring. The wiper O-ring cannot repeatedly perform as a seal for the reasons presented in Section 2.1.

2.3 MATERIALS ASSESSMENT CONCLUSIONS

2.3.1 A review of PR1221 polysulfide records concluded that potlife and tack-free time acceptance requirements were out-of-family for Lots 036 and 037. These problems resulted from a subtier supplier problem with lead oxide particle size at the manufacturer.

2.4 PROCESS ASSESSMENT CONCLUSIONS

2.4.1 All processing times and temperatures were within the previously demonstrated variability envelope.

2.4.2 There were no unique processing techniques or circumstances identified that could have contributed to gas path formation.

2.4.3 Although within previous history, a 92°F hot spot on the 20B fixed housing could be a contributing factor for gas path formation. With a dimensionally corresponding case joint temperature of 80°F, the warmer fixed housing would be expected to locally decrease PR1221 polysulfide viscosity, which could have facilitated gas path formation.

2.4.4 Low absolute humidity during cold months could retard the polysulfide cure reaction (reference TWR-60316).

2.4.5 The time interval between end of polysulfide mixing to start of application on the 20A was the shortest demonstrated in production. This circumstance would have the potential for a lower polysulfide viscosity which could have contributed to gas path formation.

2.5 LABORATORY TESTING CONCLUSIONS

2.5.1 Lot 037 demonstrated rheological characteristics that could allow gas path formation at processing times where other polysulfide lots would have acquired greater resistance to gas path formation.

2.5.2 Gas path formation resistance is increased by the viscosity increase associated with PR1221 cure reaction.

2.5.3 Gas paths were formed in the laboratory in the pressure range expected in nozzle-to-case joint assembly.

2.5.4 Gas paths formed in the polysulfide study replicated the gas path shape of the 20A.

2.5.5 A short-term temperature increase reduces the ability of polysulfide to withstand gas path formation.

2.5.6 Voids within the polysulfide can be created by poor polysulfide extrusion technique, but resulting voids do not have gas path configuration. The screeding process tends to eliminate voids caused by poor extrusion technique. However, this type of void could reduce resistance to gas path formation.

2.6 QUALITY ASSESSMENT CONCLUSIONS

2.6.1 The unusual potlife data of Lots 036 and 037 was out-of-family and justified the laboratory testing which was conducted by the Investigation Board.

2.6.2 No nonconformances or other production quality problems were identified by the Quality Assessment.

2.6.3 There are significant differences in polysulfide acceptance test results between the vendor and Thiokol analysis that warrant further study.

3

RECOMMENDATIONS

3.1 DESIGN

3.1.1 An investigation is recommended into concepts to improve the air venting capability of the nozzle-to-case joint during the assembly process, including: extending the vent slots aft to the case metal part, adding more vent ports to the fixed housing, and incorporating a bleed path around the circumference of the joint.

3.1.2 If testing demonstrates that any of the above design changes will reduce the potential for gas path formation, then additional NJAD testing is recommended to fully characterize the new configuration and process variables.

3.1.3 Expand polysulfide acceptance criteria to include a test to identify anomalous rheology and cure rate.

3.2 PROCESSING

3.2.1 Improve polysulfide application process by developing a technique for routinely producing a near void-free configuration. Train and certify operators on the selected method.

3.2.2 Implement viscosity measurement as verifiable evidence of proper polysulfide cure rate.

3.2.3 Evaluate a process change to delay nozzle seating until polysulfide has reached a viscosity level (state of cure) that laboratory testing determines to be resistant to gas path formation.

3.2.4 Change component conditioning temperature to preclude fixed housing conditioning to temperatures more than 5°F higher than case joint temperature to preclude polysulfide viscosity reduction.

3.2.5 Investigate modification of screed contour to optimize contour for new polysulfide.

3.2.6 Continue to maintain the most important statistical process control charts which were developed by this board. These charts should be utilized to identify special causes of variation at the time of occurrence.

3.3 MATERIALS

3.3.1 Identify differences between vendor and Thiokol acceptance testing and take action to correct differences.

3.3.2 Accelerate delivery of new polysulfide and assure procedures at supplier and Thiokol will preclude contamination from entering the material.

3.3.3 Develop appropriate trending charts on the new material and assign responsibility for chart maintenance.

3.3.4 Consider changing polysulfide packaging to a larger container sized to match processing needs.

3.3.5 Expand acceptance tests for new polysulfide to include evaluation of rheology and cure rate to preclude recurrence of the Lot 037 problems.

4

DISCUSSION

4.1 PROBLEM DESCRIPTION

4.1.1 The problems that were investigated by the Board included:

a. The gas path within the nozzle-to-case joint polysulfide at 57.6 deg on the 20A, extending from the motor chamber to the wiper O-ring (see Figures 4-1and 4-2).

b. Evidence of combustion gas blow-by beyond the wiper O-ring with local heat damage to the wiper O-ring (see Figure 4-2).

c. A gas path within the polysulfide at 247 deg on the 20B nozzle-to-case joint (see Figures 4-1 and 4-2).

4.2 BOARD APPOINTMENT

The Space Operations Senior Vice President and General Manager, Mr. R. E. Lindstrom, on 7 Feb 1992, appointed an Investigation Board to investigate the causes of these problems. Board membership is defined in Figure 4-3.

4.3 BOARD ACTIVITY

Board activity centered around the fault tree presented as Figure 4-4. Highlighted in the figure are the factors determined by the investigation to have significance with regard to gas path formation and wiper O-ring blow-by.

The detailed assessment activity is contained in the following appendixes, which include the following:

Appendix A: Fault Tree Assessment
Appendix B: Engineering Assessment
Appendix C: Quality Assessment
Appendix D: Manufacturing Assessment
Appendix E: Materials Assessment
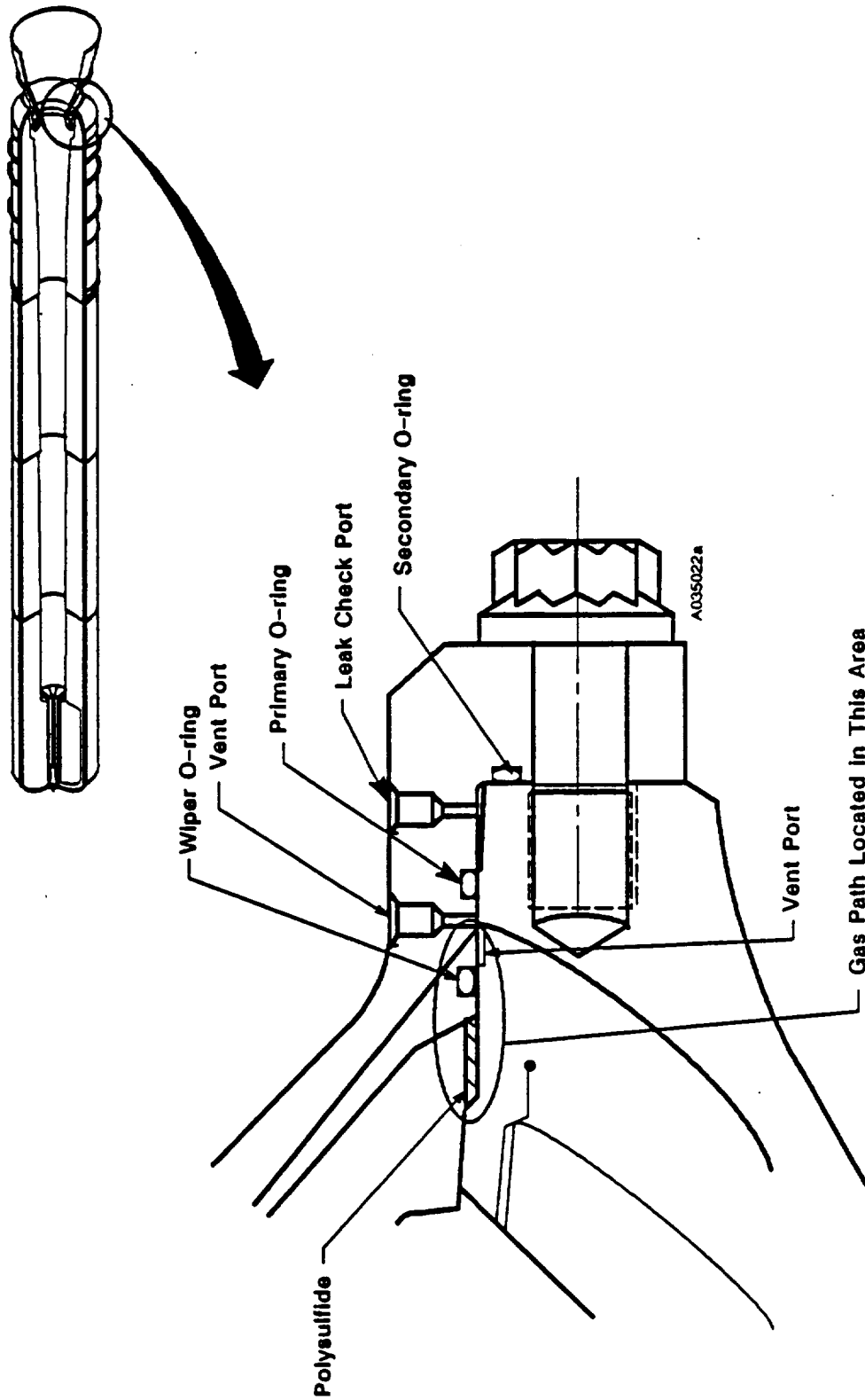
Figure 4-1. General Location of Gas Path

A035022a

- Secondary O-ring
- Leak Check Port
- Primary O-ring
- Vent Port
- Wiper O-ring
- Gas Path Located In This Area
- Vent Port
- Polysulfide
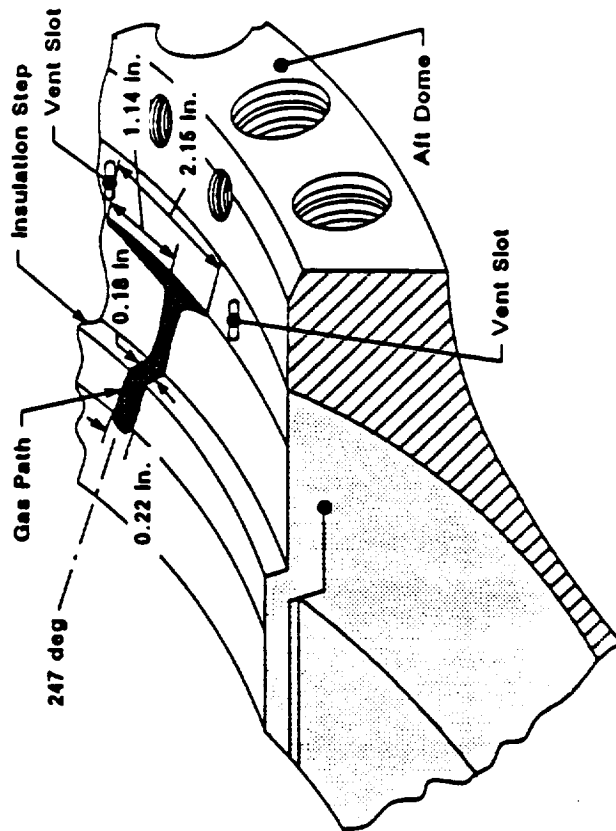
Gas Path at 247 Degrees
STS-42 (360T020) RH (B)
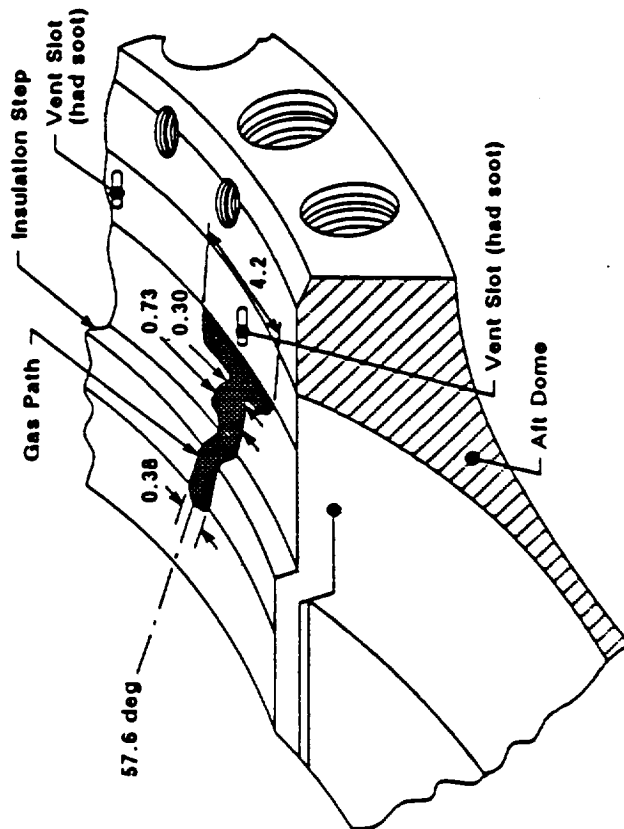
Gas Path at 57.6 Degrees
STS-42 (360T020) LH (A)

Figure 4-2. Gas Path on 20A and 20B

Thiokol CORPORATION

SPACE OPERATIONS

Robert E. Lindstrom
Senior Vice President and General Manager

7 February 1992
A100-FY92-110

TO: Space Operations Distribution A and B

FROM: R. E. Lindstrom

SUBJECT: Appointment of Board of Investigation

In accordance with Procedure 75-01-03, Paragraph 9, "Unexpected/Unintended Event or Condition, First Response to," I am appointing DelRey C. Bjorkman as Chairman of a Board of Investigation to investigate the nozzle-to-case sealant blow hole anomaly associated with Flight 20 motors. The board will conduct its investigation in accordance with the requirements of TWR-61870, "Incident Reporting and Investigation." The membership to support the chairman full-time is as follows:

<u>Chairman</u>:   DelRey C. Bjorkman

<u>Board Members</u>:

Program Support	Jerry Walters
Design Assessment	Roger Cook
Materials Assessment	Charlie Bown/Reed Haddock
Manufacturing Assessment	Dave Sebahar
Quality Assessment	Scott Smith/Don Coziar
Fault Tree Analysis	Craig Walker/Bill Morphet
Secretary	Connie Huggins

Additional members and advisors may be assigned as required by the chairman. All organizational elements are requested to provide the Board of Investigation with their full support in the conduct of its activities.

R. E. Lindstrom

Figure 4-3. Board of Investigation Appointment
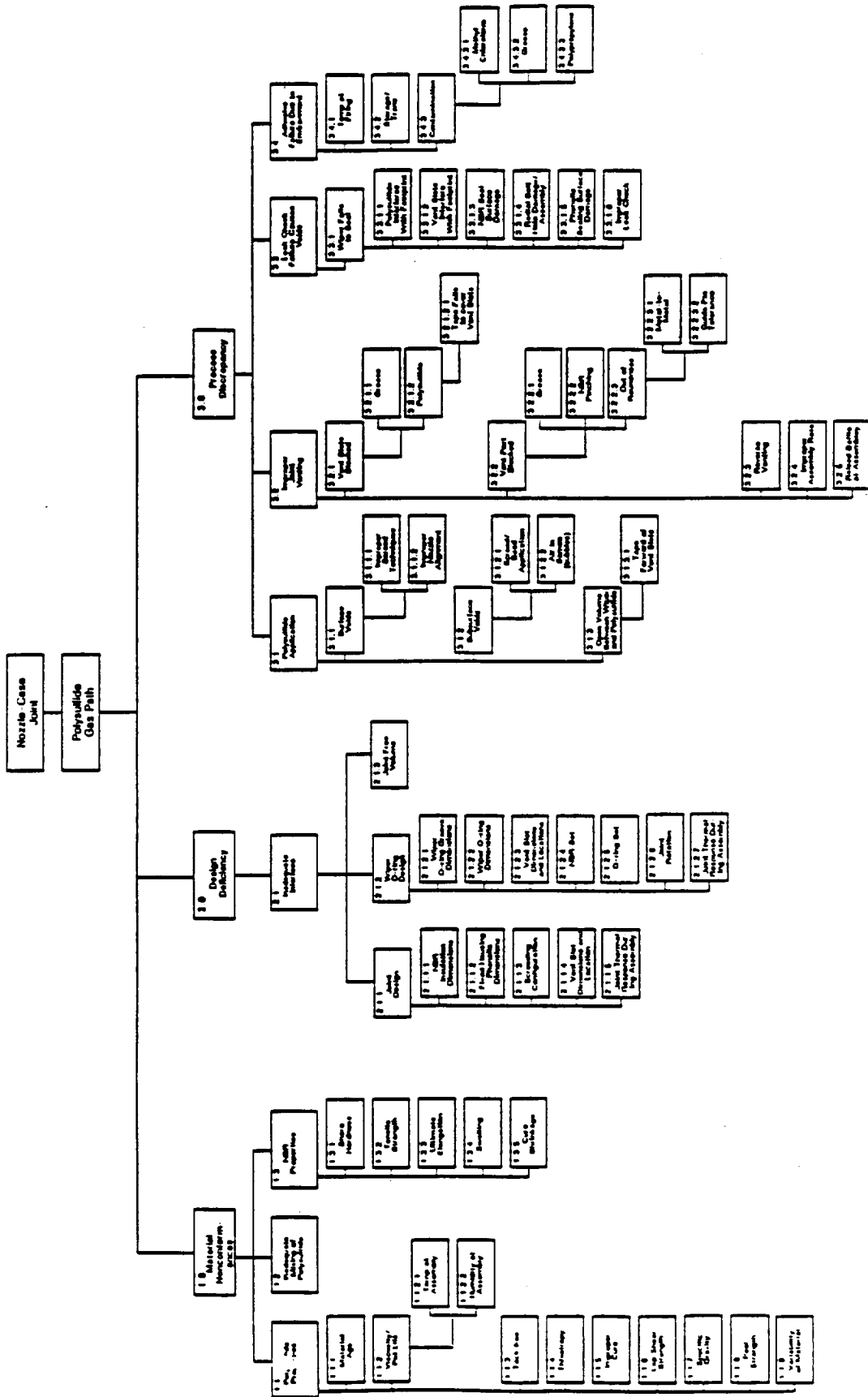
Figure 4-4. Fault Tree

APPENDIX A - FAULT TREE ASSESSMENT

1.0 INTRODUCTION

A Fault Tree analysis was developed as the backbone of the investigative activity. A straw man fault tree outline was developed as focal point at the beginning of board deliberations and was repeatedly reviewed and revised as insight was gained by team members. The fault tree was invaluable in ensuring all factors associated with the nozzle to case design were fully considered in the investigation. The finalized fault tree block diagram was presented in summary form as Figure A-1. The detailed fault tree constitutes the balance of this appendix.

The fault tree flowed down into three main areas: Material Properties, Joint Design, and Process. These main areas were further subdivided into a total of 74 specific fault possibilities which were investigated. It will be noted in the detailed fault tree that action assignments and close-out rationales are identified.

Figure A-1. Fault Tree
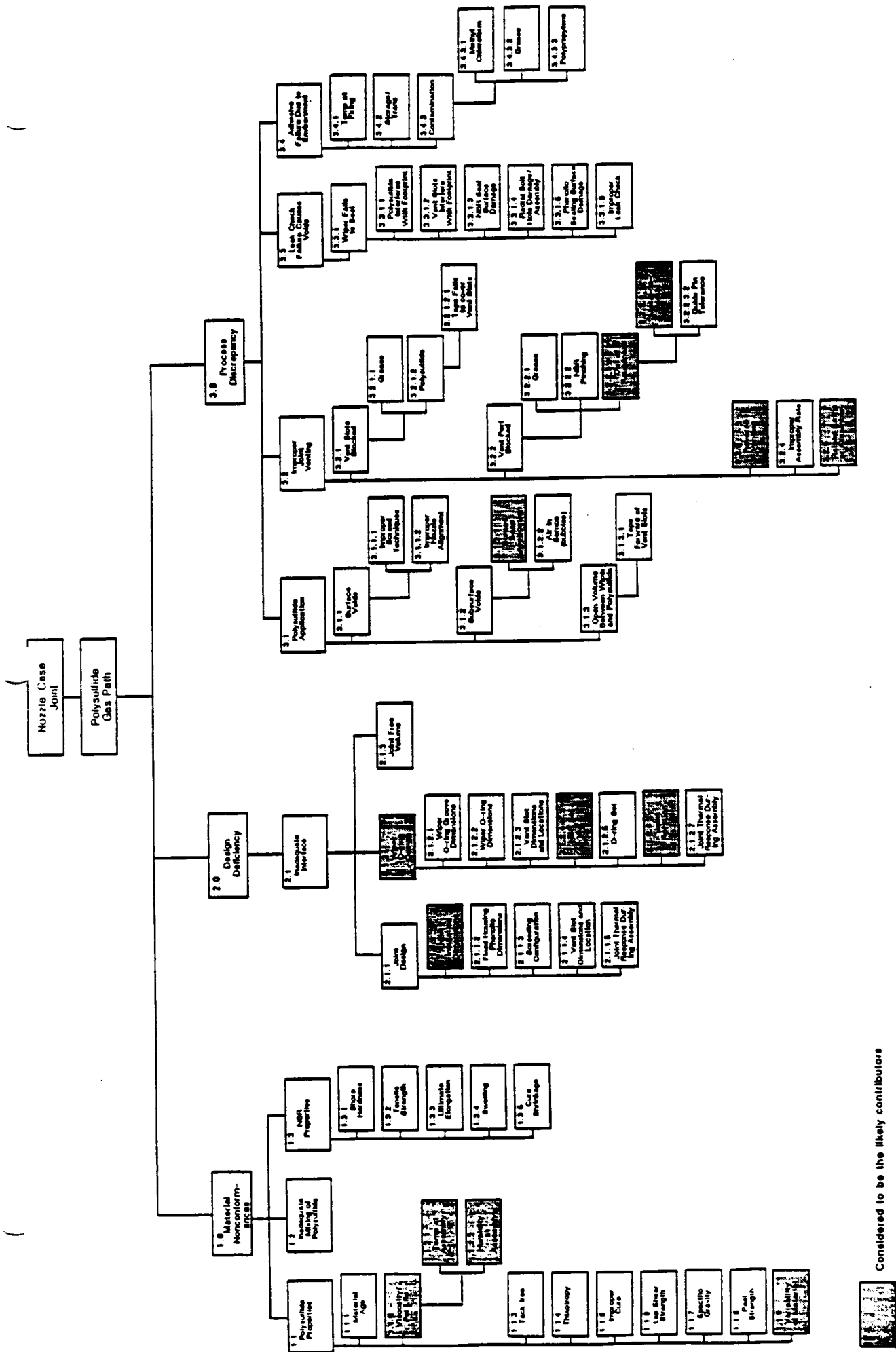
Considered to be the likely contributors

12

FAULT TREE
NOZZLE-TO-CASE JOINT (RSRM-20)
GAS PATH IN POLYSULFIDE
March 19, 1992

1.0 MATERIAL
1.1 POLYSULFIDE PROPERTIES
1.2 POLYSULFIDE MIXING
1.3 NBR PROPERTIES

CAUSE	ACTIONEE	ACTION	CLOSURE RATIONALE
1.1.1 AGE OF MATERIAL	SCOTT SMITH	VERIFY RSRM-20 DATA. COMPARE WITH DATA HISTORY.	RSRM-20 ACCEPTANCE DATA MET REQUIREMENTS. DATA COMPARISON SHOWS NOTHING UNUSUAL.
	JERRY WALTERS	EVALUATE VENDOR DATA HISTORY.	VENDOR ACCEPTANCE DATA VARIES LESS THAN THIOKOL ACCEPTANCE DATA. THIS IS DUE TO VENDOR CONTROLLED ENVIRONMENTS AND POSSIBLY DIFFERENT LOTS ARE FROM THE SAME MIX.
1.1.2 VISCOSITY/POT LIFE	ROGER COOK	EVALUATE VISCOSITY VARIATION HISTORY.	VISCOSITY VARIES SIGNIFICANTLY AT SIMILAR CONDITIONS. FROM 3.38 KILOPOISE TO 9.0 KILOPOISE.
	REED HADDOCK	TEST POLYSULFIDE VISCOSITY FROM LOT 37 (LOT 36 NOT AVAILABLE) AND COMPARE WITH OTHER LOTS.	LOT 37 SHOWS AN "OUT OF FAMILY" SLOW CURE RATE COMPARED WITH LOTS 41, 42, AND 43.
	SCOTT SMITH	VERIFY RSRM-20 POT LIFE DATA. COMPARE WITH DATA HISTORY.	RSRM-20 ACCEPTANCE DATA MET REQUIREMENTS. DATA COMPARISON SHOWS RSRM-20 DATA ON THE HIGH SIDE.

Item	Name	Action	Findings
1.1.2.1 TEMPERATURE AT ASSEMBLY	DAVE SEBAHAR	VERIFY RSRM-20 DATA. COMPARE WITH DATA HISTORY.	RSRM-20 ACCEPTANCE DATA MET REQUIREMENTS. 20B DATA COMPARISON SHOWS BOND SURFACE WITH LARGE DELTA TEMPERATURE. THIS IS ATTRIBUTED TO THE HEATER BLOWING ON ONE SIDE OF THE NOZZLE DURING THE WINTER SEASON. 20B NOZZLE WAS 92 DEGREES F AT LOCATION OF GAS PATH. LABORATORY TESTING SHOWS 90 DEGREE POLYSULFIDE IS LESS RESISTANT TO GAS PATH THAN 70-80 DEGREE F POLYSULFIDE.
1.1.2.2 HUMIDITY AT ASSEMBLY	JAY RUSSELL	VERIFY RSRM-20 DATA. COMPARE WITH DATA HISTORY.	RSRM-20 ACCEPTANCE DATA MET REQUIREMENTS. DATA COMPARISON SHOWS RSRM-20 DATA ON THE LOW SIDE DUE TO THE WINTER SEASON. LOW HUMIDITY HAS BEEN SHOWN TO SLOW THE CURE REACTION.
1.1.3 TACK FREE	SCOTT SMITH	VERIFY RSRM-20 DATA. COMPARE WITH DATA HISTORY.	RSRM-20 ACCEPTANCE DATA MET REQUIREMENTS. TACK FREE TIME REQUIREMENT WAS INCREASED EFFECTIVE LOT 35 AND SUBSEQUENT. HENCE DATA COMPARISON NOT AVAILABLE.
1.1.4 THIXOTROPY	REED HADDOCK	TEST POLYSULFIDE FROM LOT 37 (LOT 36 NOT AVAILABLE) AND COMPARE WITH OTHER LOTS.	LOT 37 FLOWED THE LEAST (HIGHEST THIXOTROPY) WHEN COMPARED TO LOTS 41, 42, AND 43.
	MART COOK	ANALYZE WITH AND WITHOUT POLYSULFIDE SLUMP.	TESTING FROM POLYSULFIDE LOTS 37, 41, 42, AND 43 AT 5, 30, AND 60 MINUTES AFTER APPLICATION SHOWED THAT NO SIGNIFICANT SLUMPING OCCURRED. THE PROFILES FROM EACH LOT, APPLIED WITH THE SAME SCREED, WERE APPROXIMATELY THE SAME.
1.1.5 IMPROPER CURE	SCOTT SMITH	VERIFY RSRM-20 DATA. COMPARE WITH DATA HISTORY.	RSRM-20 ACCEPTANCE DATA MET REQUIREMENTS. DATA COMPARISON SHOWS NOTHING UNUSUAL.
	TREVOR FRESTON	ANALYZE RSRM-20 POLYSULFIDE	POLYSULFIDE SAMPLES FROM RSRM-20 SHOWS NO NON-CONFORMANCES. (2463-FY92-P026)

2

Item	Responsible	Action	Result
1.1.6 LAP SHEAR STRENGTH	SCOTT SMITH	VERIFY RSRM-20 DATA. COMPARE WITH DATA HISTORY.	RSRM-20 ACCEPTANCE DATA MET REQUIREMENTS. DATA COMPARISON SHOWS NOTHING UNUSUAL.
1.1.7 SPECIFIC GRAVITY	SCOTT SMITH	VERIFY RSRM-20 DATA. COMPARE WITH DATA HISTORY.	RSRM-20 ACCEPTANCE DATA MET REQUIREMENTS. DATA COMPARISON SHOWS NOTHING UNUSUAL.
1.1.8 PEEL STRENGTH	SCOTT SMITH	VERIFY RSRM-20 DATA. COMPARE WITH DATA HISTORY.	RSRM-20 ACCEPTANCE DATA MET REQUIREMENTS. DATA COMPARISON SHOWS NOTHING UNUSUAL.
1.1.9 VARIABILITY OF MATERIAL	REED HADDOCK	SUBSCALE TESTING.	LAB TESTING SHOWS LOT 37 AND LOT 41 ARE ANOMALOUS.
		COMPOSITION TESTING.	FTIR FROM LOTS 37, 42 AND 43 SHOW THERE WERE NO DIFFERENCES IN THE MATERIAL.
1.2 INADEQUATE MIXING OF POLYSULFIDE	SCOTT SMITH	VERIFY RSRM-20 MIX SHEETS/BATCH CARDS	RSRM-20 DATA MET REQUIREMENT.
	TREVOR FRESTON	ANALYZE RSRM-20 POLYSULFIDE	POLYSULFIDE SAMPLES FROM RSRM-20 SHOWS NO NON-CONFORMANCES. (2463-FY92-P026)
1.3.1 NBR SHORE HARDNESS	SCOTT SMITH	VERIFY RSRM-20 DATA. COMPARE WITH DATA HISTORY.	RSRM-20 ACCEPTANCE DATA MET REQUIREMENTS. DATA COMPARISON SHOWS NOTHING UNUSUAL.
1.3.2 NBR TENSILE STRENGTH	SCOTT SMITH	VERIFY RSRM-20 DATA. COMPARE WITH DATA HISTORY.	RSRM-20 ACCEPTANCE DATA MET REQUIREMENTS. DATA COMPARISON SHOWS NOTHING UNUSUAL.
1.3.3 ULTIMATE ELONGATION	SCOTT SMITH	VERIFY RSRM-20 DATA. COMPARE WITH DATA HISTORY.	RSRM-20 ACCEPTANCE DATA MET REQUIREMENTS. DATA COMPARISON SHOWS NOTHING UNUSUAL.
1.3.4 SWELLING	REED HADDOCK	SUBSCALE TESTING.	IT IS UNLIKELY THAT SANDING AND METHYL CHLOROFORM CLEANING OF THE NBR AFT DOME MATING SURFACE CAUSED SIGNIFICANT SWELLING.
1.3.5 CURE SHRINKAGE	TREVOR FRESTON	ANALYZE RSRM-20 NBR	

2.0 DESIGN
2.1 INADEQUATE INTERFACE CONFIGURATION
2.1.1 JOINT DESIGN

CAUSE	ACTIONEE	ACTION	CLOSURE RATIONALE
2.1.1.1 NBR INSULATION DIMENSIONS	MART COOK	MEASURE AND VERIFY RSRM-20 DIMENSIONS. ANALYZE DIMENSIONS.	NO PRE-FLIGHT DRs. POSTFLIGHT MEASUREMENTS EXCEEDED ENGINEERING TOLERANCES AT GAS PATH/SOOTED VENT SLOTS: 20A: 0.019 INCHES AT 57.6 DEGREES 20A: 0.030 INCHES AT 64.8 DEGREES 20B: 0.038 INCHES AT 247 DEGREES ENGINEERING TOLERANCE IS: 0-.020 INCHES. FIRST TIME FOR POSTFLIGHT MEASUREMENTS, HENCE DATA COMPARISON NOT AVAILABLE.
2.1.1.2 FIXED HOUSING PHENOLIC DIMENSIONS	MART COOK	MEASURE AND VERIFY RSRM-20 DIMENSIONS. ANALYZE DIMENSIONS.	NO PRE-FLIGHT DRs. POSTFLIGHT MEASUREMENTS MEET DIMENSIONAL REQUIREMENTS AT GAS PATH/SOOTED VENT SLOTS.
2.1.1.3 SCREED CONFIGURATION	SCOTT SMITH	MEASURE AND VERIFY SCREED DIMENSIONS.	SCREED MEETS DIMENSIONAL REQUIREMENTS (8272-FY92-M135).
	POSTFLIGHT		POSTFLIGHT INSPECTIONS SHOW THE POLYSULFIDE THICKNESS AT NOMINAL CONDITION.
2.1.1.4 VENT SLOT DIMENSIONS AND LOCATION	POSTFLIGHT	MEASURE AND VERIFY RSRM-20 DIMENSIONS. ANALYZE DIMENSIONS.	NO PRE-FLIGHT DRs. POSTFLIGHT MEASUREMENTS MEET DIMENSIONAL REQUIREMENTS AT GAS PATH/SOOTED VENT SLOTS.
2.1.1.5 JOINT THERMAL RESPONSE	DENNIS BRIGHT	PERFORM CALCULATIONS.	CALCULATIONS SHOW NO EFFECT: DELTA T=10F, HOUSING GROWTH=0.0034" DELTA T=15F, HOUSING GROWTH=0.0051" DELTA T=20F, HOUSING GROWTH=0.0068" DELTA T=25F, HOUSING GROWTH=0.0085"

16

2.1.2 WIPER O-RING DESIGN	GARY NELSON	ANALYZE WIPER O-RING INTEGRITY.	THE WIPER O-RING IS NOT A PRESSURE SEAL. ITS FUNCTION IS TO PREVENT POLYSULFIDE FROM REACHING THE PRIMARY O-RING AND TO ACT AS A THERMAL BARRIER TO PREVENT HOT GAS DEGRADATION OF THE PRIMARY O-RING AND JOINT METAL HARDWARE. BASED ON THE POTENTIALLY LARGE TOTAL GAP (ASSEMBLY, RELAXATION, DYNAMIC), THE TRACKING FACTOR OF THE WIPER O-RING COULD BE LESS THAN 1.0 AND CANNOT BE GUARANTEED TO CONTAIN PRESSURE.
2.1.2.1 WIPER O-RING GROOVE DIMENSIONS	HART COOK	MEASURE AND VERIFY RSRM-20 DIMENSIONS. ANALYZE DIMENSIONS.	NO PRE-FLIGHT DRs. POSTFLIGHT MEASUREMENTS MEET DIMENSIONAL REQUIREMENTS AT GAS PATH/SOOTED VENT SLOTS.
2.1.2.2 WIPER O-RING DIMENSIONS	GARY NELSON	MEASURE AND VERIFY RSRM-20 DIMENSIONS. ANALYZE DIMENSIONS.	POSTFLIGHT WIPER O-RING MEASUREMENTS MEET DIMENSIONAL REQUIREMENTS OF 0.275 +/- 0.003 INCHES: (LH) MEASURED 0.2736 INCHES. (RH) MEASURED 0.2721 INCHES.
2.1.2.3 VENT SLOT DIMENSIONS AND LOCATIONS	POSTFLIGHT	MEASURE AND VERIFY RSRM-20 DIMENSIONS. ANALYZE DIMENSIONS.	NO PRE-FLIGHT DRs. POSTFLIGHT MEASUREMENTS MEET DIMENSIONAL REQUIREMENTS AT SOOTED/VENT SLOTS.
2.1.2.4 NBR SET	GARY NELSON	ANALYZE COMPRESSION/SQUEEZE.	THE ANALYSIS INDICATED AN NBR INDENTATION OF 0.038 INCHES DUE TO THE RADIAL DEFLECTION OF THE WIPER O-RING.
2.1.2.5 O-RING SET	ROGER COOK	ANALYZE COMPRESSION/SQUEEZE.	UNKNOWN DUE NBR WRAP AROUND THE O-RING.
2.1.2.6 JOINT ROTATION	ROGER COOK	ANALYZE ROTATION.	THE NOZZLE-TO-CASE JOINT HAS A DYNAMIC GAP OPENING OF APPROXIMATELY 0.021 INCHES DUE TO JOINT PRESSURIZATION.

2.1.2.7
JOINT THERMAL RESPONSE
DURING ASSEMBLY

DENNIS BRIGHT

PERFORM CALCULATIONS.

CALCULATIONS SHOW NO EFFECT:
DELTA T=10F, HOUSING GROWTH=0.0034"
DELTA T=15F, HOUSING GROWTH=0.0051"
DELTA T=20F, HOUSING GROWTH=0.0068"
DELTA T=25F, HOUSING GROWTH=0.0085"

2.1.3
JOINT FREE VOLUME

MIKE O'MALLEY

PERFORM THERMAL ANALYSIS.

CONSERVATIVE THERMAL ANALYSIS SHOWS
PRIMARY O-RING EROSION IF THE WIPER O-
RING HAD NOT SEALED BY 0.25 SECONDS.

3.0 PROCESS
3.1 INADEQUATE APPLICATION OF POLYSULFIDE
3.1.1 SURFACE VOIDS WITHIN THE POLYSULFIDE
3.1.2 SUBSURFACE VOIDS WITHIN THE POLYSULFIDE
3.1.3 OPEN VOLUME BETWEEN THE WIPER O-RING AND POLYSULFIDE

CAUSE	ACTIONEE	ACTION	CLOSURE RATIONALE
3.1.1.1 IMPROPER SCREED TECHNIQUES CAUSES DIPS/VOIDS	DAVE SEBAHAR	DOCUMENT PROCESS FLOW AND COMPARE WITH PREVIOUS AND SUBSEQUENT EXPERIENCE.	PLANNING REVIEW, VIDEO COVERAGE AND CREW INTERVIEWS SHOW NO NON-CONFORMANCES. DESIGN PREVENTS SCREED FROM ROCKING.
3.1.1.2 IMPROPER ALIGNMENT OF NOZZLE DURING INSTALLATION	DAVE SEBAHAR	REVIEW PROCESS DOCUMENTATION INTERVIEW INSTALLATION CREWS.	PLANNING REVIEW, VIDEO COVERAGE AND CREW INTERVIEWS SHOW NO NON-CONFORMANCES.
3.1.2.1 SCREED/BEAD APPLICATION OF POLYSULFIDE	CHARLES BOWN	SUBSCALE TESTING.	SUBSCALE TESTING SHOWED THAT IMPROPER SCREED TECHNIQUE COULD CAUSE SUBSURFACE VOIDS. THESE VOIDS ARE NOT OF THE CONFIGURATION NOTED ON STS-42. THESE VOIDS COULD BE CONSIDERED A CONTRIBUTOR BUT NOT THE CAUSE.
	BILL LESKCO	SUBSCALE TESTING.	
3.1.2.2 AIR IN SEMCO	CHARLIE BOWN	SUBSCALE TESTING.	SUBSCALE TESTING SHOWED THAT THERE ARE AIR BUBBLES WITHIN THE SEMCO TUBE, BUT THE BUBBLES OF SIGNIFICANT SIZE BURST UPON EXTRUSION FROM THE TUBE. SMALL VOIDS, PRESENT WITHIN THE CURED POLYSULFIDE, MAY CONTRIBUTE BUT ARE NOT THE CAUSE.
	POSTFLIGHT	REVIEW RSRM-20 SMALL VOID DATA. COMPARE WITH DATA HISTORY.	RSRM-20A: NONE. RSRM-20B: VERY SLIGHT POROSITY AT THE STEP BETWEEN THE 50 AND 60 DEGREE LOCATION. NO OTHERS SEEN. DATA COMPARISON SHOWS VOIDS AND POROSITY WITHIN THE POLYSULFIDE ARE TYPICAL.

3.1.3.1
TAPE TOO FAR FORWARD OF
VENT SLOTS

DAVE SEBAHAR

REVIEW PROCESS DOCUMENTATION.

PLANNING CONTROLS ENSURE PROPER TAPE
PLACEMENT. PLANNING REVIEW SHOWS NO NON-
CONFORMANCES.

8

3.0 PROCESS
3.2 IMPROPER VENTING OF JOINT
3.2.1 AIR FLOW THROUGH VENT SLOTS BLOCKED
3.2.2 AIR FLOW TO OR AT VENT PORT BLOCKED

CAUSE	ACTIONEE	ACTION	CLOSURE RATIONALE
3.2.1.1 GREASE	POSTFLIGHT	REVIEW RSRM-20 VENT SLOTS.	KSC POSTFLIGHT INSPECTIONS SHOW NOTHING WAS OBSERVED ON CONSEQUENCE.
3.2.1.2 POLYSULFIDE	POSTFIRE ROGER COOK	MEASURE RSRM-20 VENT SLOT FILL. COMPARE DATA.	VENT SLOT FILLS RECORDED. RSRM-20A: 30% FILL AT GAS PATH WITH 46% FILL OVERALL, NOTHING UNUSUAL. RSRM-20B: 0% FILL AT GAS PATH (11 CONSECUTIVE VENT SLOTS) WITH 40% FILL OVERALL.
			DATA COMPARISON SHOWS 11 CONSECUTIVE 0% VENT SLOT FILL NOT TYPICAL.
3.2.1.2.1 TAPE FAILS TO COVER VENT SLOTS DURING POLYSULFIDE APPLICATION	DAVE SEBAHAR	REVIEW PROCESS DOCUMENTATION AND VIDEO TO VALIDATE/REFUTE.	PLANNING CONTROLS ENSURE PROPER TAPE PLACEMENT. PLANNING SHOWS NO NON-CONFORMANCES.
3.2.2.1 GREASE	DAVE SEBAHAR	REVIEW PROCESS DOCUMENTATION INTERVIEW INSTALLATION CREWS.	PLANNING REVIEW AND CREW INTERVIEW SHOWS NO NON-CONFORMANCES. FLOW METER WORKED DURING ASSEMBLY.
3.2.2.2 NBR PINCHING	ROGER COOK MART COOK	ANALYZE.	VENTING CAN BE A PROBLEM ANYWHERE CLOSE PROXIMITY OCCURS.
			MEASUREMENTS AT GAS PATH/SOOTED VENT SLOTS SHOWED INSULATION GAPS, SO NO NBR PINCHING OCCURRED AT THESE LOCATIONS.

9

3.2.2.3 OUT OF ROUNDNESS	DAVE SEBAHAR	REVIEW PROCESSING DOCUMENTATION INTERVIEW INSTALLATION CREW.	PLANNING REVIEWS SHOWS NO NON-CONFORMANCES. ANALYSIS OF TOOLING TO COMPONENT STACK-UP IS NOT A CONCERN.
	ROGER COOK MART COOK	ANALYZE.	VENTING CAN BE A PROBLEM ANYWHERE CLOSE PROXIMITY OCCURS. METAL-TO-METAL CONTACT CAN RESTRICT VENTING.
3.2.2.3.1 METAL-TO-METAL	ROGER COOK MART COOK	ANALYZE.	VENTING CAN BE A PROBLEM ANYWHERE CLOSE PROXIMITY OCCURS. METAL-TO-METAL CONTACT CAN RESTRICT VENTING.
3.2.2.3.2 GUIDE PIN TOLERANCE	DAVE SEBAHAR	MEASURE GUIDE PINS CALCULATE ECCENTRICITY.	ACTUAL GUIDE PIN MEASUREMENT INDICATES WITHIN TOLERANCE.
	ROGER COOK MART COOK	ALLOWED BY TOLERANCE CONDUCT ANALYSIS TO EVALUATE.	FIXED HOUSING CONTACTS AFT DOME PRIOR TO POLYSULFIDE CONTACT AT APPROXIMATELY 0.8 INCHES FROM SEATING. JOINT CONTACT INFLUENCES ALIGNMENT FROM APPROXIMATELY 2.7 INCHES UNTIL SEATING.
3.2.3 REVERSE VENTING	ROGER COOK MART COOK	ANALYZE.	VENTING IN THE FORWARD DIRECTION THROUGH THE VENT SLOTS COULD OCCUR WHEN THE CHANNEL BETWEEN THE WIPER AND PRIMARY O-RINGS BECOME BLOCKED. IF THE PATH TO THE VENT PORT IS BLOCKED, THEN THE ENTRAPPED AIR COULD TRAVEL ALONG THE WIPER/PRIMARY CHANNEL AND BURP BACK THROUGH THE POLYSULFIDE AT THE WEAKEST LOCATION (THINNEST BONDLINE) IN LINE WITH A VENT SLOT.
			TWO OF THE THREE GAS PATHS OBSERVED ON RSRM FLIGHT MOTORS (11B AND 20A) WERE IN LINE WITH VENT SLOTS. A REVIEW OF ALL RSRM FLIGHT MOTORS WITH MULTIPLE VOIDS GREATER THAN 1.0 INCH IN THE AXIAL DIMENSION HAS REVEALED THAT 8 OUT OF THE 17 VOIDS DOCUMENTED WERE IN LINE WITH A VENT SLOT. THE RANDOM PROBABILITY OF A VOID BEING LOCATED AT A VENT SLOT LOCATION IS ONLY 1 IN 36.

3.2.4
IMPROPER ASSEMBLY RATE   DAVE SEBAHAR   REVIEW PROCESS DOCUMENTATION AND VIDEO TO VALIDATE/REFUTE.   PLANNING REVIEW AND VIDEO COVERAGE SHOW NO NON-CONFORMANCES.

3.2.5
RAISED BAFFLE AT ASSEMBLY   MART COOK   ANALYZE   NOMINAL AND WORST CASE JOINT TOLERANCE STUDIES SHOWED THAT FIXED HOUSING CONTACTS THE POLYSULFIDE PROFILE AT APPROXIMATELY 0.8 INCHES FROM SEATING. BUT POTENTIALLY ENTRAPS AIR VENTING FORWARD.

3.0 PROCESS
3.3 VOIDS DUE TO LEAK CHECK FAILURE
3.3.1 WIPER O-RING FAILS TO SEAL

CAUSE	ACTIONEE	ACTION	CLOSURE RATIONALE
3.3.1.1 POLYSULFIDE INTERFERES WITH WIPER O-RING FOOTPRINT	GARY NELSON	REVIEW RSRM-20 CONDITIONS	POLYSULFIDE IS TYPICALLY FOUND PAST THE WIPER O-RING AT THE VENT SLOT LOCATIONS. THIS CONDITION COULD AFFECT THE O-RING FOOTPRINT. NO TESTING HAS BEEN PERFORMED.
3.3.1.2 VENT SLOTS INTERFERE WITH WIPER O-RING FOOTPRINT	MART COOK	PERFORM DIMENSIONAL ANALYSIS REVIEW RSRM-20 CONDITIONS	STUDY OF THE ACTUAL WIPER O-RING CONFIGURATION AT EACH GAS PATH/SOOTED VENT SLOT SHOWED THE FOOTPRINT WAS FORWARD OF THE VENT SLOTS.
3.3.1.3 NBR SEALING SURFACE DAMAGE (NICKS, GOUGES)	GARY NELSON ROGER COOK SCOTT SMITH DAVE SEBAHAR	REVIEW RSRM-20 NBR	PLANNING REVIEW SHOW NO NON-CONFORMANCES. OBSERVATION: ABRADING AND METHYLCHLOROFORM WIPE WAS COMPLETED TWICE ON BOTH RSRM-20 SEGMENTS. NO DAMAGE WAS NOTED FROM THE KSC POSTFLIGHT INSPECTIONS.
3.3.1.4 RADIAL BOLT HOLES DAMAGE WIPER O-RING DURING NOZZLE ASSEMBLY	GARY NELSON POSTFLIGHT	REVIEW RSRM-20 O-RINGS	NO ASSEMBLY DAMAGE. KSC POSTFLIGHT INSPECTIONS (TWR-60682) SHOWED: (LH) NONE. (RH) DISASSEMBLY GOUGES IN WIPER O-RING AT RADIAL BOLT HOLE LOCATIONS 343.8, 347.4, AND 354.6. THIS DAMAGE DOES NOT CORRESPOND WITH THE GAS PATH AT 247 DEGREES.

3.3.1.5
PHENOLIC SEALING SURFACE
DAMAGE

POSTFLIGHT

REVIEW RSRM-20 PHENOLICS

NO DAMAGE WAS NOTED FROM THE KSC
POSTFLIGHT INSPECTIONS.

3.3.1.6
IMPROPER LEAK CHECK

WAYNE SPERRY

VERIFY RSRM-20 DATA.
COMPARE WITH DATA HISTORY.

LEAK CHECK DATA MET REQUIREMENTS PER TWR-
60429A. 22 +/-3 PSIG LEAK CHECK IS
PERFORMED BETWEEN THE PRIMARY-TO-WIPER
CAVITY AFTER THE POLYSULFIDE IS CURED, NO
VOLUME IS RECORDED. DATA COMPARISON
SHOWS NOTHING UNUSUAL.

13

3.0 PROCESS
3.4 ADHESIVE FAILURE OF POLYSULFIDE
3.4.3 CONTAMINATION

CAUSE	ACTIONEE	ACTION	CLOSURE RATIONALE
3.4.1 TEMPERATURE DURING FIRING	SID HENDERSON	REVIEW RSRM-20 EXPERIENCE	DATA COMPARISON SHOWS NOTHING UNUSUAL. POSTFLIGHT EVIDENCE OF THE GAS PATH SUPPORT THIS CAUSE.
3.4.2 STORAGE AND TRANSPORTATION	BRUCE MCWHORTER	DEFINE POINT OF DEVIATION IN RSRM-20 PROCESS	DATA COMPARISON SHOWS NOTHING UNUSUAL. POSTFLIGHT EVIDENCE OF THE GAS PATH SUPPORT THIS CAUSE.
3.4.3.1 METHYL CHLOROFORM	REED HADDOCK	SUBSCALE TESTING	
3.4.3.2 GREASE	REED HADDOCK	SUBSCALE TESTING	
3.4.3.3 POLYPROPYLENE			

APPENDIX B - ENGINEERING ASSESSMENT

1.0 INTRODUCTION

This appendix summarizes the results of the Engineering Team effort in the RSRM-20 A & B Nozzle to Case Joint Gas Path Investigation. This effort focused on; extracting information from the postflight inspection of the nozzle to case joints, postflight trending, the design of the joint configuration and any deviation from the engineering tolerances in the RSRM-20 A & B hardware, structural analysis, modeling the joint configuration during the assembly process, potential problems during the assemblies that could cause gas path formation, and a thermal analysis of the joints during motor operation.

2.0 SUMMARY

- A single gas path was observed in the RSRM-20A nozzle to case joint at 57.6 degrees through the polysulfide bondline to the wiper O-ring. This gas path was in line with a vent slot.

- A single gas path was observed in the RSRM-20B nozzle to case joint at 247 degrees through the polysulfide bondline to the wiper O-ring.

- Both gas paths were formed at joint assembly.

- Heat effect was observed on the glass cloth phenolic, carbon cloth phenolic and NBR over the lengths of both gas paths.

- Soot reached the wiper O-rings in the RSRM-20 A & B nozzle to case joints through gas paths in the polysulfide, both wiper O-rings experienced erosion over a small circumferential length, and soot was observed past the RSRM-20A wiper O-ring only.

- Observations indicate that the RSRM-20A wiper O-ring leaked initially and then resealed soon after pressurization since only minimal soot reached past the groove. Thermal analysis predicts that the blowby resealed after 0.15 seconds.

- The nozzle-to-case wiper O-rings performed as designed. Polysulfide did not reach the primary O-ring and no hot gas degradation was observed to the primary O-ring and the joint metal hardware.

- Both RSRM RSRM-20A & B joints were of proper configuration

- Postflight trending does not show an increase in the number of gas paths or significant voids.

27

- Postflight trending does show a trend of increasing CCP adhesive failure mode, decreasing NBR failure mode and decreasing cohesive failure mode since RSRM-10.

- The RSRM-20 A & B nozzle to case joint configurations and all individual components were within the current flight history.

- A structural analysis has indicated that an 0.038 inch deep indentation in the NBR could be formed due to wiper O-ring assembled contact pressure. This indentation along with joint rotation could result in a wiper O-ring tracking factor of less than 1.0.

- The polysulfide profile variation due to application and slump seen with the current polysulfide has little effect on when the fixed housing first contacts the adhesive bead during the assembly.

- The air trapped in the nozzle to case joint during an assembly could reach a maximum of 1.15 psi before venting is initiated, assuming no vent path blockage and no polysulfide blow through.

- Several conditions can occur during a nozzle to case joint assembly that would restrict air evacuation and/or contribute to gas path formation, including; NBR pinch-off, out of roundness/metal to metal contact, plugged vent port, excessive grease and reverse venting through the vent slots.

- The most likely scenario for the RSRM-20A gas path formation is an unknown form of vent path blockage which resulted in reverse venting through a vent slot and then through the polysulfide.

- The most likely scenario for the RSRM-20B gas path formation would include an egg shaped aft dome which resulted in metal to metal contact in two locations around the circumference of the joint. This would have prevented the air between these two areas of blockage from reaching the vent port. The trapped air would have had to vent through the polysulfide.

- It has been determined by the Gas Path Investigation Team that the present design of the joint has an inherent potential to form gas paths.

3.0 RECOMMENDATIONS

- Investigate extending the vent slots aft to the metal hardware.

- Investigate adding additional vent ports to the fixed housing.

- Investigate adding a bleed path around the circumference of the joint to prevent air flow blockage.

- Perform a comprehensive study program to identify corrective actions. Prove gas path causes and remedies.

    - Investigate out-of-round hardware at assembly.

    - Validate joint venting by capturing/measuring vented air.

28

- Round hardware with oversize O-ring.

- Investigate modifying the screed contour to account for the different slump characteristics of the replacement polysulfide (STW4-3829).

- Change polysulfide packaging size to better match process requirement.

- Investigate an increased diameter wiper O-ring to improve sealing by compensating for NBR shrinkage, stress relaxation, and motor firing joint rotation.

4.0 DISCUSSION

4.1 Postflight Inspection Results

The RSRM-20 A & B nozzle to case joint post-flight assessment performed at KSC and H7 revealed the following conditions:

4.1.1 RSRM-20A Postflight Inspection Results

- A single gas path was observed at 57.6 degrees through the polysulfide bondline to the wiper O-ring, Figure B-1. This gas path was in line with a vent slot. No other voids greater than 0.42 inch in diameter were observed in the bondline.

- The gas path was filled with a tar like residue (decomposed polysulfide and soot).

- The polysulfide at the forward end of the gas path exhibited a much higher concentration of heat effect than the aft end, which indicates a low volume of flow through the gas path.

- Some portions of the polysulfide on the walls of the gas path were smooth and shiny, and not heat affected. This indicates that the gas path was formed during the joint assembly.

- The polysulfide immediately in front of the wiper O-ring was heat affected full circumference as evidenced by a darker colored polysulfide.

- Soot was observed on the forward wall, aft wall and on the bottom of the wiper O-ring groove in the fixed housing intermittently between 50 and 79 degrees.

- Soot was observed past the wiper O-ring groove at the vent slot locations at 57.6 and 64.8 degrees. No soot was observed to the primary O-ring.

- Soot was not observed across the wiper O-ring footprint in the bottom of the groove, i.e., the blowby occurred on the NBR side of the wiper O-ring.
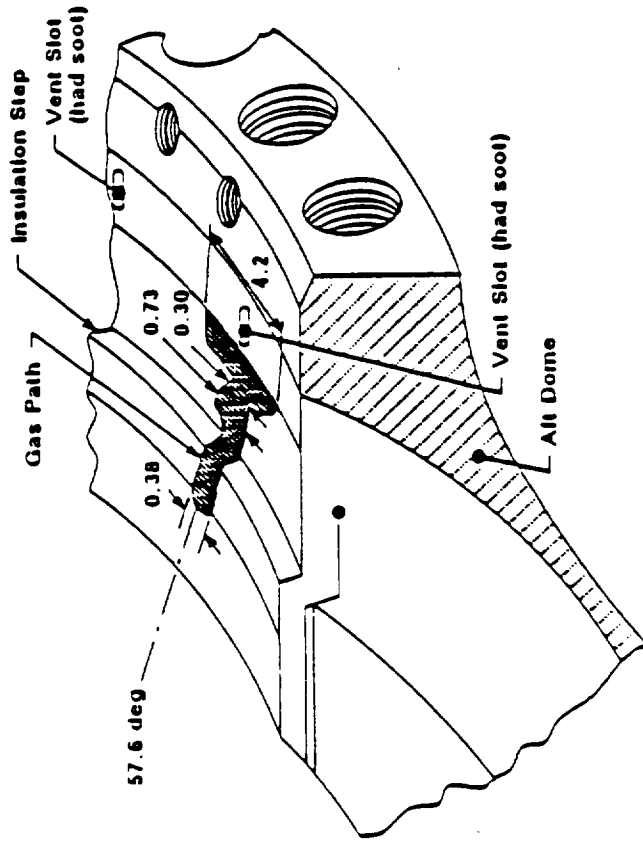
Gas Path at 57.6 Degrees

SIS-42 (360T020) LH (A)

Figure B-1. Gas Path on RSRM-20A Aft Dome
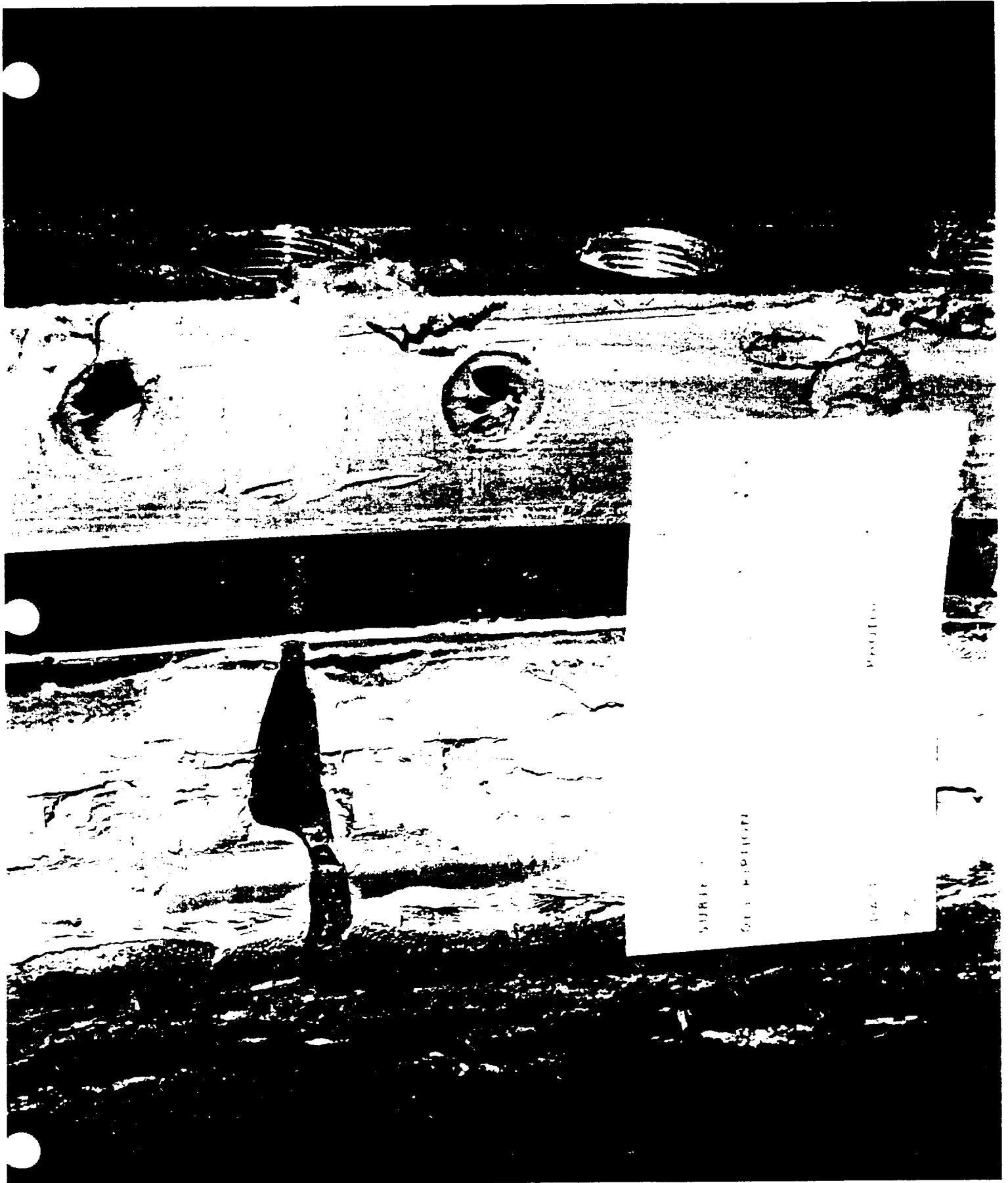
- Circumferential heat effect and erosion were observed on the wiper O-ring centered at 57.6 degrees and measured 2.2 inches long by 0.020 inch maximum depth, Figure B-2.

- Heat effect to the carbon cloth phenolic (CCP) was observed over the length of the gas path, but had no measurable depth.

- Heat effect to the glass cloth phenolic (GCP) on the forward edge of the wiper O-ring groove was observed to have a maximum depth of 0.020 inch. No heat effect was observed aft of the wiper O-ring.

- Heat effect to the aft dome NBR was observed over the length of the gas path. Erosion in the NBR was observed at the joint step and forward of the wiper O-ring. A band of non-heat affected polysulfide was observed on the aft dome immediately prior to the wiper O-ring.

- EDAX and FTIR indicated no unusual materials or contamination in the residue found in the gas path or in the adjacent polysulfide. The analysis also verified the correct concentration of lead in the materials, which indicates proper mixing.

- The thickness and hardness of the polysulfide was consistent around the circumference of the joint.

- The amount of insulation erosion, failure mode (65% cohesive and 35% adhesive) and vent slot fill (ave 48%) were all within the postflight database.

4.1.2 RSRM-20B Postflight Inspection Results

- A single gas path was observed at 247 degrees through the polysulfide bondline to the wiper O-ring, Figure B-3. No other voids greater than 0.55 inch in diameter were observed in the bondline.

- The gas path was filled with a tar like residue (decomposed polysulfide and soot).

- The polysulfide at the forward end of the gas path exhibited a high concentration of heat effect. The aft end had no indications of heat effect, which indicates a low volume of flow through the gas path.

- Some portions of the polysulfide on the walls of the gas path were smooth and shiny, and not heat affected. This indicates that the gas path was formed during the joint assembly.

- The polysulfide immediately in front at the wiper O-ring was heat affected full circumferential as evidenced by a darker colored polysulfide.
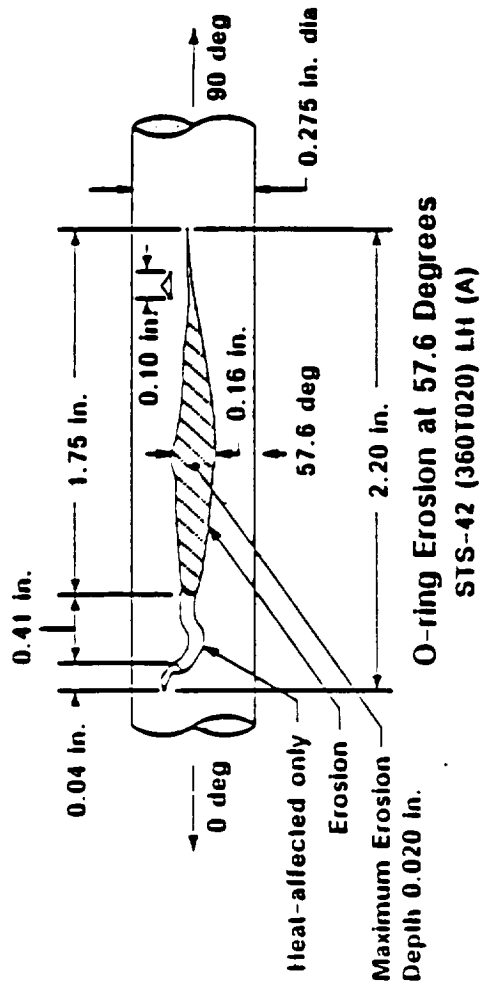
Figure B-2. RSRM-20A Wiper O-Ring
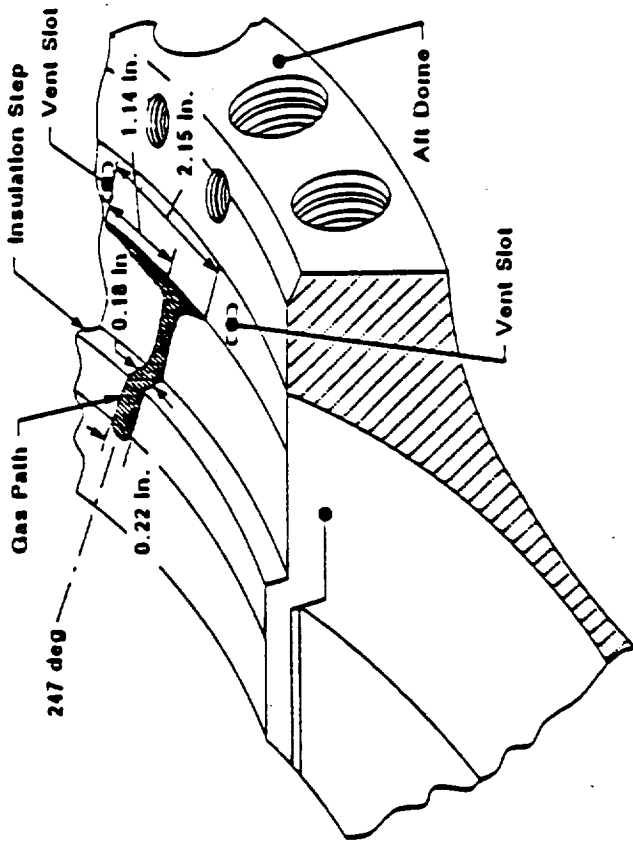
Gas Path at 247 Degrees
STS-42 (360T020) RH (B)

Figure B-3. Gas Path on RSRM-20B Aft Dome
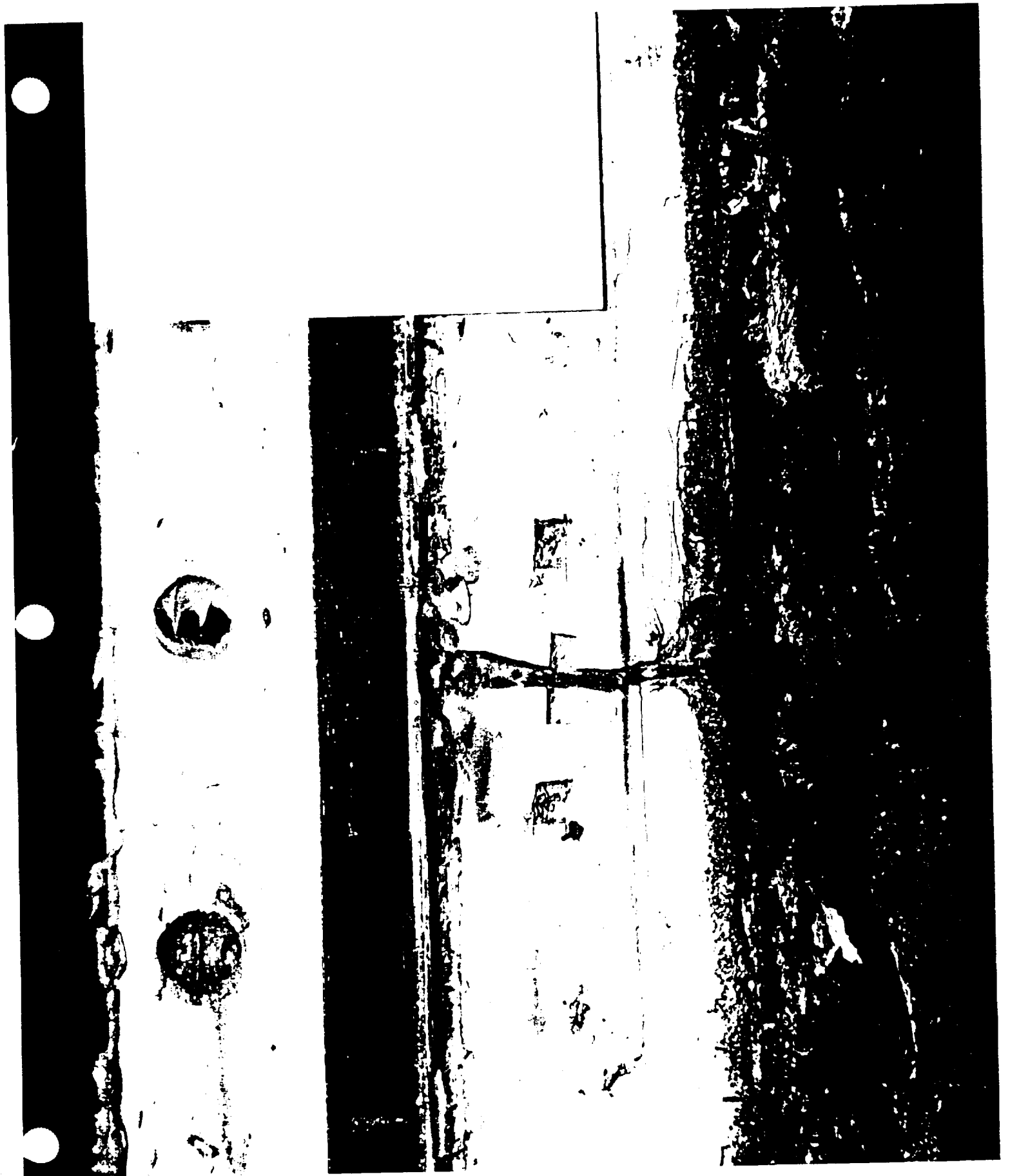
- Soot was observed on the forward wall of the wiper O-ring groove in the fixed housing between 246 and 250 degrees.

- No soot or any evidence of blowby was observed past the wiper O-ring.

- Circumferential heat effect and erosion were observed on the wiper O-ring in three locations centered at 247 degrees and measured 1.52 inches long overall by 0.024 inch maximum depth, Figure B-4.

- Heat effect to the carbon cloth phenolic was observed over the length of the gas path, but had no measurable depth.

- Heat effect to the glass cloth phenolic on the forward edge of the wiper O-ring was observed to have a maximum depth of 0.040 inch. The forward edge of the wiper O-ring groove appeared to be rounded (possible erosion) along a 0.40 inch circumferential width. No heat effect was observed aft of the wiper O-ring.

- Heat effect to the aft dome NBR was observed over the length of the gas path. Erosion in the NBR was observed at the joint step and forward of the wiper O-ring. A band of non-heat affected polysulfide was observed on the aft dome immediately prior to the wiper O-ring.

- EDAX and FTIR indicated no unusual materials or contamination in the residue found in the gas path or in the adjacent polysulfide. The analysis also verified the correct concentration of lead in the materials, which indicates proper mixing.

- The thickness and hardness of the polysulfide was consistent around the circumference of the joint.

- The amount of insulation erosion, failure mode (40% cohesive and 60% adhesive) and vent slot fill (ave 40%) were all within the postflight database.

4.2 Postflight Trending Analysis

Postflight nozzle to case joint trending data through RSRM-20 was compiled and is given in Table B-I.

4.2.1 Gas Penetration

As Table B-I shows, gas penetration aft of the insulation step has occurred on only three motors; RSRM-11B, 20A, 20B. No evidence of multiple gas paths has been seen.

4.2.2 Void Formation

Attached are plots of voids greater than 1.0-inch axial length and voids greater than 0.5-inch axial length for flight motors (Figures B-5 and B-6). The charts do not shown an increase in the number of significant voids observed. Also plotted were the degree location of voids larger than

0.275 in. dia

0.276 in.

0.13 in.

0.125 in.

0.240 in.

0.70 in.

0.17 in.

0.135 in.

1.52 in.

0.12 in.

Maximum Erosion
Depth 0.024 in.
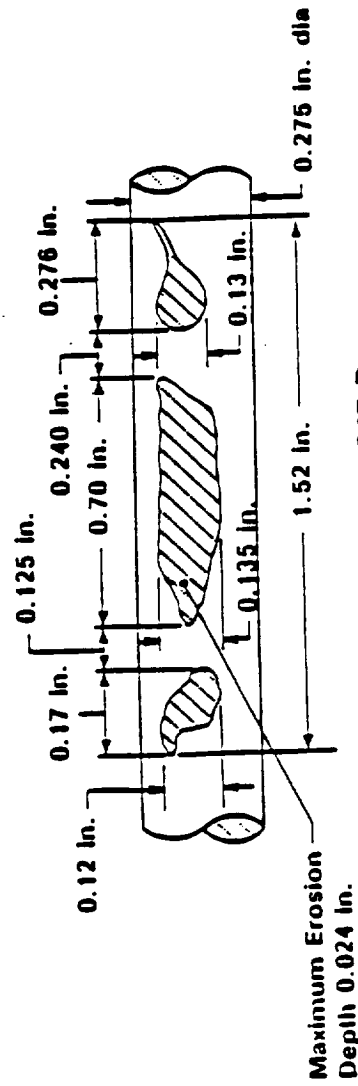
O-ring Erosion at 247 Degrees
STS-42 (360T020) RH (B)

Figure B-4. RSRM-20B Wiper O-Ring

TABLE R-1

RSRM NOZZLE-TO-CASE JOINT POSTFL(INSPECTION FLIGHT HISTORY

	01A	01B	02A	02B	03A	03B	04A	04B	05A	05B
Gas Path:	0	0	0	0	0	0	0	0	0	0
Foreign Material	0	0	0	0	0	0	0	0	0	0
Voids Forward of Step	0	1	0	0	0	3	several	0	0	0
Voids at Wiper O-ring	1	7	0	0	0	0	2	2	2	2
Voids Aft of Step	3	12	7	0	2	0	0	several	3	several
Porosity	slight	slight	slight	slight	typical	typical	none	none	slight	slight
Extrusion Past Wiper										
Adhesive-to-NBR Failure	60	10	20	2	75	3	30	15	5	20
Adhesive-to-CCP Failure	0	0	0	0	0	2	0	0	15	10
Cohesive Failure	40	90	80	98	25	95	70	85	80	70
Aft Dome Edge Unbonds	0	0	0	0	0	0	0	0	0	0
Torn Baffle	no	no	no	no	no	no	no	no	no	no
Vent Slot Percentage Fill	80	70		62	11	5	60	64	41.4	8.6
Erosion - Inboard Depth										
0 deg			6.12	6.00					6.20	6.20
90 deg			6.25	6.12					6.20	6.10
180 deg			6.12	6.00					6.00	5.90
270 deg			6.25	6.25					6.20	6.30
Erosion Outboard Depth										
0 deg			5.62	5.75					5.80	5.70
90 deg			5.75	5.75					5.60	5.70
180 deg			5.75	5.62					5.70	5.60
270 deg			6.00	5.75					5.70	5.90

38

TABLE B-I (CONT)

	06A	06B	07A	07B	08A	08B	09A	09B	10A	10B
Gas Paths	0	0	0	0	0	0	0	0	0	0
Foreign Material	0	0	0	0	0	0	0	0	0	0
Voids Forward of Step	0	0	0	0	16	14	several	0	0	1
Voids at Wiper O-ring	1	0	1	0	0	0	0	0	1	0
Voids Aft of Step	0	0	0	0	14	12	several	1	10	15
Porosity	slight	slight	typical	slight	typical	typical	slight	slight	slight	typical
Extrusion Past Wiper	0	0	0	0	0	0	0	0	0	0
Adhesive-to-NBR Failure	0	100	15	10	3.5	16	0	0	0	0
Adhesive-to-CCP Failure	5	0	2	1	1.5	4	5	10	45	40
Cohesive Failure	95	0	83	89	95	80	95	90	55	60
Aft Dome Edge Unbonds	3	0	0	0	0	0	0	0	0	0
Torn Baffle	no	no	no	no	no	no	no	no	no	no
Vent Slot Percentage Fill	38	57	32	84	45	50.3	44	34	23	1
Erosion – Inboard Depth										
0 deg	6.25	6.40	6.00	5.95	6.10	6.10	6.00	6.00	6.05	6.00
90 deg	6.25	6.40	6.40	6.10	6.20	6.15	6.25	6.00	6.00	6.00
180 deg	6.30	6.35	6.25	6.10	6.20	6.35	6.00	5.75	6.20	5.95
270 deg	6.20	6.25	6.35	6.05	6.10	6.40	6.25	6.00	6.35	6.10
Erosion – Outboard Depth										
0 deg	6.05	6.10	5.78	5.60	5.60	5.60	5.75	5.75	5.75	5.65
90 deg	6.00	5.90	5.90	5.60	5.60	5.50	5.75	5.75	5.75	5.70
180 deg	6.05	5.90	5.95	5.70	5.00	5.50	5.50	5.40	5.95	5.70
270 deg	6.00	5.83	5.05	5.70	5.40	5.65	5.75	5.70	5.70	5.85

39

TABLE B-I (CONT)

	11A	11B	12A	12B	13A	13B	14A	14B	15A	15B	16A
Gas Paths	0	1	0	0	0	0	0	0	0	0	0
Foreign Material	0	0	0	0	0	0	0	0	0	0	0
Voids Forward of Step	2	0	3	2	several	several	0	0	several	0	0
Voids at Wiper O-ring	6	1	0	0	0	0	0	0	several	0	0
Voids Aft of Step	5	several	0	1	several	0	0	1	several	0	0
Porosity	noe	slight	typical	typical	typical	extensive	heavy	typical	typical	moderate	heavy
Extrusion Past Wiper	0	0	0	0	0	0	0	0	0	several	0
Adhesive-to-NBR Failure	1	0	10	0	10	0	15	10	0	10	0
Adhesive-to-CCP Failure	49	50	60	70	30	90	70	50	15	50	75
Cohesive Failure	50	50	30	30	60	10	15	40	85	40	25
Aft Dome Edge Unbonds	0	0	0	0	0	0	0	0	0	0	0
Thin Baffle	no	no	no	no	no	no	no	no	no	no	no
Vent Slot Percentage Fill	33	21	61.3	51	70.3	33.1	25.8	31	17.2	88.6	37.9
Erosion – Inboard Depth											
0 deg	6.10	6.10	6.40	6.20	6.30	6.40	6.20	6.10	6.25	6.00	6.00
90 deg	6.30	6.08	6.30	6.00	6.50	6.30	6.25	6.05	6.30	6.10	6.10
100 deg	6.05	6.00	6.30	6.30	6.10	6.20	6.20	6.00	6.30	6.20	6.10
270 deg	6.10	6.12	6.20	6.10	6.30	6.10	5.90	6.10	6.20	6.30	6.10
Erosion – Outboard Depth											
0 deg	5.70	5.90	5.80	5.80	5.80	5.80	5.85	5.70	6.00	5.70	5.70
90 deg	5.95	5.70	5.70	5.60	5.80	5.90	5.05	5.80	5.90	5.80	5.70
100 deg	5.75	5.75	5.60	5.80	5.70	5.80	5.75	5.70	5.90	5.80	5.70
270 deg	5.65	5.05	5.80	5.70	5.80	5.80	5.65	5.75	5.70	5.90	5.50

|	16B	17A	17B	18A	18B	19A	19B	20A	20B
Gas Paths	0	0	0	0	0	0	0	1	1
Foreign Material	0	0	0	yes	yes	yes	0	0	0
Voids Forward of Step	several	0	several	0	several	2	0	0	0
Voids at Wiper O-ring	several	0	several	1	0	0	0	1	2
Voids Aft of Step	several	several	several	0	0	5	0	9	2
Porosity	heavy	slight	slight	typical	heavy	slight	typical	none	slight
Extrusion Past Wiper	majority	several	0	4	6	3	0	3	0
Adhesive-to-NBR Failure	30	0	0	0	0	0	0	15	0
Adhesive-to-CCP Failure	10	25	2	60	50	40	15	20	60
Cohesive Failure	60	75	90	40	50	60	85	65	40
Aft Dome Edge Unbonds	0	0	0	0	0	0	0	0	0
Torn Baffle	no	yes	no	no	no	no	no	no	no
Vent Slot Percentage Fill	95.8	96	66	70	56	70	23	46	40
Erosion - Inboard Depth									
0 deg	6.10	5.95	5.95	5.90	6.20	6.30	6.20	6.00	6.00
90 deg	6.10	6.05	6.20	6.00	6.00	6.05	6.20	6.10	6.10
180 deg	6.20	5.90	5.95	6.25	6.00	6.20	6.15	6.10	6.10
270 deg	6.20	6.30	6.15	6.00	6.25	6.10	6.25	6.10	6.00
Erosion - Outboard Depth									
0 deg	5.70	5.75	5.70	5.75	5.75	5.90	5.85	5.80	5.60
90 deg	5.80	5.80	5.80	5.60	5.50	5.75	5.75	5.80	5.70
180 deg	5.80	5.70	5.70	5.75	5.50	5.80	5.75	5.80	5.60
270 deg	5.80	5.85	5.95	5.75	5.75	5.70	5.90	5.70	5.65
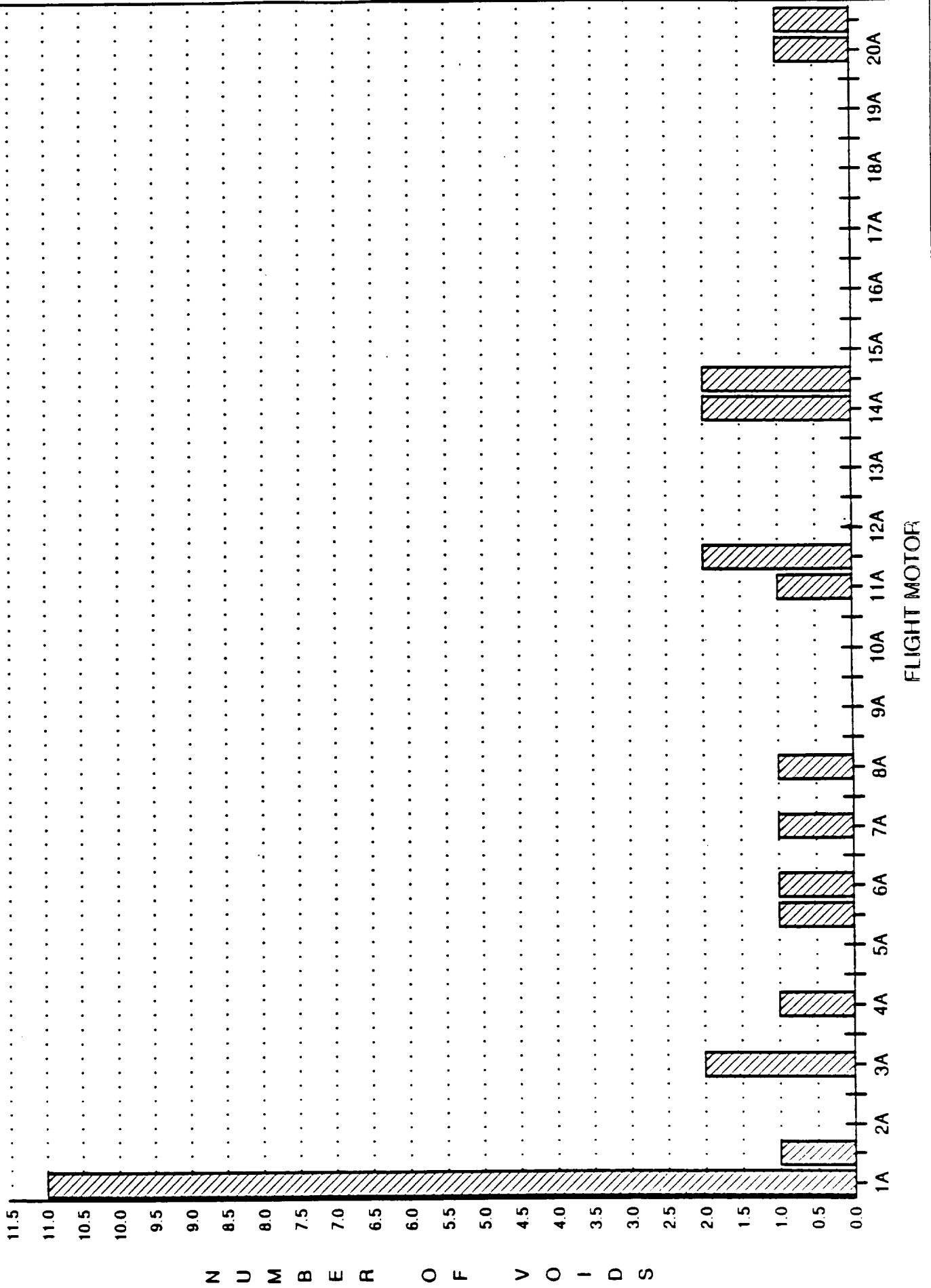
Figure B-5. Void Formation

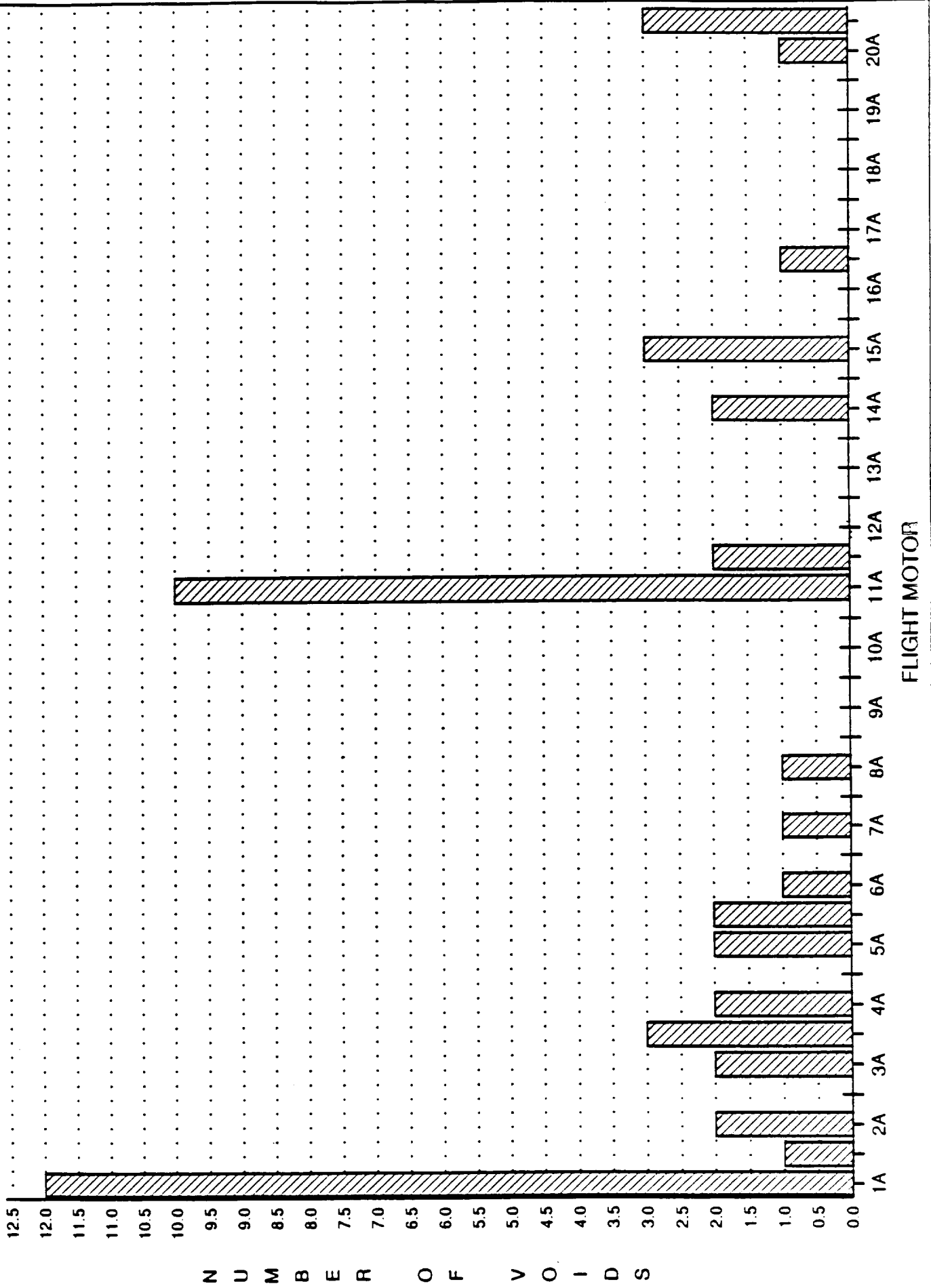NUMBER OF VOIDS > 0.5 INCH VS. FLIGHT MOTOR

Figure B-6   Void Formation

43

0.5-inch axial length, Figure B-7. The voids do not appear to concentrate in any area.

4.2.3 Polysulfide Extrusion Past Wiper O-Ring

Table B-I and Figure B-8 seems to indicate that polysulfide extrusion past the wiper O-ring is a recent phenomenon. This is the result of recent documentation of polysulfide extrusion past the wiper O-ring which has occurred at vent slot locations only. This condition has been seen on flight motors previous to RSRM-15, but was not documented because it was considered a normal and acceptable condition. Polysulfide extrusion past the wiper at locations other than at vent slots has not been observed.

4.2.4 Failure Mode

A trend of increasing CCP adhesive failure and decreasing NBR adhesive failure is evident, Figures B-9 and B-10. These trends are due in part to improved NBR surface preparation prior to bonding. A slight downward trend has also been observed in the cohesive failure mode since RSRM-10, Figure B-11.

4.2.5 Vent Slot Fill

The average vent slot fill is highly variable from motor to motor, Figure B-12. The extent of vent slot fill is a function of the polysulfide (thixotropy and viscosity) and the assembly process (rate, temperature, humidity and time). Although high vent slot fill is generally considered desirable, since it is an indication of good air evacuation and adhesive flow, postflight observations have not shown a direct correlation between vent slot fill and the joints ability to function (i.e., low or no vent slot fill does not always result in a gas path, but does indicate that the air trapped between the wiper and polysulfide during the assembly was not completely evacuated or, at a minimum, was not evacuated until late in the assembly).

4.3 Nozzle to Case Joint Configuration

The RSRM fixed housing carbon and glass cloth phenolics are bonded onto the fixed housing metal hardware and then machined to the drawing tolerances. The RSRM aft dome NBR insulation is vulcanized to the metal hardware using a mold which forms the joint surface. The aft dome insulation joint profile is mold controlled, meaning that the configuration of the joint surface is accepted based on the use of a specified mold tool and not by a Quality verification of the engineering tolerances. Therefore, dimensions on the aft dome NBR are at times not within drawing tolerance, but still acceptable because the mold tooling is producing hardware that is basically identical to the hardware that was qualified during the redesign.

4.3.1 Aft Dome Joint Surface Profile

Tables B-II and B-III and Figure B-13 list the aft dome NBR profiles for RSRM-20 A & B. The profile measurements for both aft domes were not always in the engineering tolerances, for the reason stated above, but were within the current flight history, Table B-IV.
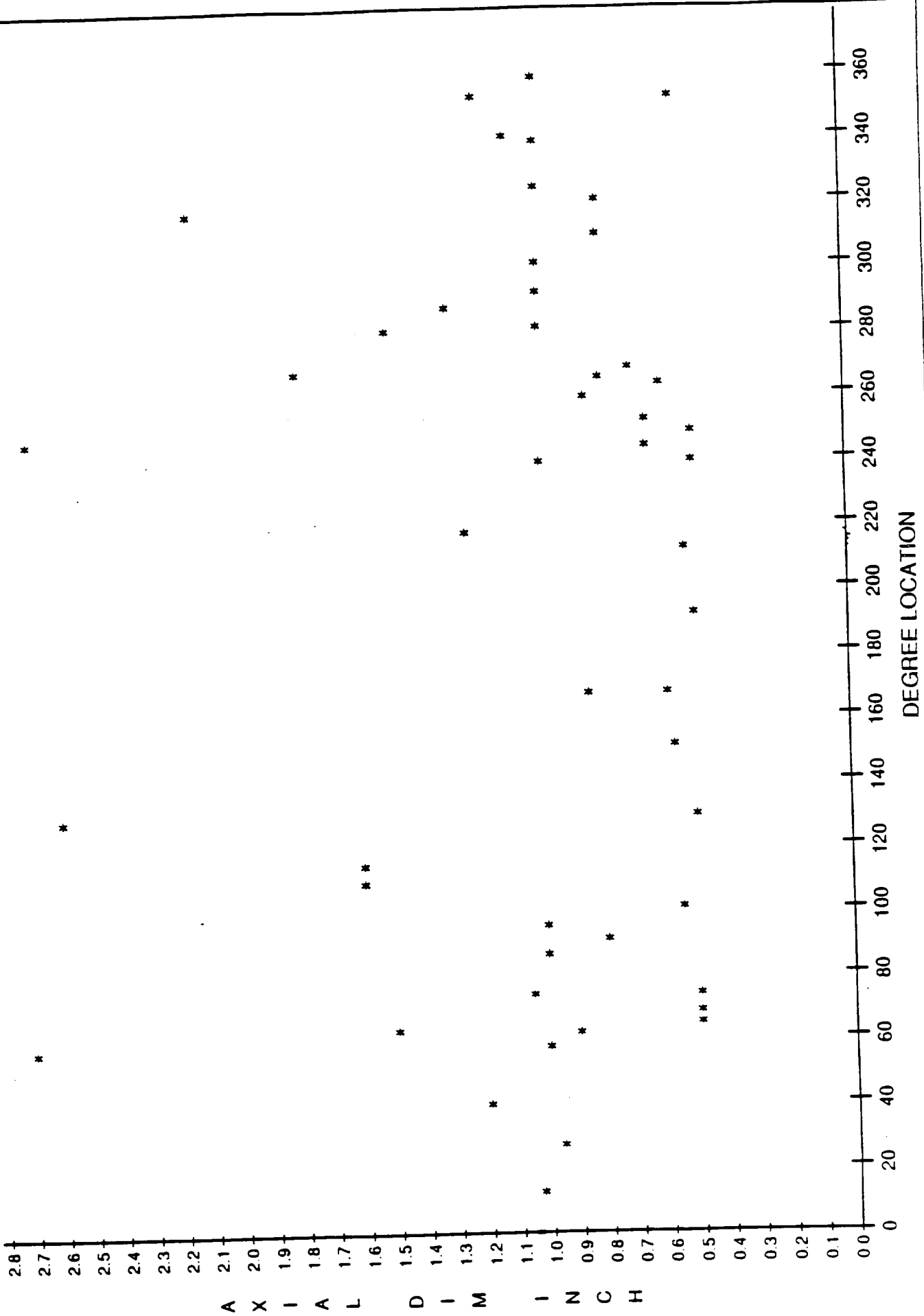
Figure B-7. Void Formation

POLYSULFIDE EXTRUSION PAST WIPER VS. FLIGHT MOTOR
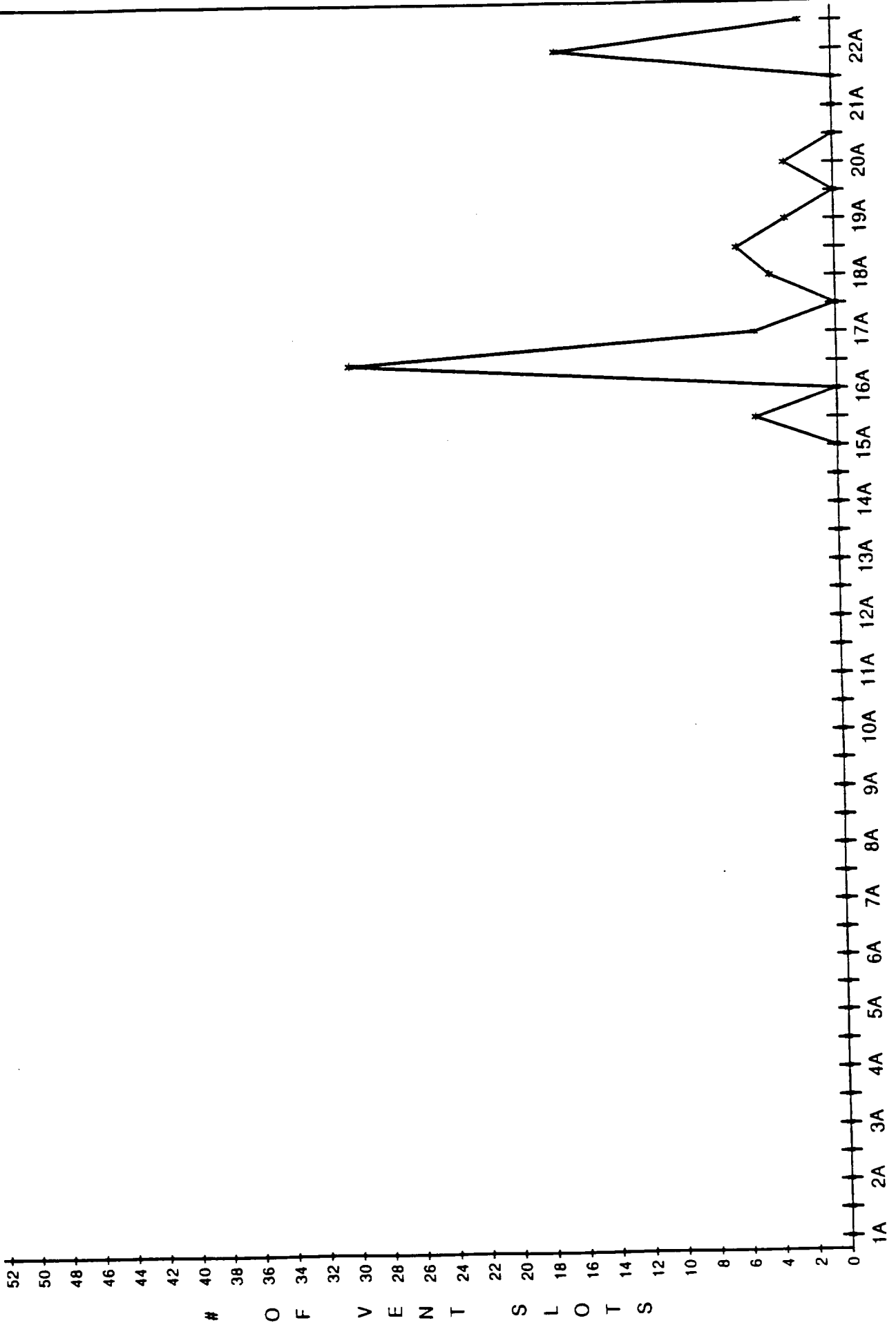
FLIGHT MOTOR

% CCP ADHESIVE FAILURE VS. FLIGHT MOTOR
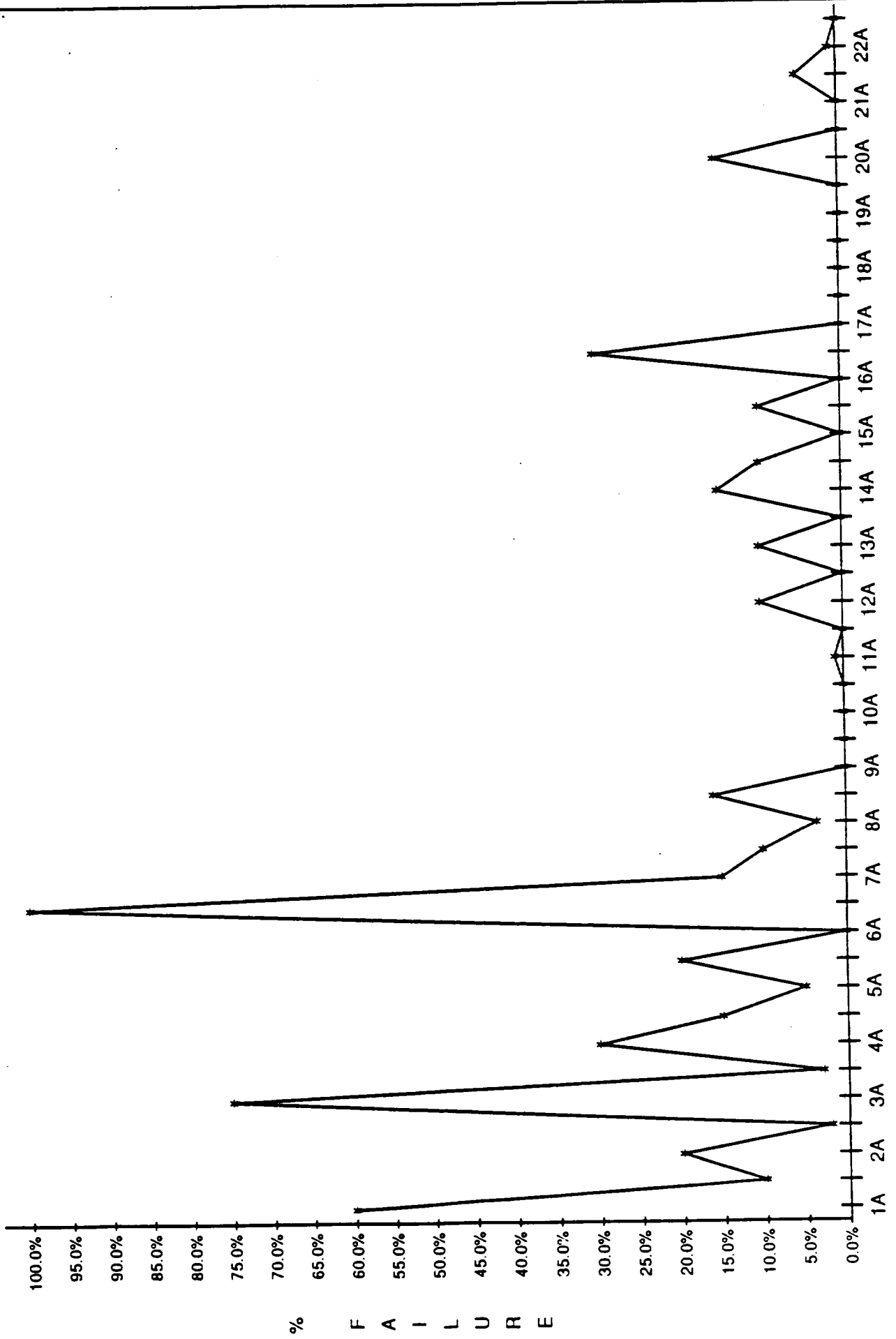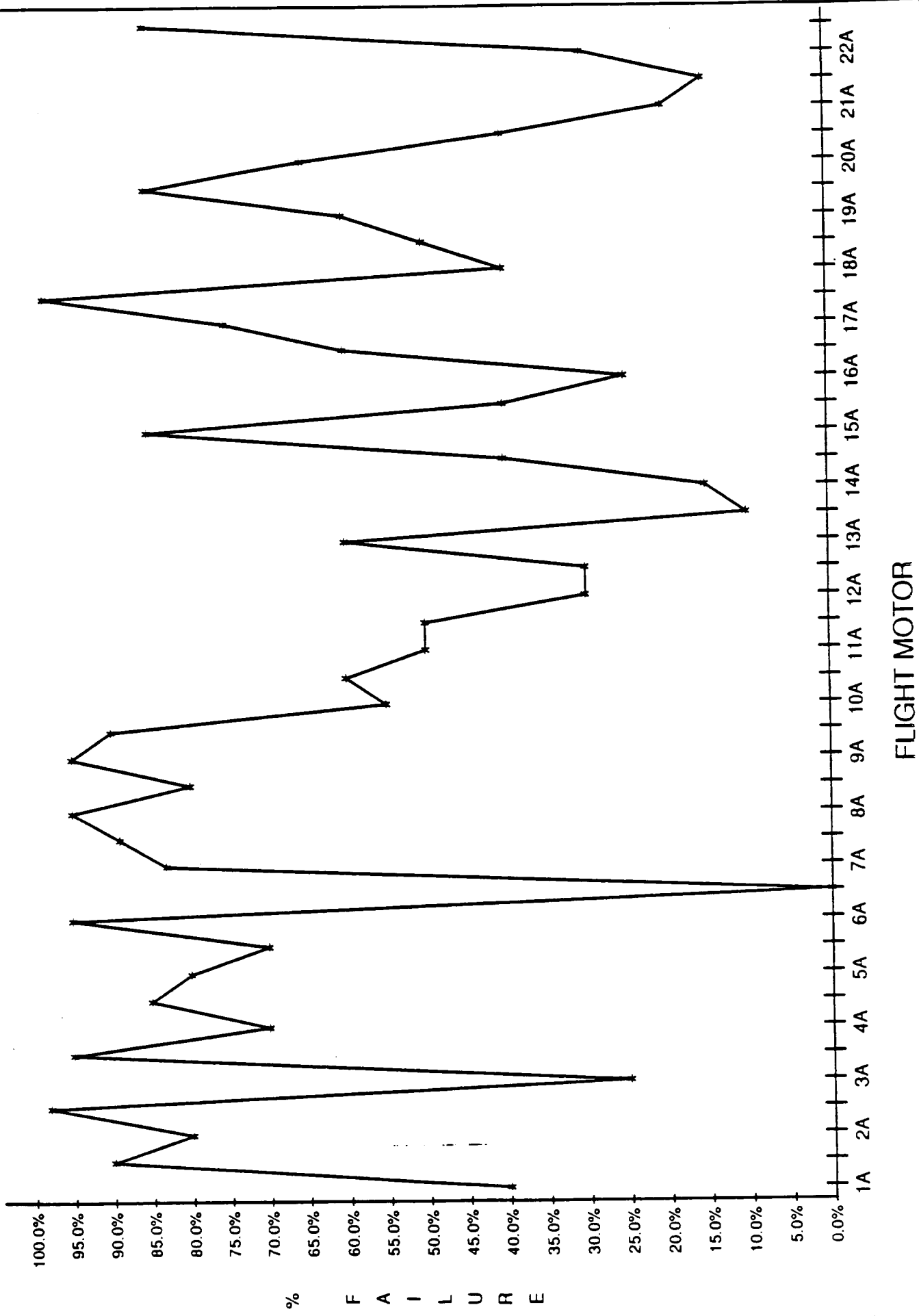
Figure B-10. NBR Adhesive Failure

Figure B-11. Cohesive Failure

% AVG VENT SLOT FILL VS. FLIGHT MOTOR

FLIGHT MOTOR

1A 2A 3A 4A 5A 6A 7A 8A 9A 10A 11A 12A 13A 14A 15A 16A 17A 18A 19A 20A 21A 22A

100.0% 95.0% 90.0% 85.0% 80.0% 75.0% 70.0% 65.0% 60.0% 55.0% 50.0% 45.0% 40.0% 35.0% 30.0% 25.0% 20.0% 15.0% 10.0% 5.0% 0.0%

%
F
L
L
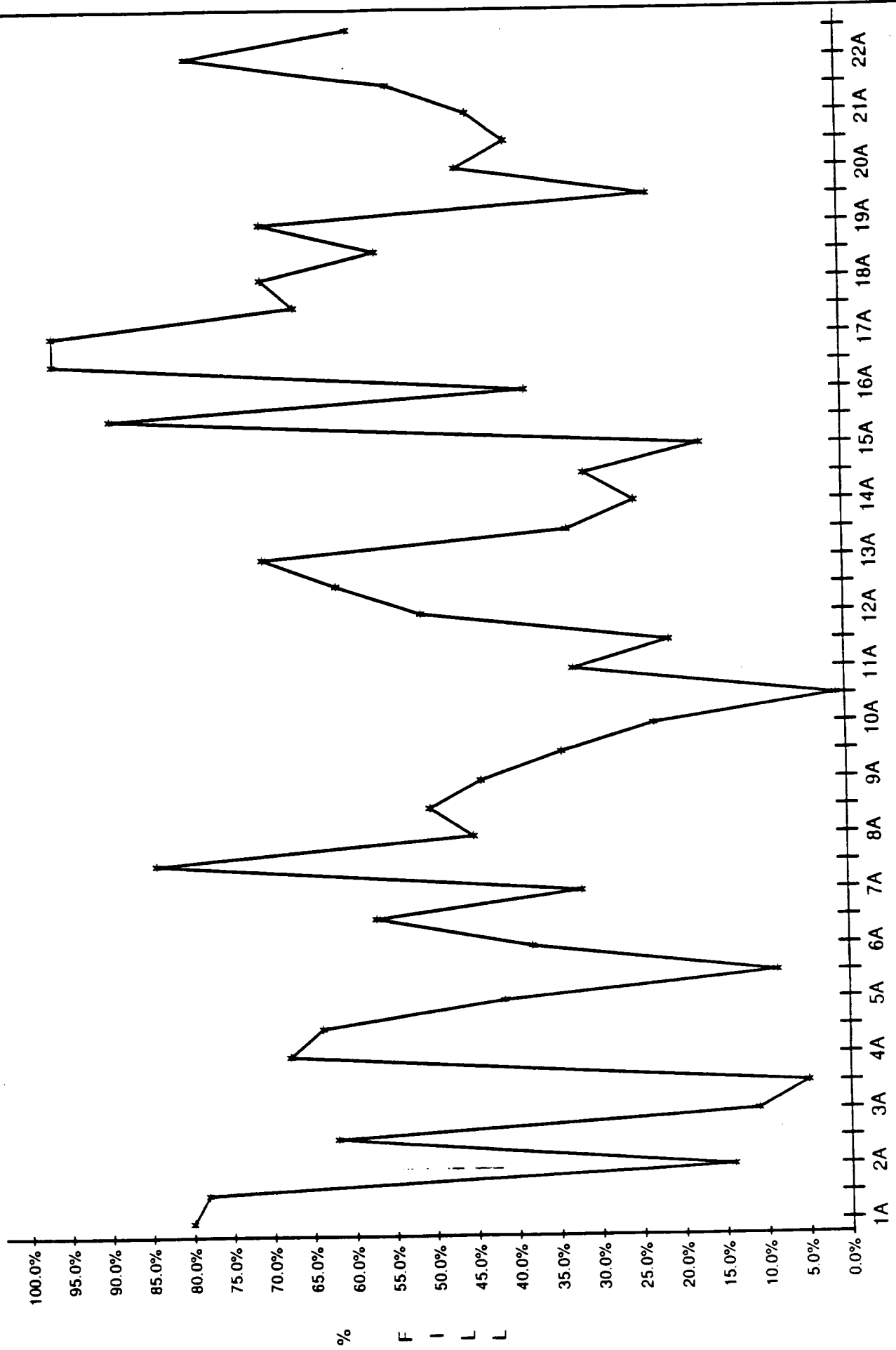
RSRM-20A AFT DOME JOINT PROFILE

A	B	C	D	E	F	G	H	I	DEG.
-.002	3.135	-.006	5.115*	.153*	5.211*	.430	7.757*	.812	0.0
-.007	3.130	-.011	5.121*	.110	5.204*	.391	7.755*	.827	21.6
0.000	3.120*	0.000	5.109*	.153*	5.198*	.430	7.756*	.835*	46.8
-.007	3.153	-.024*	5.118*	.109	5.220*	.385	7.732*	.820	68.4
-.006	3.144	-.007	5.115*	.138	5.225*	.418	7.716*	.859*	90.0
-.005	3.125	-.011	5.126*	.142	5.230*	.418	7.759*	.808	111.6
-.002	3.117*	-.011	5.125*	.141	5.230*	.424	7.753*	.805	136.8
-.002	3.117*	-.011	5.120*	.137	5.232*	.418	7.757*	.804	158.4
0.000	3.124*	-.007	5.109*	.140	5.213*	.428	7.765*	.805	180.0
-.001	3.122*	-.007	5.105*	.144	5.200*	.426	7.769*	.809	201.6
0.000	3.112*	-.005	5.103*	.146	5.199*	.428	7.770*	.808	226.8
0.000	3.122*	-.007	5.102*	.147*	5.201*	.428	7.745*	.825	248.4
-.003	3.116*	-.011	5.104*	.141	5.204*	.429	7.747*	.817	270.0
-.002	3.135	-.013	5.115*	.132	5.207*	.415	7.741*	.815	291.6
-.004	3.131	-.012	5.110*	.143	5.206*	.425	7.753*	.817	316.8
-.001	3.130	-.010	5.101*	.139	5.200*	.423	7.740*	.820	338.4
0.000	3.153	0.000	5.126	.153*	5.232	.430	7.770	.859*	MAX.
-.007	3.112*	-.024*	5.101*	.109	5.198*	.385	7.716*	.804	MIN.

ENGINEERING RANGE

A	B	C	D	E	F	G	H	I	
0.000	3.185	0.000	5.190	.146	5.300	.433	7.868	.830	MAX.
-.020	3.125	-.020	5.130	.086	5.240	.383	7.808	.770	MIN.

57.6°

TABLE B-III

RSRM-20B AFT DOME JOINT PROFILE

A	B	C	D	E	F	G	H	I	DEG.
-.003	3.088*	-.011	5.114*	.140	5.225*	.420	7.710*	.836*	0.0
-.001	3.097*	-.013	5.114*	.141	5.227*	.425	7.735*	.828	21.6
-.003	3.090*	-.013	5.121*	.139	5.232*	.429	7.738*	.827	46.8
-.004	3.051*	-.015	5.117*	.145	5.228*	.422	7.712*	.820	68.4
-.004	3.059*	-.015	5.106*	.143	5.230*	.416	7.731*	.815	90.0
-.004	3.091*	-.018	5.106*	.131	5.222*	.410	7.710*	.826	111.6
-.006	3.082*	-.026*	5.106*	.115	5.230*	.396	7.728*	.817	136.8
-.003	3.062*	-.014	5.109*	.134	5.226*	.423	7.719*	.820	158.4
-.008	3.069*	-.025*	5.097*	.113	5.225*	.394	7.722*	.828	180.0
-.003	3.043*	-.014	5.096*	.139	5.220*	.410	7.720*	.823	201.6
-.004	3.065*	-.015	5.087*	.135	5.209*	.423	7.736*	.814	226.8 247°
-.003	3.074*	-.013	5.105*	.141	5.230*	.422	7.743*	.825	248.4
-.001	3.074*	-.012	5.116*	.142	5.237*	.424	7.746*	.820	270.0
-.001	3.066*	-.013	5.114*	.144	5.228*	.424	7.747*	.821	291.6
-.001	3.071*	-.010	5.118*	.142	5.226*	.428	7.746*	.815	316.8
.001	3.054*	-.010	5.119*	.141	5.227*	.421	7.723*	.823	338.4
-.001	3.097	-.010	5.121	.145	5.237	.429	7.747	.836*	MAX.
-.008	3.043*	-.026*	5.087*	.113	5.209*	.394	7.710*	.814	MIN.

ENGINEERING RANGE

A	B	C	D	E	F	G	H	I	DEG.
0.000	3.185	0.000	5.190	.146	5.300	.433	7.868	.830	MAX.
-.020	3.125	-.020	5.130	.086	5.240	.383	7.808	.770	MIN.

52
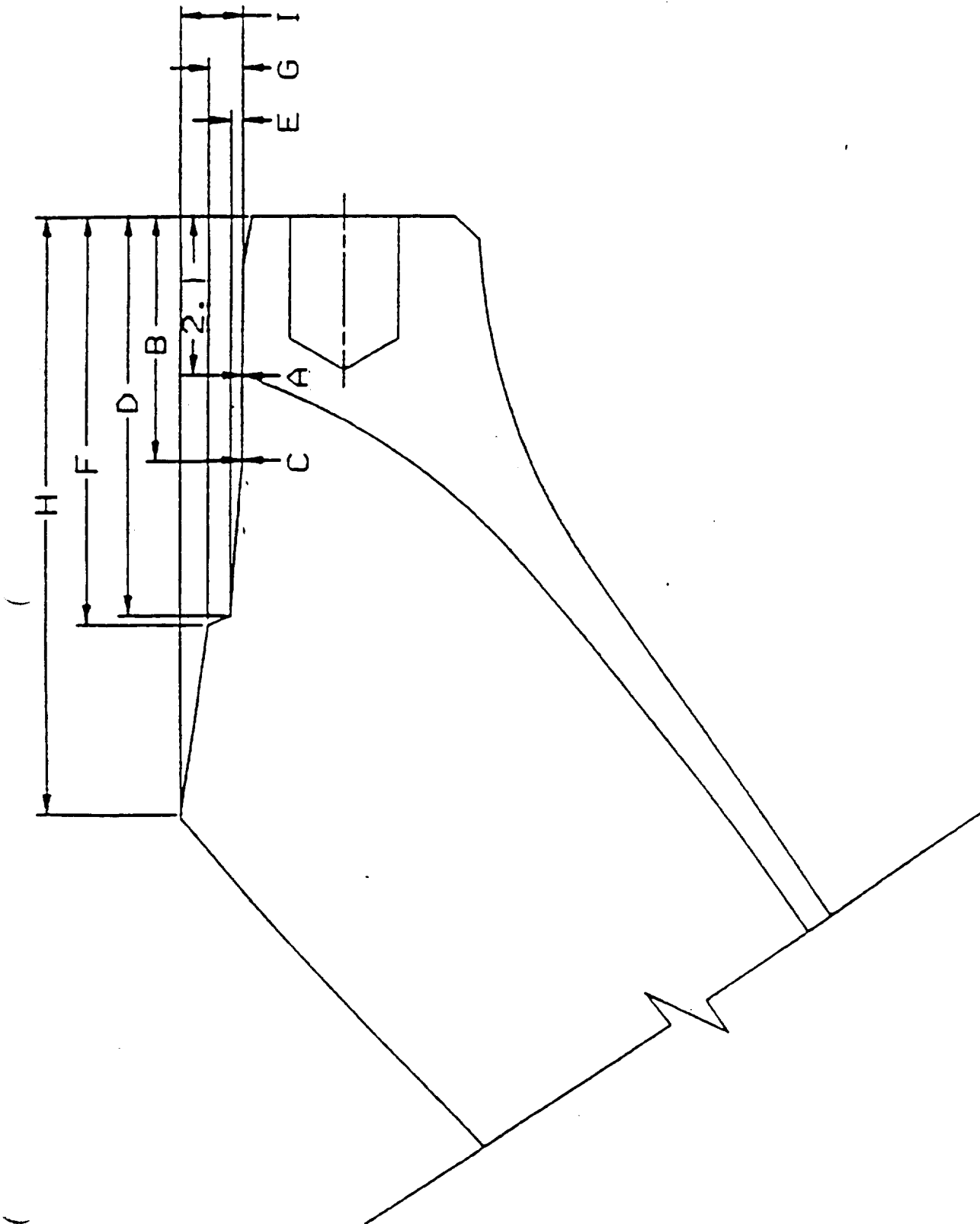
Figure B-13. RSRM Aft Dome Measurement Locations

53

TABLE B-IV

RSRM AFT DOME JOINT NBR PROFILE

	A	B	C	D	E	F	G	H	I
Max	0.000	3.214	0.019	5.204	0.173	5.374	0.483	7.875	0.878
Min	0.022	2.937	0.030	5.070	0.088	5.110	0.385	7.520	0.726
Ave	0.005	3.138	0.010	5.126	0.142	5.262	0.424	7.768	0.796
Eng Max	0.000	3.185	0.000	5.190	0.146	5.300	0.433	7.868	0.830
Eng Min	0.020	3.125	0.020	5.130	0.086	5.240	0.383	7.808	0.770

NBR standoff gap measurements at locations adjacent to the gas paths/sooted vent slots were taken during postflight assessment. These measurements were taken between the 'A' and 'C' locations on Figure B-13. The average of these measurements were: 20A at 57.6 degrees, 0.019 inch; 20A at 64.8 degrees, 0.030 inch; and 20B at 247 degrees, 0.038 inch. The engineering tolerance for this gap is 0.0 to 0.020 inch. The postflight measurements are either exceeding or on the high end of the current flight history. These measurements were taken by hand, rather than with the profile measuring tool used preflight, and may include more error than the preflight measurements in Table B-II and B-III.

4.3.2 Fixed Housing Joint Surface Profile

The fixed housing joint surface preflight measurements were not documented for RSRM-20 A & B, however, the engineering tolerances are listed in Table B-V and Figure B-14 for reference to the aft dome measurements.

Glass cloth phenolic standoff dimensions were taken at each of the gas path locations and all dimensions were within engineering tolerances, Figure B-15 and Table B-VI. A thermal analysis of the fixed housing has estimated that the housing diameter will expand at a rate of 0.0034 inch every 10 degrees due to thermal effects. An analysis of the aft dome did not estimate any significant thermal expansion.

4.3.3 Nozzle to Case Joint Bondline Gap Analysis

The thickness of the nozzle to case joint bondline can be analytically predicted by using the aft dome NBR joint measurements and the fixed housing drawing tolerances. The bondline thicknesses for RSRM-20 A & B are listed in Table B-VII and B-VIII and Figure B-16. These bondlines are within the current flight history, Table IX.

4.3.4 Vent Slots

Vent slots are cut into the aft dome NBR after the vulcanization process is complete. The vent slots were designed to start venting air trapped between the wiper O-ring and the polysulfide adhesive bead before a significant amount of pressure can build up due to the decreased joint volume caused by the assembly process. The engineering tolerance for the aft end of the vent slot, or the end that controls when vent is initiated, is 2.21 - 2.26 inches forward of the aft dome boss, Figure B-15 and Table B-VI. Cutting this end of the vent slot further aft in the NBR would allow venting to start earlier in the assembly process. Concerns raised during the RSRM redesign, of scoring the metal hardware during the vent slot fabrication dictated that the end of the groove be away from the metal. The forward end of the vent slot is located at 2.80 - 2.85 inches forward of the aft dome boss. This dimension allows the air venting to cease as late in the assembly process as possible and still have the wiper O-ring seated on a solid NBR surface.

Table B-VI and Figure B-15 list the forward and aft dimensions of the vent slots in the vicinity of the gas paths on RSRM-20 A & B. All dimensions were within the engineering tolerance.

<div align="center">

TABLE B-V

RSRM FIXED HOUSING JOINT ENGINEERING TOLERANCES

</div>

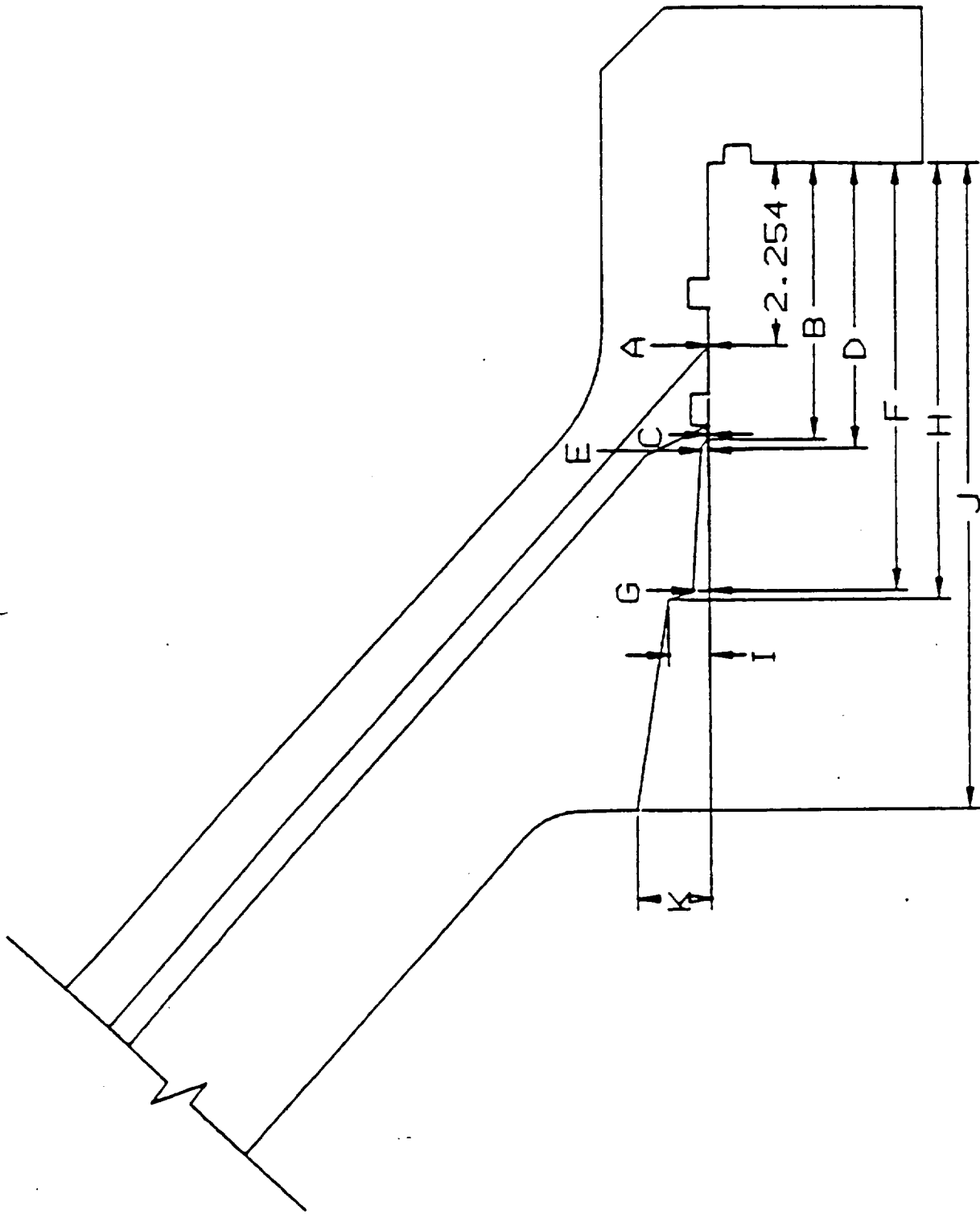|	A	B	C	D	E	F	G	H	I	J	K
Max	0.020	3.304	0.053	3.413	0.116	5.099	0.213	5.206	0.503	7.740	0.877
Min	0.000	3.298	0.027	3.406	0.090	5.084	0.188	5.190	0.480	7.660	0.862

Figure B-14. Fixed Housing Measurement Locations

NOZZLE TO CASE JOINT WIPER O-RING AND VENT SLOT DIMENSIONS

WIPER O-RING GROOVE

VENT SLOT

A

B

E

C

F

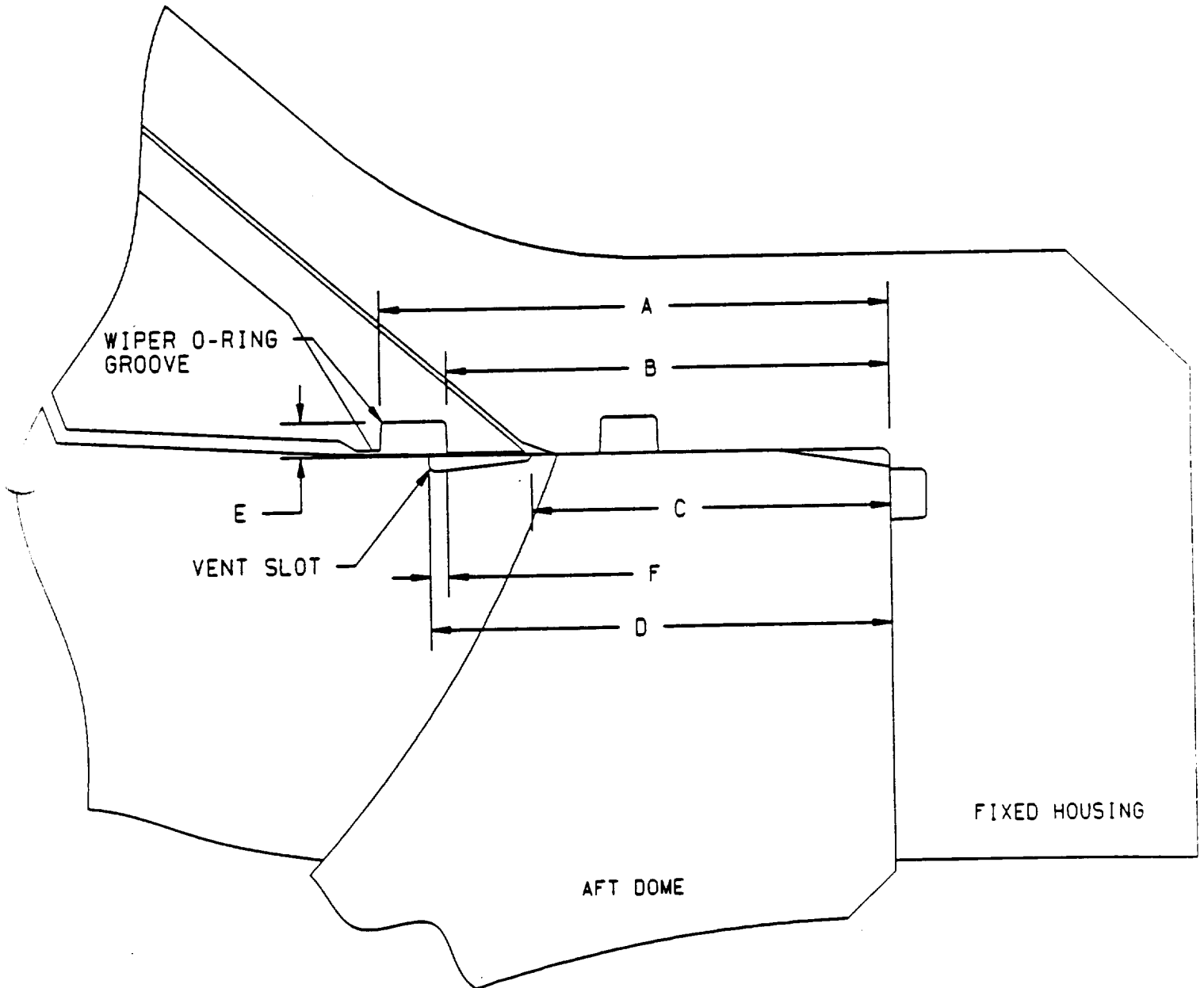D

AFT DOME

FIXED HOUSING

Figure B-15.   Nozzle-to-Case Joint Wiper O-Ring and Vent
Slot Dimensions

TABLE B-VI

NOZZLE-TO-CASE JOINT WIPER O-RING GROOVE AND VENT SLOT DIMENSIONS

NOZZLE-TO-CASE JOINT WIPER O-RING GROOVE AND VENT SLOT DIMENSIONS

MOTOR, LOCATION	DIMENSION						
	A	B	C	D	E*	F**	G***
20A, 57.6°	3.134	2.753	2.245	2.818	.201	.067	.009
20A, 64.8°	3.135	2.755	2.232	2.799	.201	.050	.009
20B, 247°	3.134	2.758	2.26****	2.809****	.196	.042****	.011
ALLOWABLE	3.152 3.113	2.777 2.738	2.26 2.21	2.85 2.80	.205 .195	.112 .023	.020 .000

* Maximum groove depth, measured from fixed housing metal surface.

** Vent slot/wiper O-ring groove overlap (D-B).

*** Not shown, radial distance between fixed housing CCP and metal surface, aft of the wiper O-ring groove.

**** Vent slot dimensions for 20B were taken at the slots adjacent to the 247° blowhole, at 244.8° and 252°.

TABLE B-VII

RSRM-20A NOZZLE-TO-CASE JOINT GAP ANALYSIS

POINT AA	POINT BB	POINT CC	POINT DD	POINT EE	POINT FF	POINT GG	POINT HH	DOME DEG.	NOZZLE DEG.
0.003	0.019	0.073	0.036*	0.027*	0.022*	0.050	0.052	0.0	MAX.
0.008	0.027	0.084	0.079	0.047	0.029*	0.087	0.037*	21.6	MAX.
0.000	0.013*	0.067*	0.036*	0.021*	0.010*	0.048	0.029*	46.8	MAX.
0.009	0.041	0.096	0.080	0.045	0.046	0.096	0.040*	68.4	MAX.
0.006	0.022	0.077	0.051	0.032*	0.039*	0.064	-.001*	90.0	MAX.
0.006	0.024	0.079	0.048	0.041*	0.044*	0.065	0.056	111.6	MAX.
0.003	0.024	0.078	0.049	0.041*	0.042*	0.059	0.058	136.8	MAX.
0.003	0.024	0.079	0.052	0.037*	0.046	0.065	0.060	158.4	MAX.
0.001	0.021	0.075	0.049	0.026*	0.024*	0.052	0.060	180.0	MAX.
0.002	0.020	0.075	0.044	0.021*	0.013*	0.053	0.057	201.6	MAX.
0.001	0.017	0.072	0.042*	0.018*	0.011*	0.050	0.058	226.8	MAX.
0.001	0.020	0.074	0.041*	0.017*	0.013*	0.051	0.037*	248.4	MAX.
0.004	0.024	0.078	0.047	0.021*	0.016*	0.050	0.046	270.0	MAX.
0.004	0.028	0.082	0.057	0.034*	0.023*	0.064	0.047	291.6	MAX.
0.005	0.025	0.080	0.046	0.026*	0.019*	0.054	0.046	316.8	MAX.
0.002	0.024	0.078	0.049	0.019*	0.014*	0.055	0.042	338.4	MAX.
0.023	0.046	0.100	0.062	0.050	0.045	0.075	0.079	0.0	MIN.
0.028	0.054	0.110	0.105	0.070	0.052	0.113	0.065	21.6	MIN.
0.020	0.039	0.094	0.062	0.044	0.033*	0.073	0.056	46.8	MIN.
0.029	0.067	0.123	0.106	0.068	0.069	0.121	0.068	68.4	MIN.
0.026	0.049	0.103	0.077	0.055	0.062	0.089	0.027*	90.0	MIN.
0.026	0.051	0.105	0.074	0.064	0.067	0.090	0.083	111.6	MIN.
0.023	0.050	0.105	0.075	0.063	0.065	0.084	0.085	136.8	MIN.
0.023	0.050	0.105	0.078	0.060	0.069	0.090	0.087	158.4	MIN.
0.021	0.047	0.102	0.075	0.049	0.047	0.078	0.087	180.0	MIN.
0.022	0.046	0.101	0.070	0.043*	0.036*	0.078	0.083	201.6	MIN.
0.021	0.044	0.098	0.068	0.041*	0.034*	0.076	0.084	226.8	MIN.
0.021	0.046	0.101	0.067	0.040*	0.036*	0.076	0.064	248.4	MIN.
0.024	0.050	0.105	0.073	0.044	0.039*	0.075	0.072	270.0	MIN.
0.024	0.054	0.109	0.083	0.057	0.046	0.090	0.074	291.6	MIN.
0.025	0.052	0.106	0.072	0.048	0.042*	0.080	0.073	316.8	MIN.
0.022	0.050	0.105	0.075	0.041*	0.037*	0.081	0.069	338.4	MIN.

SUMMARY OF GAP ANALYSIS

AA	BB	CC	DD	EE	FF	GG	HH		
0.000	0.013*	0.067*	0.036*	0.017*	0.010*	0.048	-.001*	MINIMUM GAP	
0.014	0.036	0.091	0.063	0.041*	0.037*	0.073	0.059	AVERAGE GAP	
0.029	0.067	0.123	0.106	0.070	0.069	0.121	0.087	MAXIMUM GAP	

ENGINEERING RANGE - BASED ON ENGINEERING DESIGN AFT DOME AND FIXED HOUSING

AA	BB	CC	DD	EE	FF	GG	HH		
0.000	0.014	0.069	0.044	0.044	0.045	0.042	0.042	MINIMUM GAP	
0.020	0.040	0.097	0.088	0.093	0.095	0.088	0.089	NOMINAL GAP	
0.040	0.067	0.124	0.132	0.143	0.145	0.135	0.137	MAXIMUM GAP	

MEASUREMENTS WHICH GENERATE THE GAPS

AA	BB	CC	DD	EE	FF	GG	HH		
A	B/C	B/C	D/E	D/E	F/G	F/G	H/I	DOME	
A	B/C	D/E	F/G	F/G	H/I	H/I	J/K	NOZZLE	

RSRM-20B NOZZLE-TO-CASE JOINT GAP ANALYSIS

POINT AA	POINT BB	POINT CC	POINT DD	POINT EE	POINT FF	POINT GG	POINT HH	DOME DEG.	NOZZLE DEG.
0.004	0.022	0.077	0.049	0.031*	0.038*	0.062	0.021*	0.0	MAX.
0.003	0.024	0.079	0.048	0.030*	0.039*	0.058	0.033*	21.6	MAX.
0.005	0.024	0.079	0.051	0.038*	0.042*	0.054	0.034*	46.8	MAX.
0.006	0.022	0.077	0.044	0.032*	0.041*	0.061	0.037*	68.4	MAX.
0.006	0.023	0.077	0.045	0.022*	0.045	0.067	0.045	90.0	MAX.
0.006	0.029	0.084	0.057	0.026*	0.039*	0.072	0.031*	111.6	MAX.
0.009	0.037	0.093	0.073	0.032*	0.051	0.087	0.043	136.8	MAX.
0.005	0.023	0.078	0.055	0.028*	0.038*	0.059	0.038*	158.4	MAX.
0.011	0.036	0.091	0.075	0.024*	0.047	0.088	0.031*	180.0	MAX.
0.005	0.021	0.076	0.049	0.014*	0.037*	0.071	0.036*	201.6	MAX.
0.006	0.024	0.079	0.052	0.007*	0.022*	0.057	0.047	226.8	MAX.
0.005	0.022	0.077	0.047	0.022*	0.042*	0.061	0.037*	248.4	MAX.
0.003	0.022	0.076	0.047	0.032*	0.048	0.060	0.042	270.0	MAX.
0.003	0.022	0.076	0.045	0.029*	0.040*	0.059	0.042	291.6	MAX.
0.002	0.020	0.074	0.047	0.034*	0.037*	0.054	0.047	316.8	MAX.
0.002	0.019	0.074	0.048	0.035*	0.040*	0.061	0.036*	338.4	MAX.
0.024	0.048	0.103	0.075	0.053	0.061	0.087	0.049	0.0	MIN.
0.023	0.051	0.105	0.074	0.053	0.062	0.083	0.060	21.6	MIN.
0.025	0.050	0.105	0.077	0.060	0.065	0.079	0.062	46.8	MIN.
0.026	0.049	0.103	0.070	0.054	0.063	0.086	0.065	68.4	MIN.
0.026	0.049	0.104	0.071	0.045	0.067	0.092	0.072	90.0	MIN.
0.026	0.056	0.110	0.083	0.049	0.062	0.097	0.059	111.6	MIN.
0.029	0.064	0.119	0.099	0.054	0.074	0.112	0.070	136.8	MIN.
0.025	0.050	0.105	0.081	0.051	0.061	0.084	0.066	158.4	MIN.
0.031	0.062	0.118	0.101	0.047	0.070	0.113	0.059	180.0	MIN.
0.025	0.048	0.103	0.075	0.037*	0.060	0.096	0.063	201.6	MIN.
0.026	0.051	0.105	0.078	0.030*	0.045	0.082	0.074	226.8	MIN.
0.025	0.049	0.104	0.073	0.044	0.065	0.086	0.064	248.4	MIN.
0.023	0.048	0.103	0.073	0.054	0.071	0.085	0.070	270.0	MIN.
0.023	0.048	0.103	0.071	0.052	0.063	0.084	0.069	291.6	MIN.
0.022	0.046	0.101	0.073	0.056	0.060	0.080	0.074	316.8	MIN.
0.022	0.045	0.100	0.074	0.058	0.063	0.087	0.063	338.4	MIN.

SUMMARY OF GAP ANALYSIS

0.002	0.019	0.074	0.044	0.007*	0.022*	0.054	0.021*	MINIMUM GAP
0.015	0.038	0.092	0.065	0.038*	0.052	0.077	0.051	AVERAGE GAP
0.031	0.064	0.119	0.101	0.060	0.074	0.113	0.074	MAXIMUM GAP

ENGINEERING RANGE

0.000	0.014	0.069	0.044	0.044	0.045	0.042	0.042	MINIMUM GAP
0.020	0.040	0.097	0.088	0.093	0.095	0.088	0.089	NOMINAL GAP
0.040	0.067	0.124	0.132	0.143	0.145	0.135	0.137	MAXIMUM GAP

MEASUREMENTS WHICH GENERATE THE GAPS

A	B/C	B/C	D/E	D/E	F/G	F/G	H/I	DOME
A	B/C	D/E	F/G	F/G	H/I	H/I	J/K	NOZZLE
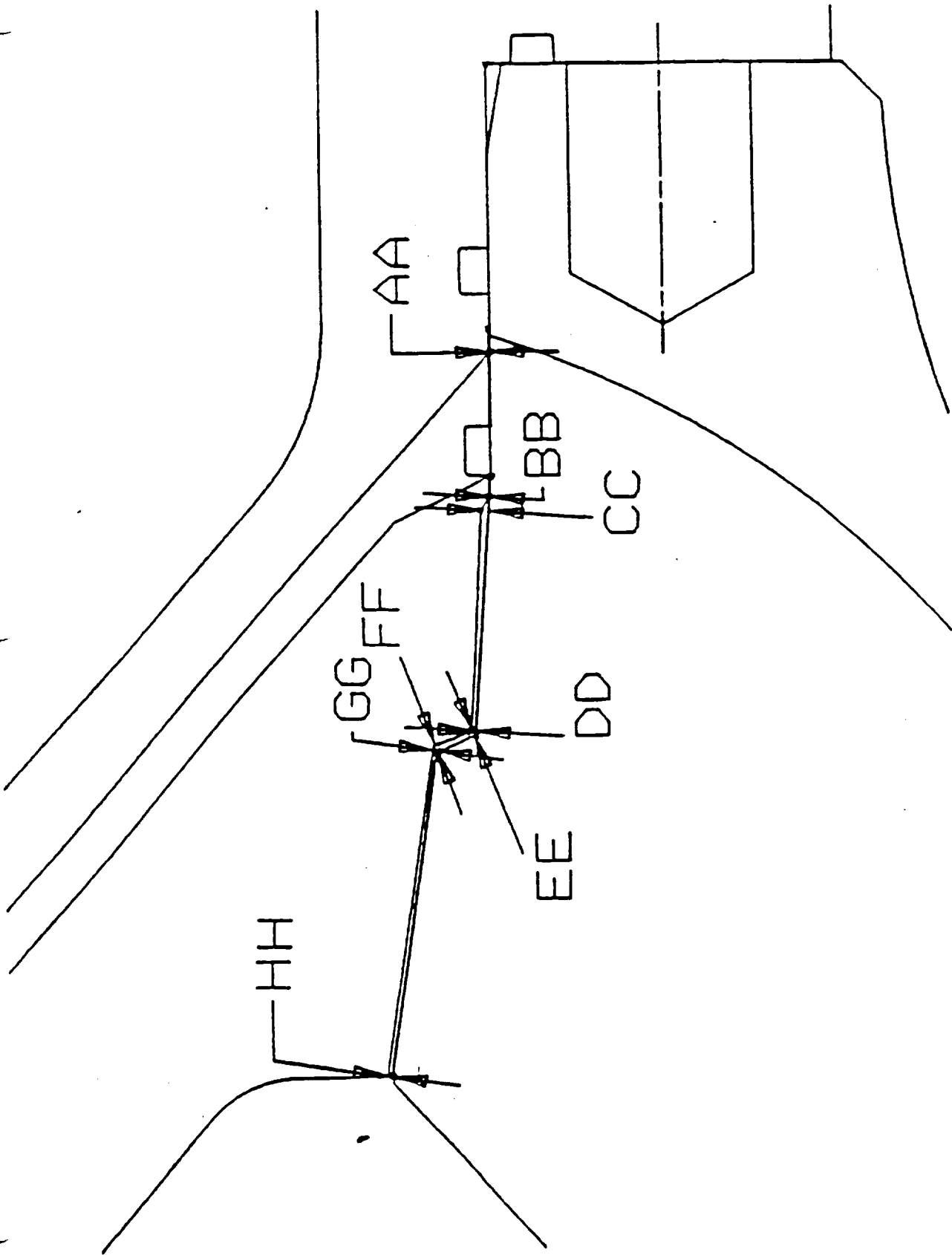
Figure B-16. RSRM Nozzle-to-Case Joint Gap Locations

62

TABLE B-IX

RSRM NOZZLE-TO-CASE JOINT GAP FLIGHT HISTORY

	AA	BB	CC	DD	EE	FF	GG	HH
Max	-0.016*	-0.003*	6.053	0.017	-0.012*	-0.068*	0.000	-0.015*
Avg	0.017	0.038	6.092	0.061	0.052	0.082	0.077	0.084
Min	0.043	0.073	0.141	0.129	0.143	0.201	0.125	0.156

*These gap thicknesses were calculated analytically from measurements taken from unassembled hardware, therefore, negative measurements would become interference fits, or 0.000 bond gap, when assembled

4.3.5 Assembled Wiper O-Ring Configuration

The configuration of the area surrounding the wiper O-ring at the gas path/sooted vent slot locations was plotted using measurements taken from the hardware during the postflight inspection, Figure B-17, B-18 and B-19. These plots assume that the nozzle has been seated, all bolts have been tightened to the final torque requirement and the wiper O-ring has not yet caused an indentation into the NBR. These figures illustrate that the hardware (wiper O-ring, wiper groove, NBR, GCP and vent slots) in these areas were all within the engineering tolerance. The wiper O-ring had passed over the vents slots and was resting on a solid NBR surface.

The wiper O-ring was not designed to be a pressure seal, although subscale and fullscale testing has demonstrated that it often will seal motor chamber pressure. It was added to the nozzle-to-case joint during the RSRM redesign to prevent polysulfide from inhibiting the sealing performance of the primary O-ring. The wiper O-ring was also designed to function as a thermal barrier to prevent hot gas degradation of the primary O-ring and joint metal hardware. The RSRM-20 wiper o-rings performed as designed. Polysulfide did not reach the primary O-ring and no hot gas degradation was observed on the primary O-ring or on the joint metal hardware. The RSRM-20B wiper O-ring did seal against motor chamber pressure, while the RSRM-20A wiper leaked for approximately 0.15 seconds before resealing.

4.3.6 Polysulfide Interference with the Wiper O-Ring Footprint

During the postflight inspections, polysulfide is commonly observed on the forward side of the wiper O-ring and often under the wiper at vent slot locations. This is a result of the wiper O-ring wiping the polysulfide away from the primary O-ring sealing surface during the assembly. This condition could affect the O-ring footprint and may have contributed to the RSRM-20A wiper blowby.

4.3.7 NBR Indentation Due to the Wiper O-Ring

NBR relaxation due to the wiper O-ring was evaluated using finite element analysis with ASF-NBR storage material properties taken from TWR-18011 Supplement B and wiper O-ring properties supplied by Joints and Seals. The bottom of the wiper O-ring was deflected radially through a distance of .0612-inches. This deflection distance was calculated based on the amount that the wiper O-ring would overlap the NBR rubber after the mating of the nozzle assembly and the aft case segment. The analysis indicated an NBR indentation of 0.038 inches due to the radial deflection of the wiper O-ring (Figures B-20 and B-21). Figure B-22 shows the radial deflection of the NBR rubber along the edge that contacts the wiper O-ring. The assembled gap between the fixed housing and the aft dome, based on a tolerance study of the joint, can range from 0.000 to 0.032 inch. The nozzle-to-case joint has a dynamic gap opening of approximately 0.021 inch due to joint pressurization. Due to the potentially large total gap (assembly, relaxation, dynamic), the tracking factor of the wiper O-ring could be less than 1.0.
Based on the above, the wiper O-ring cannot be guaranteed to contain pressure.

Based on the thermal analysis performed for the RSRM-20A gas path (Section 4.6) and the lack of material degradation observed aft of the
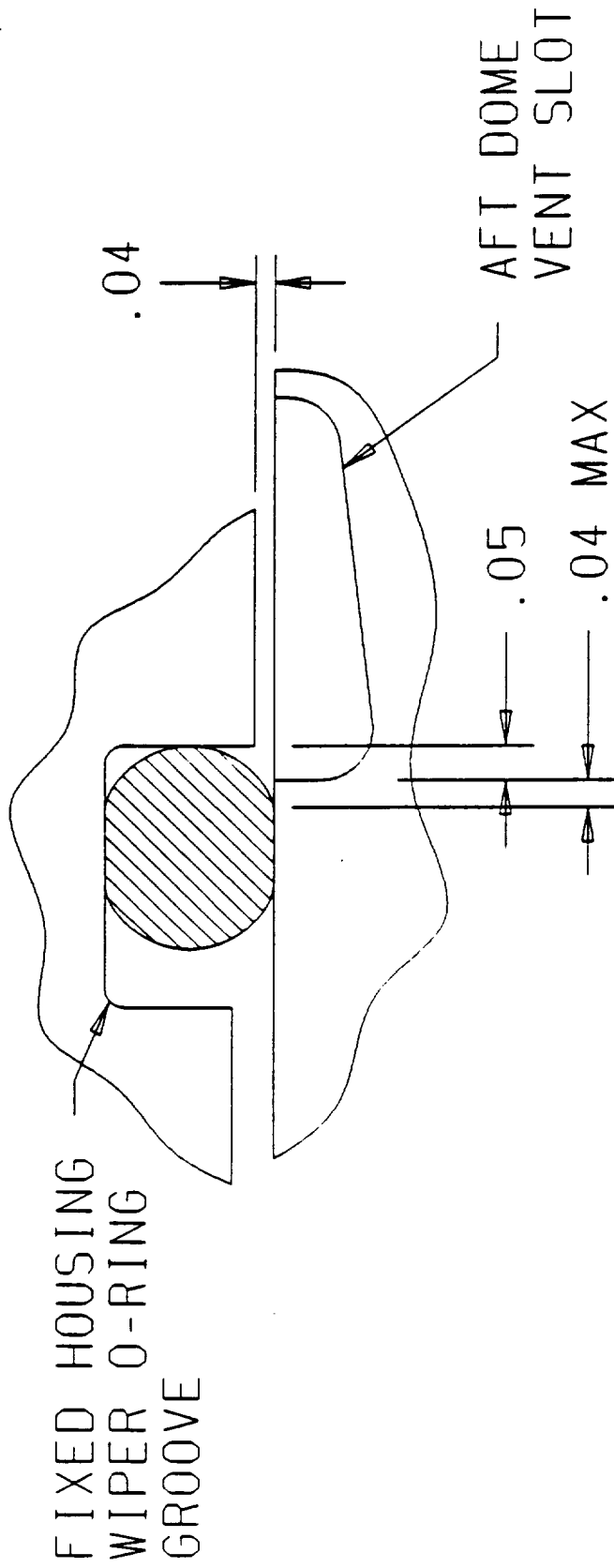
RSRM 20A, ACTUAL WIPER O-RING CONFIGURATION AT 57.6° (

FIXED HOUSING
WIPER O-RING
GROOVE

AFT DOME
VENT SLOT

.03

.07

.02 MAX
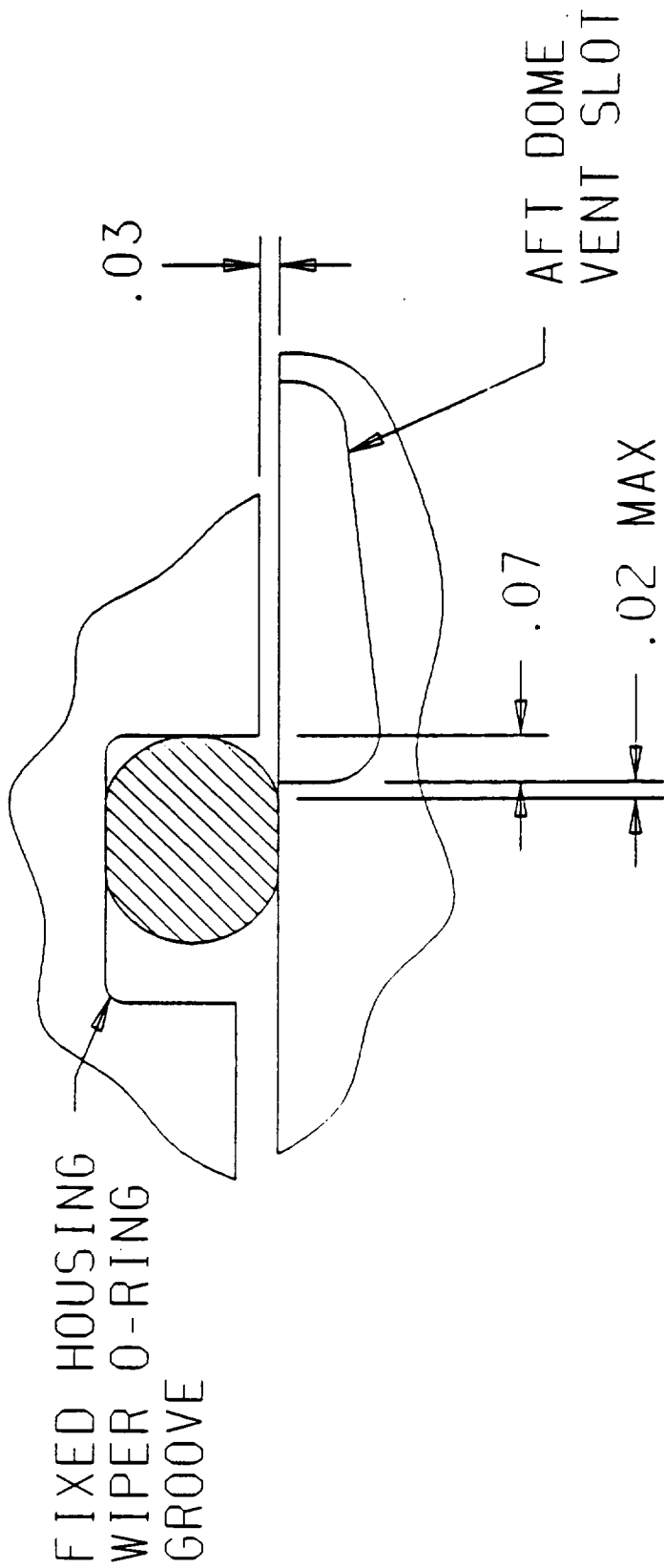
MAX O-RING GROOVE WIDTH: .381
MAX O-RING GROOVE DEPTH, FROM F.H. METAL SURFACE: .201
MIN O-RING DIAMETER: .2731
O-RING DEFORMED LENGTH: .303 - .307
O-RING FOOTPRINT: .130 - .134

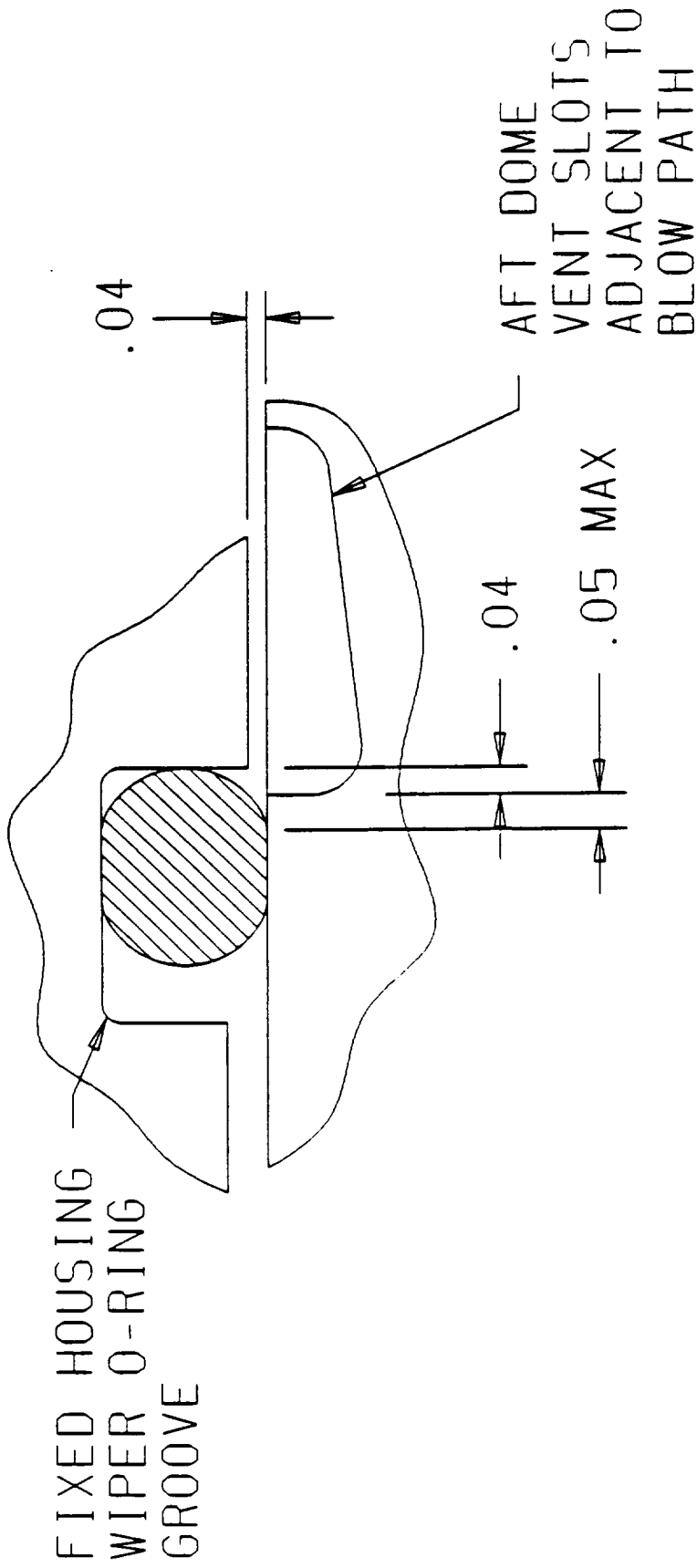Figure B-17. Assembled Wiper O-Ring Configuration

RSRM 20A, ACTUAL WIPER O-RING CONFIGURATION AT 64.8° (

FIXED HOUSING
WIPER O-RING
GROOVE

AFT DOME
VENT SLOT

.04

.05

.04 MAX

MAX O-RING GROOVE WIDTH: .380
MAX O-RING GROOVE DEPTH, FROM F.H. METAL SURFACE: .201
MIN O-RING DIAMETER: .2731
O-RING DEFORMED LENGTH: .297 - .301
O-RING FOOT PRINT: .115 - .120

Figure B-18. Assembled Wiper O-Ring Configuration

RSRM 20B, ACTUAL WIPER O-RING CONFIGURATION AT 247.0° VENT SLOT DIMENSIONS ARE AVERAGED FROM ADJACENT VENT SLOTS AT 244.8° AND 252°.

FIXED HOUSING
WIPER O-RING
GROOVE

.04

.04

.05 MAX

AFT DOME
VENT SLOTS
ADJACENT TO
BLOW PATH

MAX O-RING GROOVE WIDTH: .376
MAX O-RING GROOVE DEPTH, FROM F.H. METAL SURFACE: .196
MIN O-RING DIAMETER: .2721
O-RING DEFORMED LENGTH: .297 - .301
O-RING FOOTPRINT: .117 - .122

Figure B-19.   Assembled Wiper O-Ring Configuration

SDRC I-DEAS VI: FE_Modeling_&_Analysis

DISPLACEMENTS   STEP 1, INC 6

LOAD SET: 6 -
DISPLACEMENT - NORMAL MIN: 0.00 MAX: 0.061149
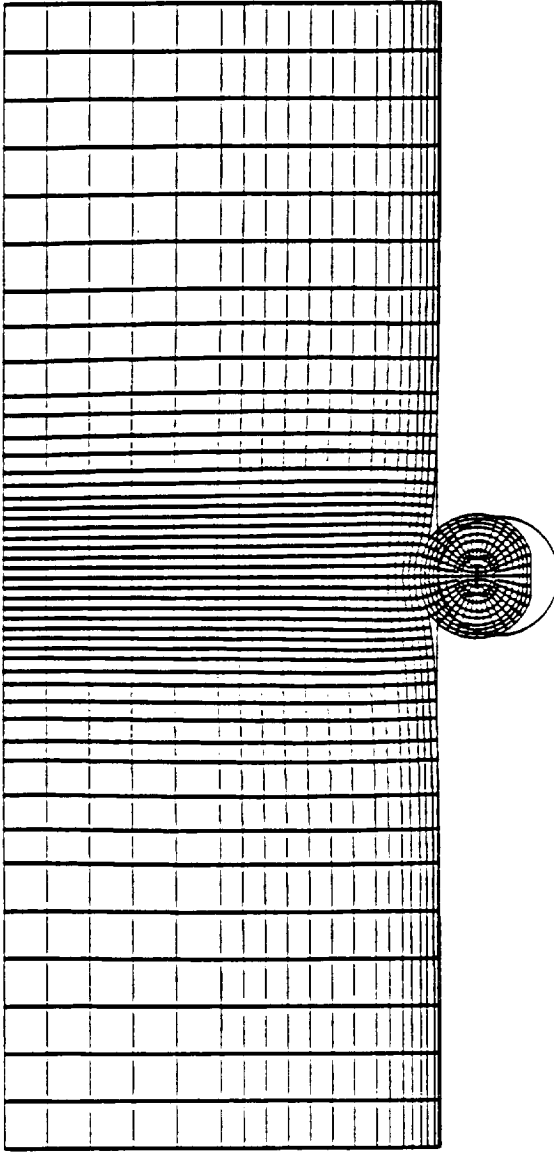
Figure B-20.   NBR Indentation
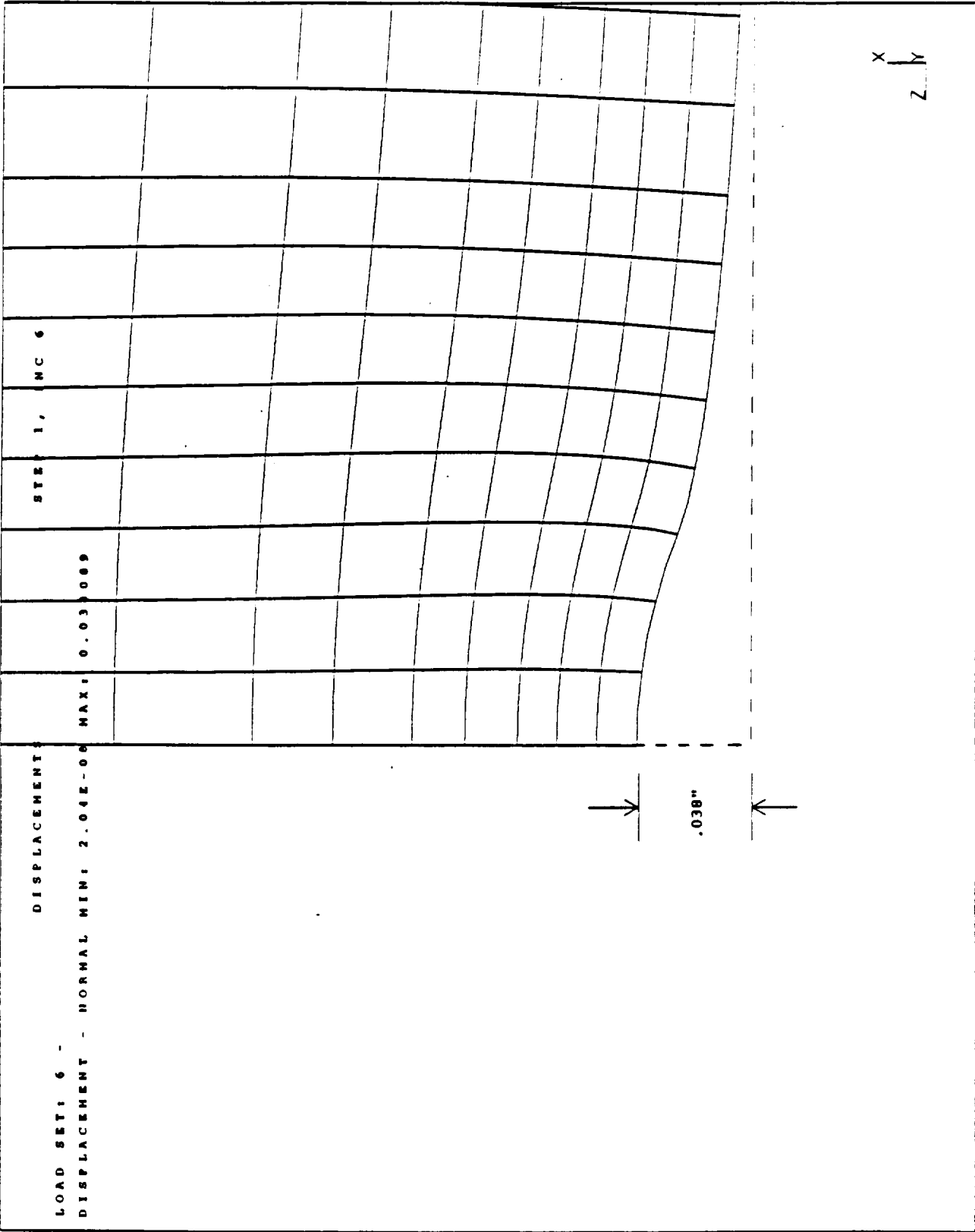
Figure B-21. NBR Indentation
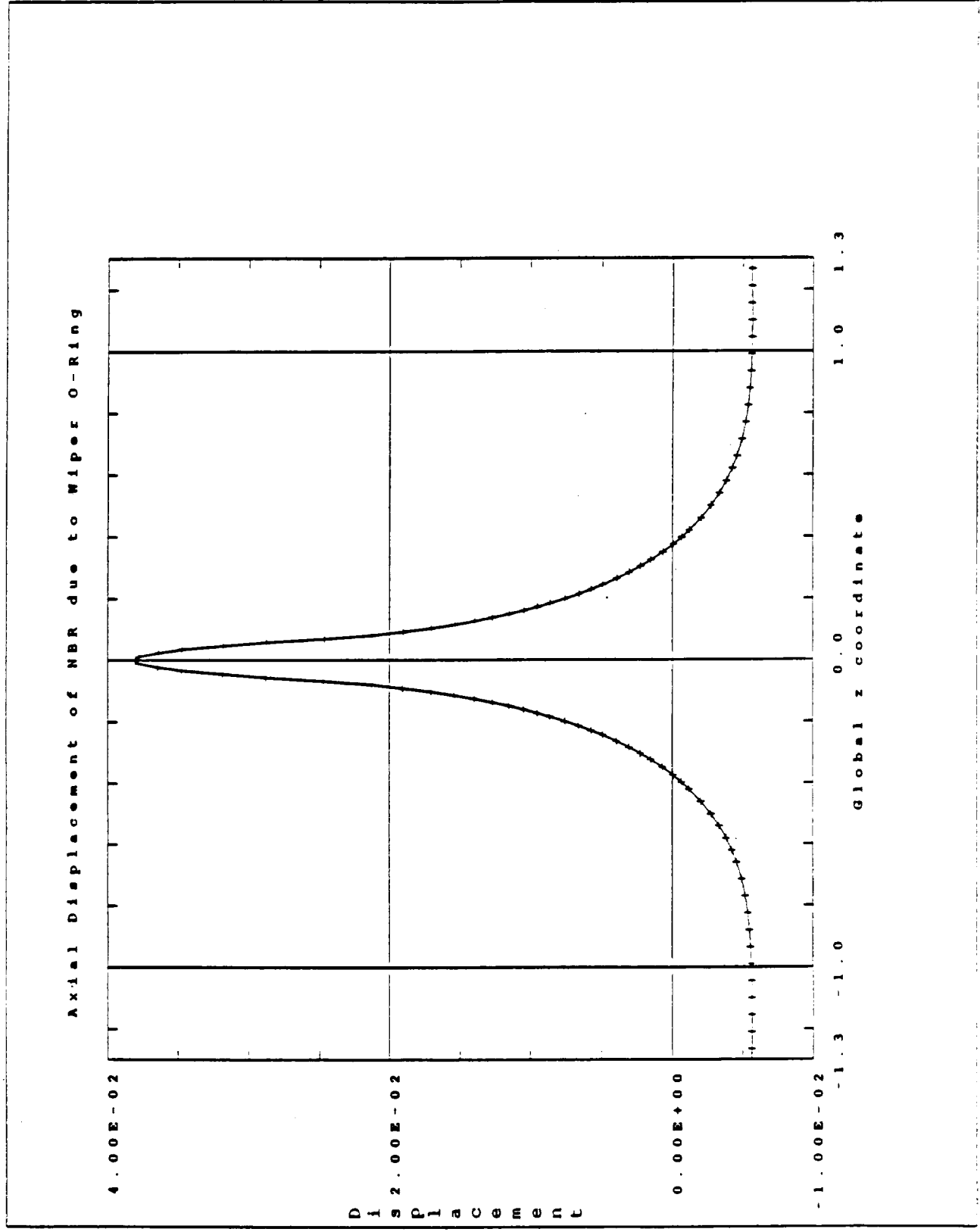
Figure 5-22. NBR Indentation

wiper O-ring during the postflight inspection, it has been determined that the wiper O-ring blowby that occurred in this joint was short lived, lasting on the order of 0.15 seconds before resealing. A probable scenario on why the O-ring leaked and then resealed is based on the indentation made in the NBR by the wiper O-ring. Due to the NBR indentation, the wiper O-ring did not have sufficient sealing capability when the joint rotated at ignition. The wiper O-ring would have been blown to the aft edge of the NBR indentation and wedged between the aft sides of the O-ring groove and the NBR indentation before resealing. The blowby would have occurred during time the O-ring was shifting.

4.3.8 Wiper O-Ring Leak Check

Table 10 lists the results of the nozzle to case joint leak check performed preflight. All leak checks were within the engineering allowable limits. It was determined by engineering that the leak checks were not a factor in the formation of the gas paths, because these checks were performed without anomalies and the primary to wiper leak check is performed after the completion of the polysulfide cure.

4.4 Nozzle to Case Joint Assembly CAD Analysis

4.4.1 Screed Design

The screed used to apply the polysulfide to the RSRM nozzle to case joint was designed with the goal to apply a sufficient amount of polysulfide to fill the widest joint gap and to trap the least amount of air possible during the assembly. The polysulfide selected during the motor redesign period (STW4-3311) has a tendency to slump and shrink back from the screed during the assembly process. This results in a smaller adhesive bead located further forward on the aft dome than the opening in the screed. These factors were considered in the screed design. A CAD analysis has shown that the lot to lot variation in slump and shrink back seen with STW4-3311 has little affect on the distance from seating when the fixed housing first contacts the polysulfide (see Section 4.4.2). Testing has demonstrated that the replacement polysulfide (STW4-3829), which is currently scheduled for use on RSRM-30, slumps much less and shrinks back slightly more than STW4-3311. Even though STW4-3829 has been successfully qualified for use on flight motor using the current screed, the design of the screed should be reevaluated to determine if any improvements can be made for the new polysulfide.

4.4.2 Joint Assembly Using the Nominal Configuration

A CADCAM analysis of the RSRM nozzle to case joint assembly was performed using nominal dimensions, concentric hardware and a polysulfide bead profile typical of the adhesive observed at the time of assembly. The analysis showed that the wiper O-ring would contact the aft dome metal boss at a distance of 2.65 inches from seating, Figure B-23. The primary O-ring would contact the aft dome metal boss at 1.29 inches from seating, Figure B-24. At this point in the assembly, the aft end of the joint is sealed by the O-rings, but air in the joint can still vent in the forward direction.

At 0.80 inch from seating, the step in the fixed housing first contacts the polysulfide bead, Figure B-25. The air between the wiper O-ring and the polysulfide bead becomes trapped. (If the adhesive bead

TABLE B-X

20A/20B NOZZLE-TO-CASE JOINT
LEAK TEST RESULTS

PRESSURE (PSIG)	ALLOWABLE LEAK RATE (SCCS)	ACTUAL LEAK RATE LEFT-HAND (SCCS)	ACTUAL LEAK RATE RIGHT-HAND (SCCS)
920 P-S	0.0840	0.0224	0.0060
30 P-S	0.0082	-0.0015	-0.0015
25 P-W	5 PSI/ 5 MIN	0.213 PSI	0.192 PSI
0 P-S*	0.0082	0.0003	0.0001
Stat-0-Seal	0 BUBBLE/SEC	NO LEAK	NO LEAK

P-S PRIMARY-TO-SECONDARY CAVITY; P-W PRIMARY-TO-WIPER CAVITY
*   MONITOR PRESSURE RISE IN P-S CAVITY

WIPER O-RING CONTACTS AFT DOME

2.65
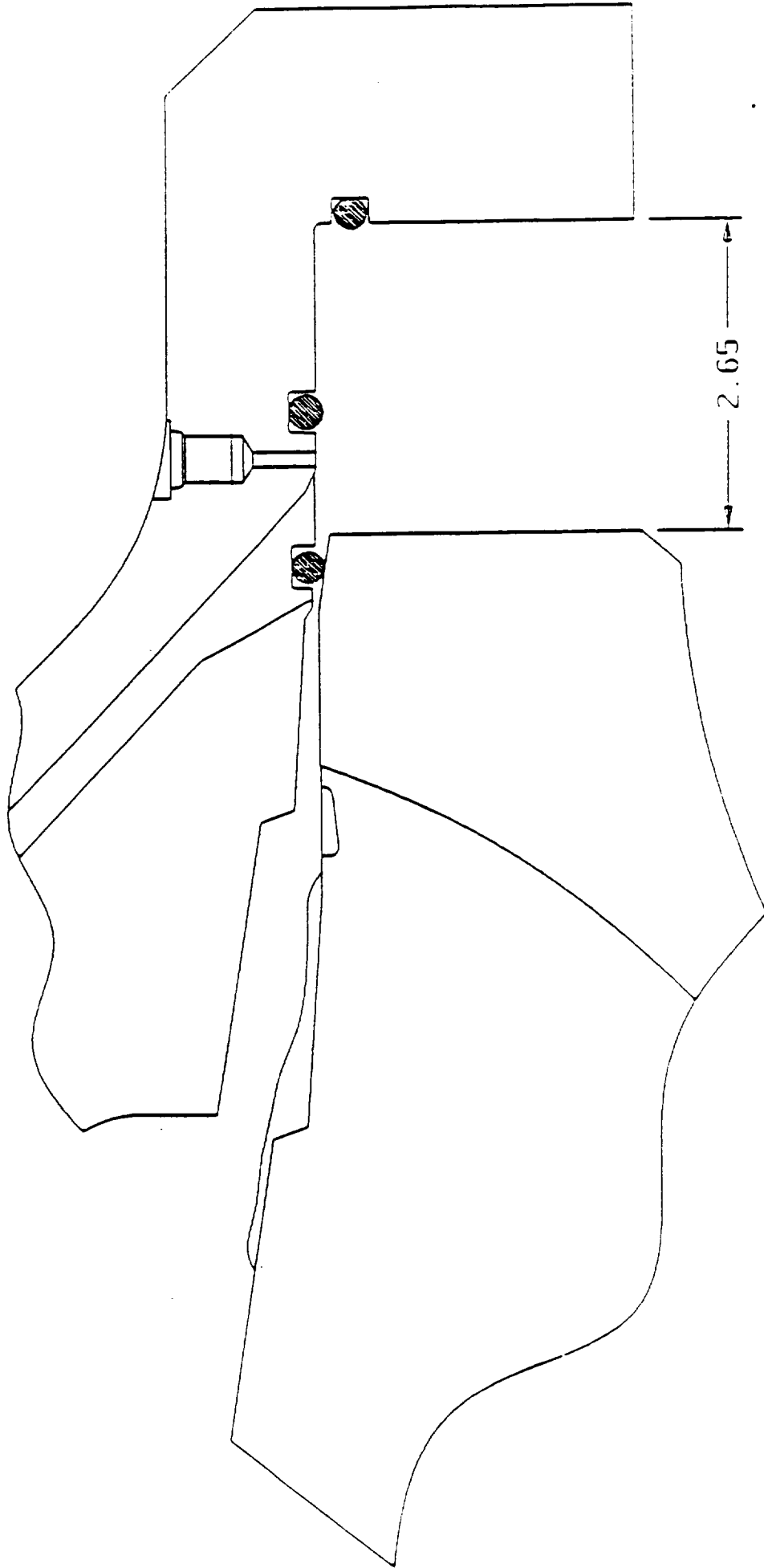
Figure B-23. Nozzle-to-Case Joint Assembly

73

PRIMARY O-RING CONTACTS AFT DOME

1.29
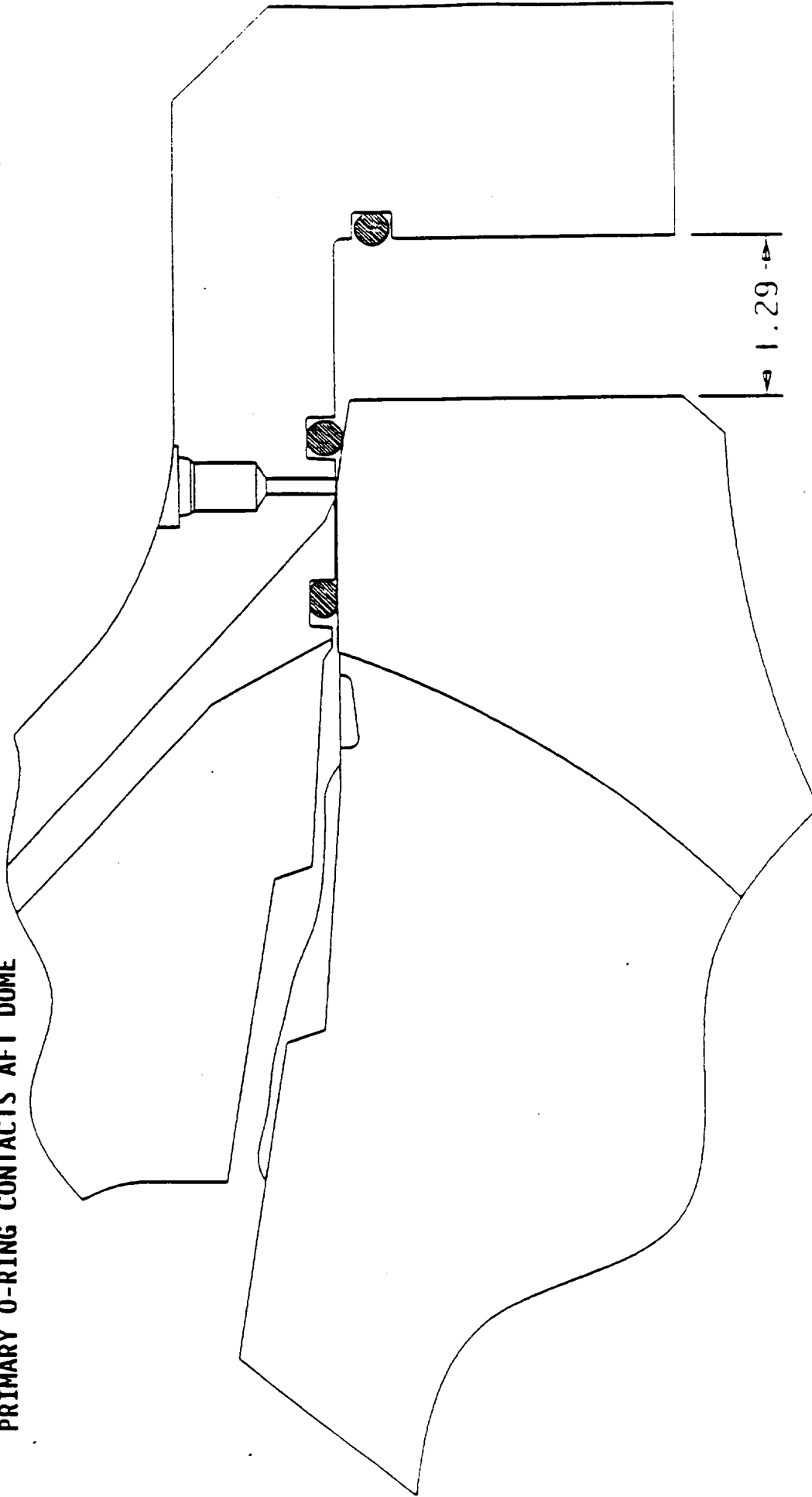
Figure B-24. Nozzle-to-Case Joint Assembly

74

0.8 GAP BETWEEN HOUSING AND DOME, FIXED HOUSING CONTACTS POLYSULFIDE

.80
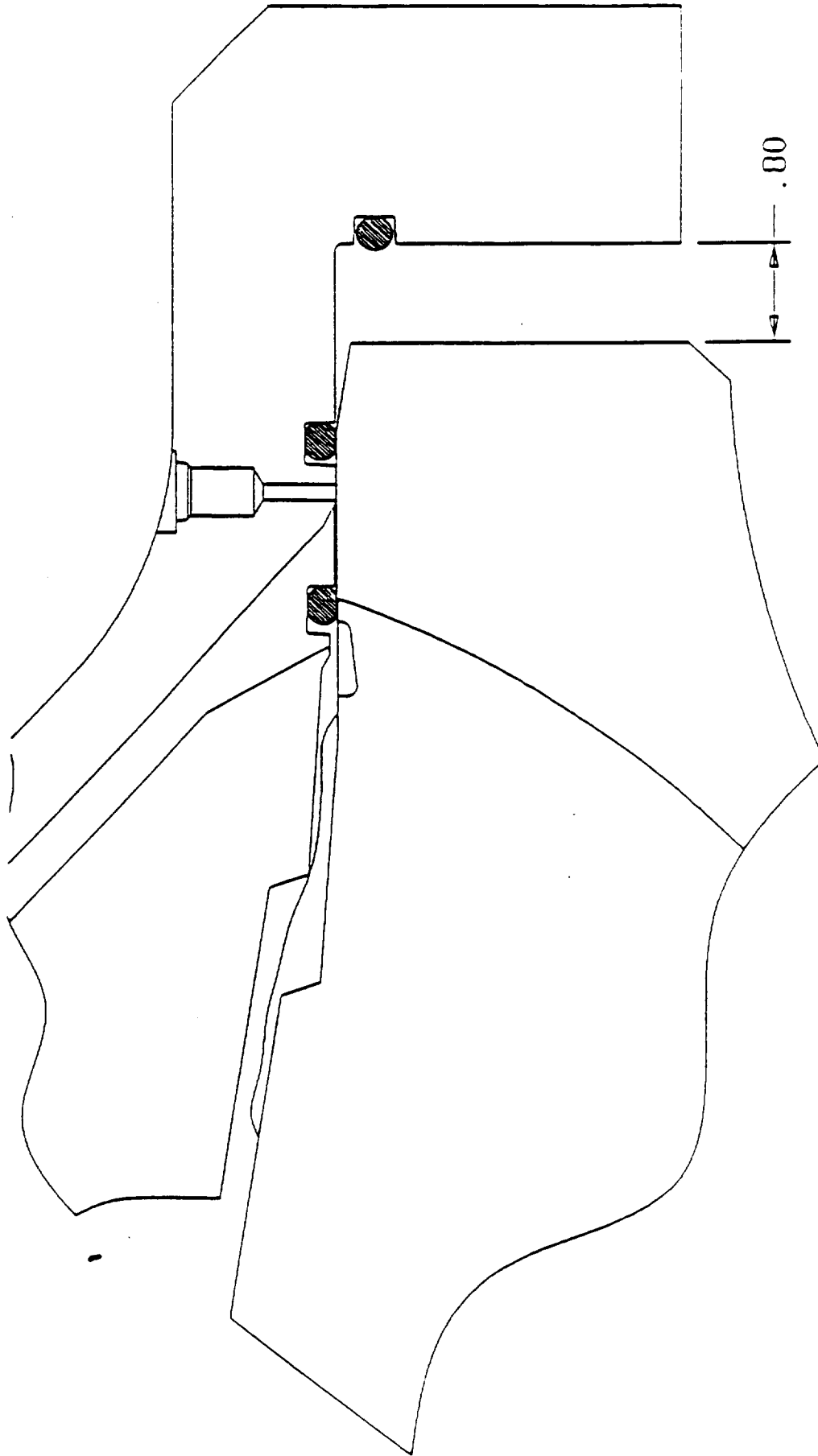
Figure B-25. Nozzle-to-Case Joint Assembly

75

remained the same shape as the screed, i.e. no slumping, then the fixed housing would first contact the bead at the same point in the assembly, Figure B-26. This demonstrates that the variation in slump commonly seen with the current polysulfide has little effect on when the fixed housing first contacts the adhesive bead, because the edge of the adhesive that is first contacted by the fixed housing does not slump significantly, due to the close proximity to the aft dome surface.)

Between 0.80 inch and 0.61 inch from seating, (where the wiper O-ring passes over the vent slots and venting begins, Figure B-27) the trapped air is either building up pressure or is venting through the polysulfide. Assuming that no air vents through the polysulfide, then the pressure differential due to the decreased volume experienced in this phase of the assembly would be equal to 1.15 psi.

Between 0.61 inch and 0.18 inch from seating (where the air flow through the vent slots becomes restricted by the wiper O-ring, Figure B-28) air is venting freely through the vent slots and out the vent port. These dimension are substantiated by the flight motor assembly history, where monitoring of the air flow out of the vent port usually begins at the 0.60 inch incremental step and ends at the 0.15 inch incremental step. During this venting period, any gas paths which may have formed in the polysulfide prior to air flowing through the vent slots should be filled in by the mechanical mixing caused by the joint assembly. By the point in the assembly process where the wiper O-ring moves forward of the vent slots, all trapped air should be evacuated from the joint and many of the vent slots have begun to fill with polysulfide (assuming nominal dimensions and concentric hardware). Between this point (0.18 gap) and seating, the wiper O-ring moves onto a solid NBR surface, Figure B-29. No significant changes should occur in the joint during this period if all the air has been evacuated.

4.4.3 Joint Assembly Using the Worst Case Configuration

A nozzle to case joint assembly was simulated on cadcam using worst case hardware dimensions (smallest axial dome assembly, largest axial fixed housing assembly) deflected baffle and metal to metal contact at the aft end of the joint) and the largest polysulfide profile measured. This configuration was modeled to determine the earliest contact between fixed housing assembly and polysulfide. This analysis showed that the step of the fixed housing phenolic would contact the polysulfide bead at approximately 1.45 inch from seating, Figure B-30. This contact could occur only in localized areas because there would be other areas of no metal/metal contact with larger joint gaps.

Using the same worst case hardware and adhesive profile, the fixed housing would first contact the polysulfide bead full circumference at 0.87 inch from seating, Figure B-31. The difference in distance from seating between this case and the nominal case is primarily due to hardware axial dimensional differences and not polysulfide slump profiles. In this worst case, more air would be trapped in the joint than in the nominal case and more venting would be required to evacuate the air.

4.5 Restricted Venting

There are several undesirable conditions that can occur during the nozzle to case joint assembly process that could potentially contribute to   76

JOINT GAP (.80) WHEN FIXED HOUSING FIRST CONTACTS POLYSULFIDE. IF
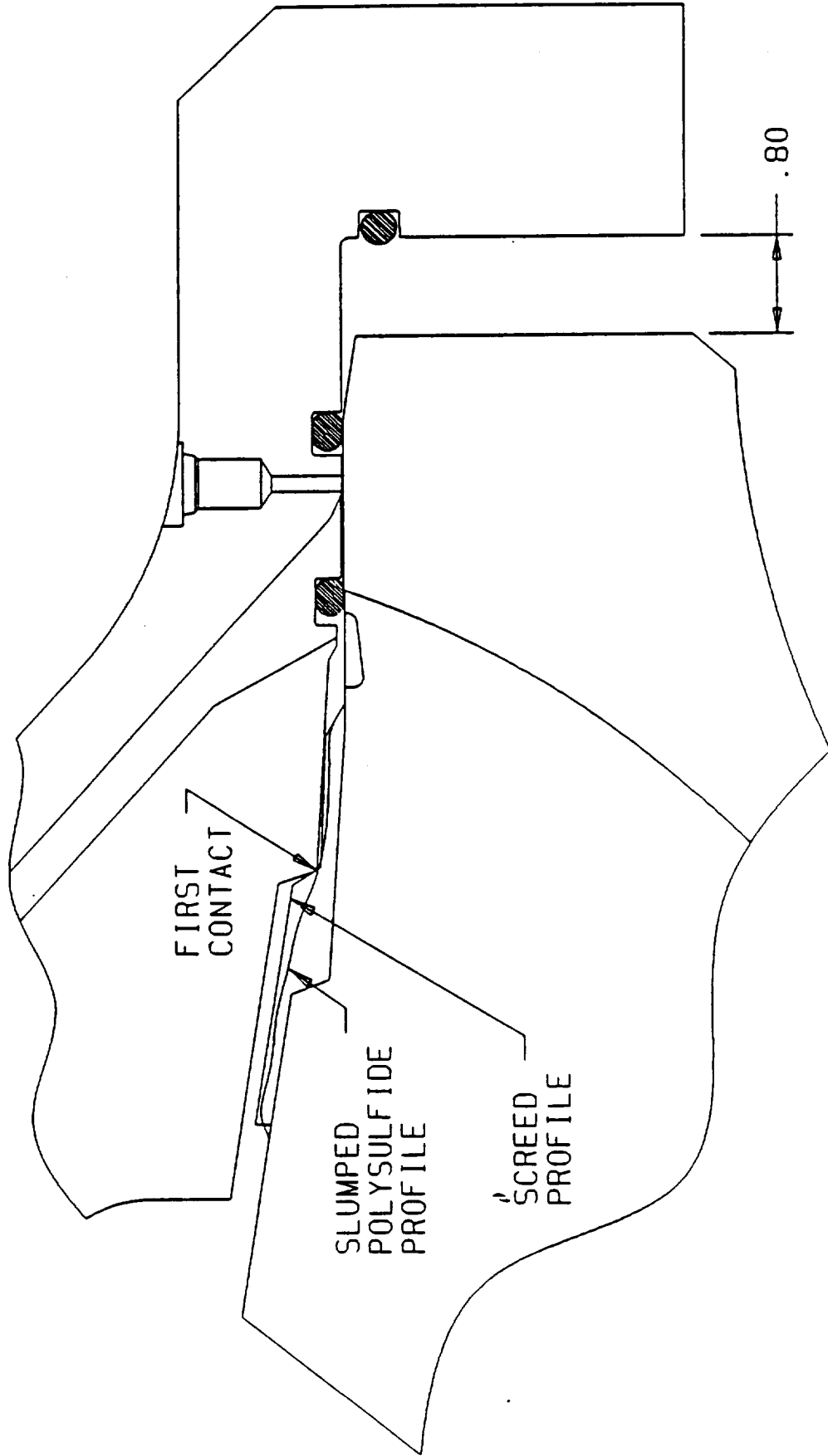POLYSULFIDE MAINTAINED THE PROFILE OF THE APPLICATION SCREED.

.80

FIRST
CONTACT

SLUMPED
POLYSULFIDE
PROFILE

SCREED
PROFILE

Figure B-26. Nozzle-to-Case Joint Assembly

77

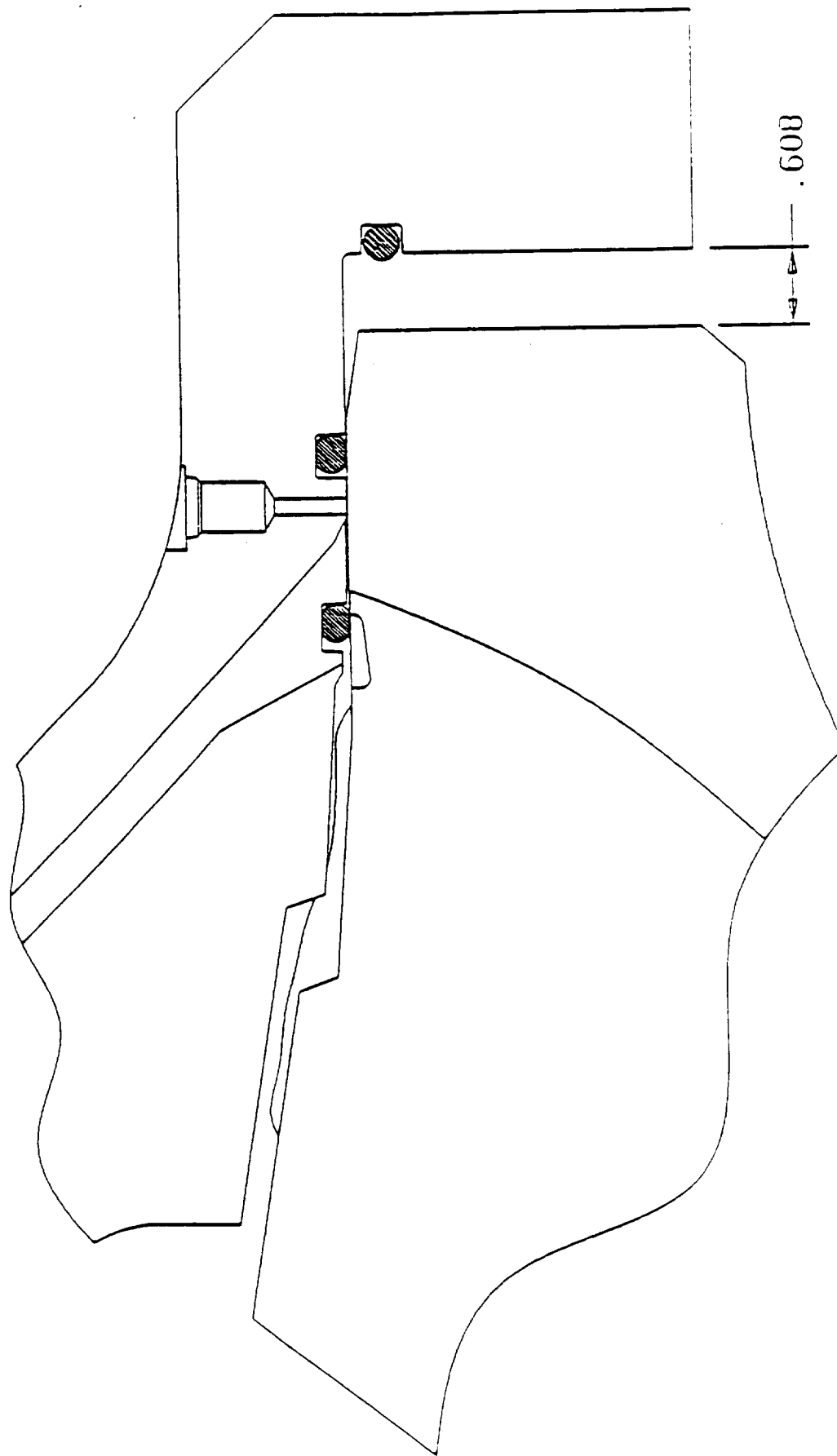**AFT EDGE OF WIPER O-RING PASSES OVER AFT EDGE OF VENT SLOT, VENTING STARTS**

.608

Figure B-27. Nozzle-to-Case Joint Assembly

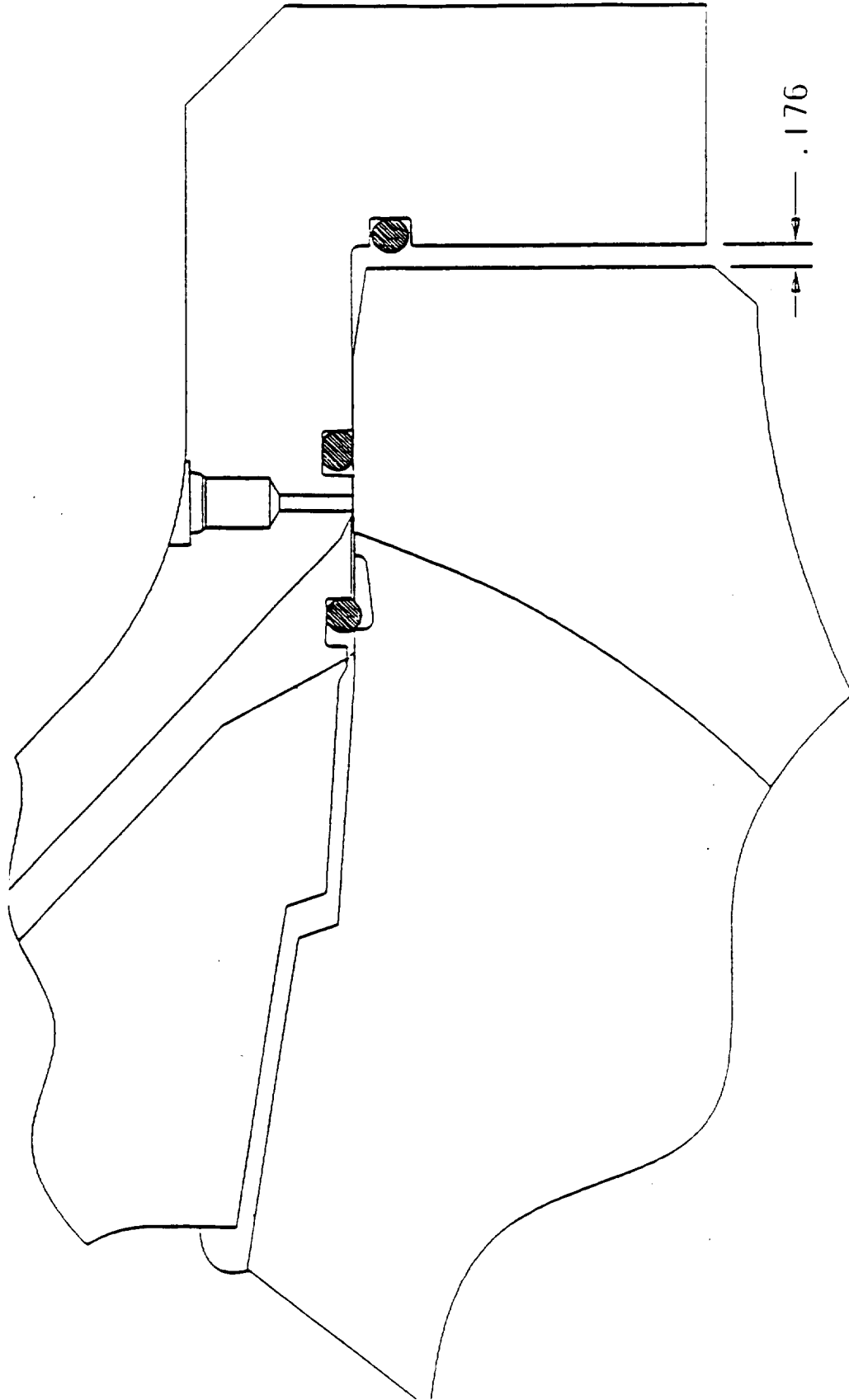# WIPER O-RING CONTACTS FORWARD EDGE OF VENT SLOT, VENTING STOPS

.176

Figure B-28. Nozzle-to-Case Joint Assembly

79

JOINT SEATED
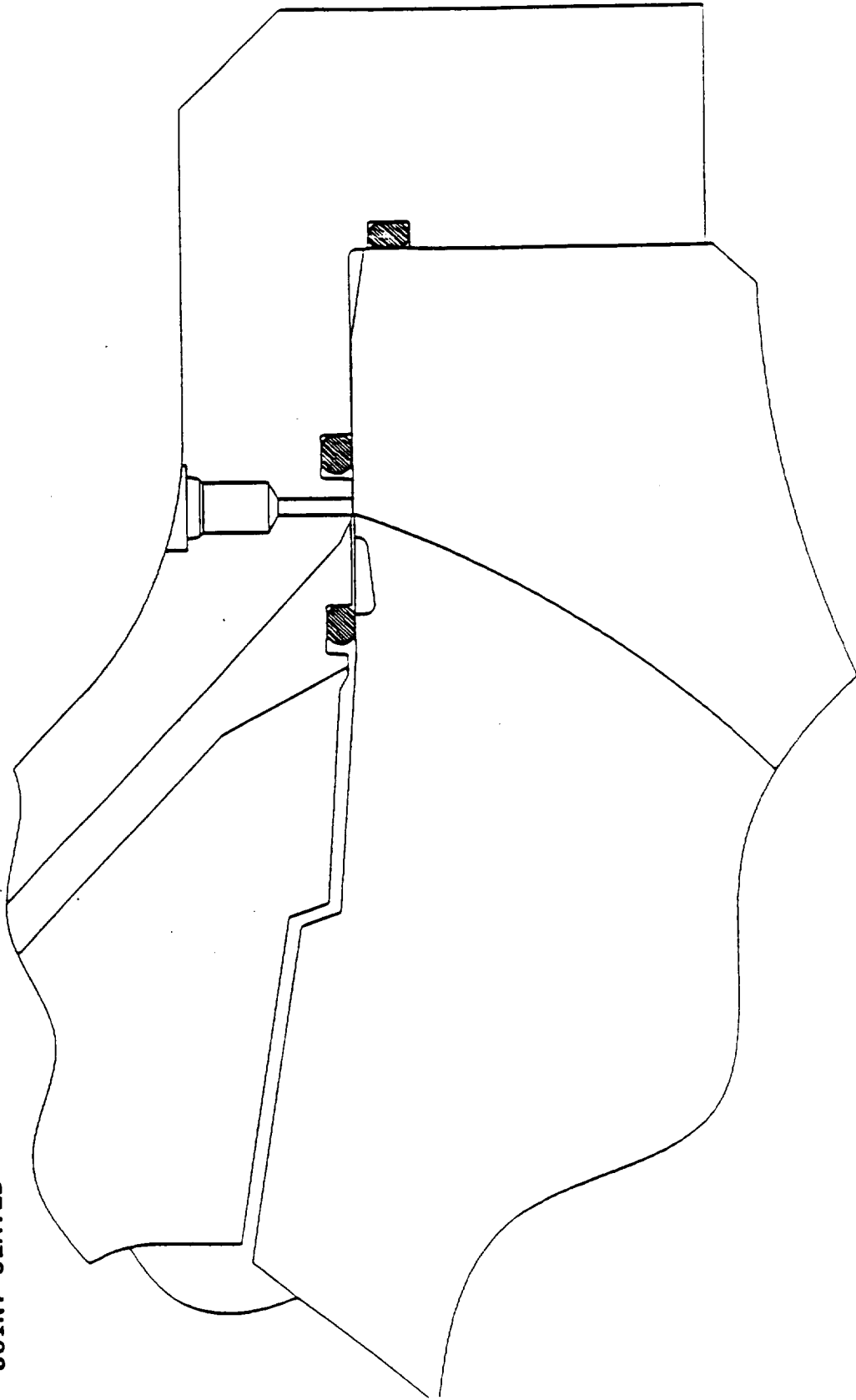
Figure B-29.   Nozzle-to-Case Joint Assembly

WORST ON WORST HARDWARE DIMENSIONS, POLYSULFIDE CONTACT.
SMALLEST DOME, LARGEST FIXED HOUSING, METAL TO METAL
O-RING GROOVES AND VENT SLOT NOMINAL
LOT 41 POLYSULFIDE PROFILE AT 60 MINUTES, WORST PROFILE

1.45

NOMINAL
PROFILE
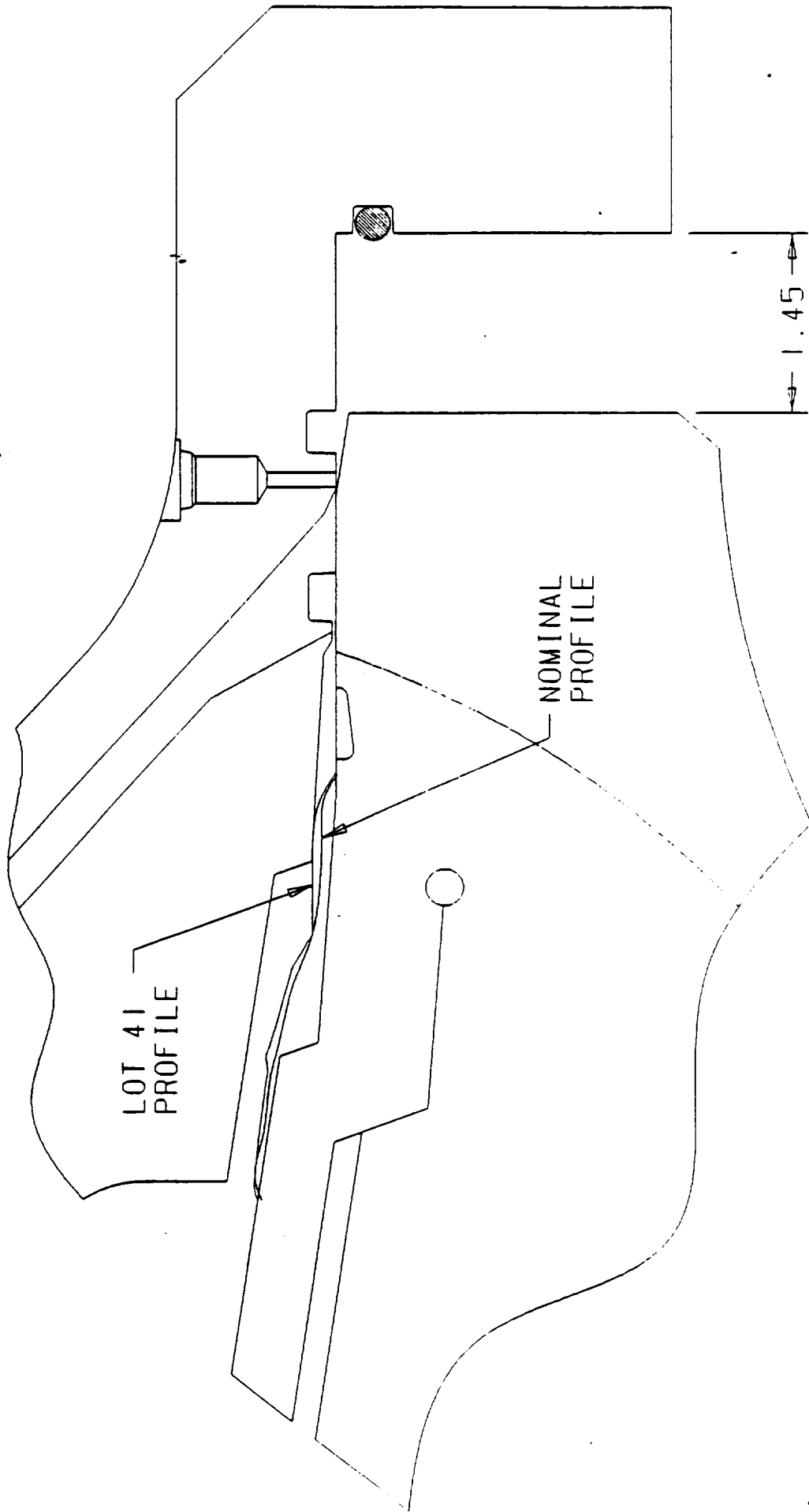
LOT 41
PROFILE

Figure B-30. Nozzle-to-Case Joint Assembly

81

WORST ON WORST HARDWARE DIMENSIONS, POLYSULFIDE CONTACT.
SMALLEST DOME, LARGEST FIXED HOUSING, METAL TO METAL
O-RING GROOVES AND VENT SLOT NOMINAL
LOT 41 POLYSULFIDE PROFILE AT 60 MINUTES, WORST PROFILE
BAFFLE RAISED .1-INCH AT FWD END

.87
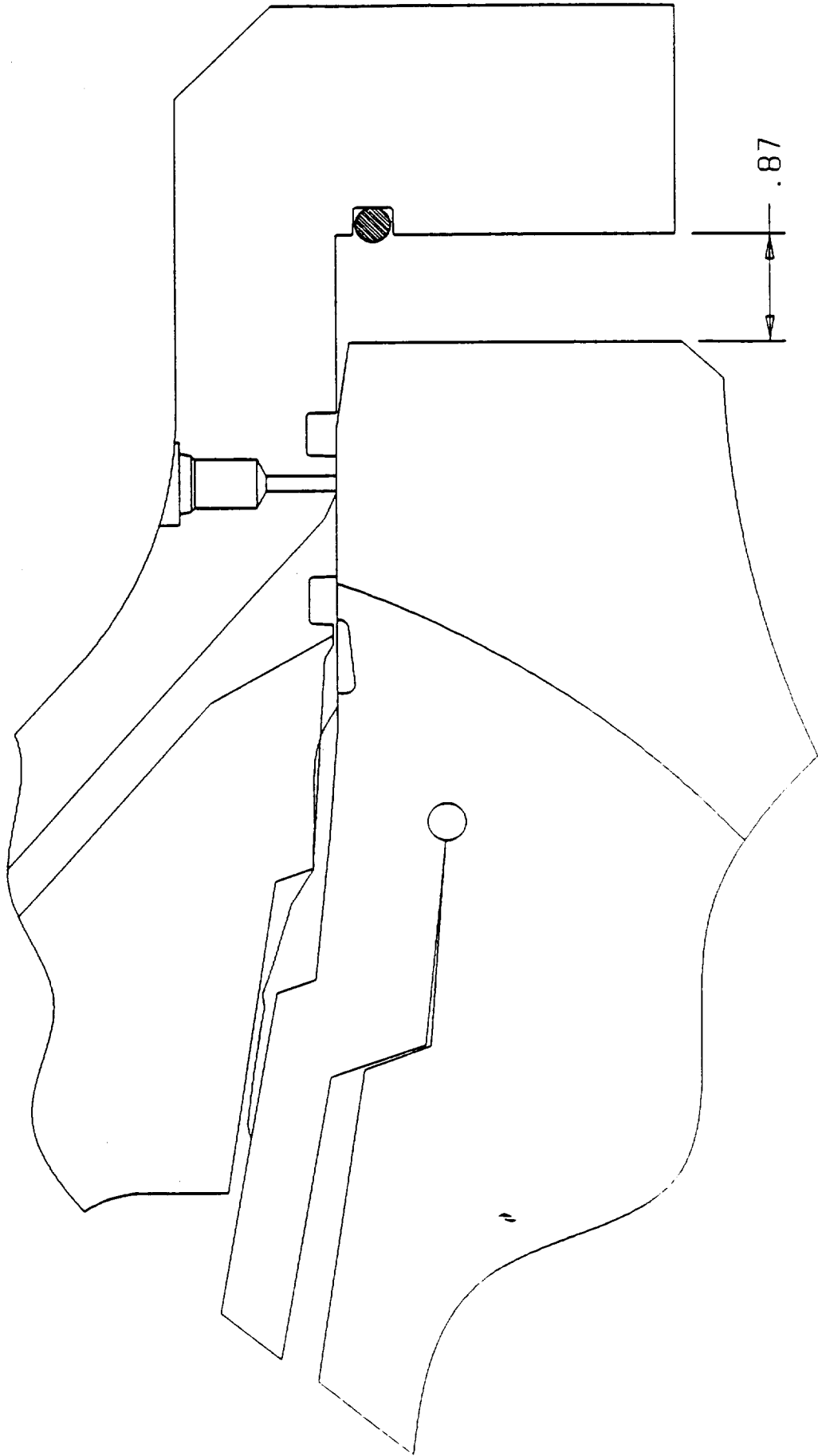
Figure B-31. Nozzle-to-Case Joint Assembly

the formation of gas paths in the polysulfide. These generally deal with the restricting of air flow through the path to the vent port. During the assembly air becomes trapped between the wiper O-ring and the adhesive bead. Under normal operating conditions, this trapped air flows through the vent slots as the wiper O-ring passes over the slots, Figure B-32. The air then flows circumferentially in the channel between the wiper and the primary O-rings towards the vent port at 43.2 deg where it is evacuated out of the joint. If any of these features along the air flow passage becomes blocked during the critical phase of the assembly when the wiper O-ring is straddling the vent slots (i.e., metal to metal contact in 2 or more places), then the air trapped in part or all of the joint will remain, causing voids, or will be forced to flow out the forward end of the joint, possibly forming gas paths in the polysulfide.

Air trapped in the joint during the assembly process will always flow in the direction of least resistance. The air trapped during the RSRM-20 A & B assembly processes flowed through the polysulfide rather than through the vent ports. Testing has shown that the polysulfide requires a reasonable amount of pressure to blow through (approximately $\geq$ 1.0 psi), see Appendix F. Under normal conditions this magnitude of pressure will not be generated in the joint if the path to the vent port is open, therefore, it can be assumed that some kind of air path blockage occurred during both the RSRM-20 A & B nozzle installations.

4.5.1 NBR Pinch-off

Contact between the NBR at the aft end of a vent slot and the adjacent GCP on the fixed housing is possible during the assembly process. This condition would require that both the NBR and the GCP be approaching the maximum drawing tolerances of standoff from the metal features. The result of this condition could prevent individual vent slots from venting. Several consecutive vent slots would have to become blocked in order for this condition to form a significant void or gas path since the trapped air can flow circumferentially forward of the wiper O-ring until an open vent slot is found.

Actual dimensions taken from the RSRM-20 A & B hardware show that gaps were present between the NBR and CCP at each of the gas path/sooted vent slot locations, eliminating the possibility of NBR pinching at these locations, Figures B-17, B-18 and B-19.

4.5.2 Out of Roundness/Metal to Metal Contact

Roundness measurements taken prior to NJAD and flight nozzle installations have shown that the aft dome has been out of round by as much as 0.208 inch on diameter (RSRM-24A). Fixed housing measurements are not taken prior to nozzle installations, but are assumed to be within 0.005 inch of round based on refurbished measurements. During the assembly, contact between the aft dome and fixed housing metal hardware and the O-rings act as rounding fixtures to force the two components to be concentric. Theoretically, there will be locations around the circumference where the gap between the hardware is at a maximum and locations where the gap is zero. The joint design could allow a condition where there is no standoff gap between the fixed housing GCP and the aft dome NBR, as well as the two metal components. With this condition the channel between the wiper and primary O-rings would not exist in localized areas, possibly isolating a large portion of the trapped air in the joint

83

TOP VIEW, WIPER O-RING MIDWAY OVER VENT SLOT

.36 JOINT GAP

43.2°

VENT PORT

VENT SLOT

FIXED HOUSING

PRIMARY O-RING

AIR FLOW

WIPER O-RING

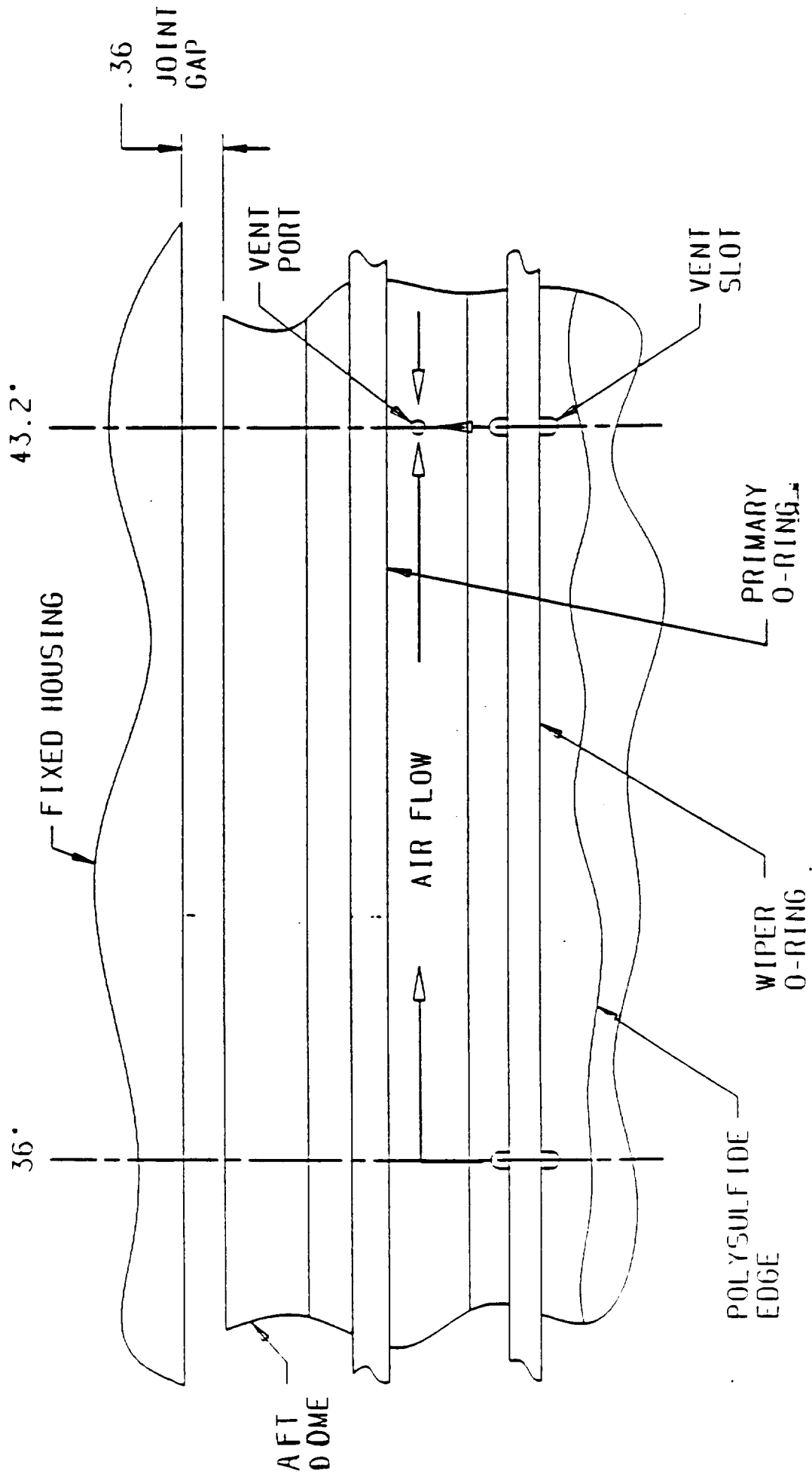36°

POLYSULFIDE EDGE

AFT DOME

Figure B-32. Nozzle-to-Case Joint Assembly

84

from the vent port. This condition could result in the formation of large voids and gas paths in the polysulfide as the assembly progressed.

At the gas path/sooted vent slot locations on RSRM-20 A & B, there was sufficient insulation-to-metal standoff gap to allow venting, Figures B-17, B-18 and B-19, although air flow could have been restricted in other areas. Roundness measurements of the RSRM-20 A & B were not taken prior to the nozzle installations.

4.5.3 Plugged Vent Port

The RSRM-3B nozzle to case joint was disassembled preflight due to a failed secondary o-ring leak check. One through and two partial gas paths were observed in the polysulfide bondline. It was determined that during the assembly, the vent port had been inadvertently filled with grease, which restricted all air flow out the aft end of the joint. A flow meter has been attached to the vent port on all subsequent nozzle installations to verify that air is flowing out of the port during the assembly process. Both RSRM-20 A & B nozzle installations had adequate air flow out of the vent port.

4.5.4 Excessive Grease

All the above mentioned conditions that potentially could restrict air flow during the assembly become more likely when grease is considered in the configuration. Grease is applied to all metal components and all O-rings. The GCP can also be covered with grease from the wiper O-ring. Testing has demonstrated that excessive grease can mask leak checks. Air pressures generated in nozzle to case joint assemblies are much lower than leak checks, on the order of 1 to 2 psi. A grease blockage could restrict air flow during a joint assembly.

4.5.5 Reverse Venting

Venting in the forward direction through the vent slots could occur if the channel between the wiper and primary O-rings becomes blocked. If the path to the vent port is blocked, then the trapped air could communicate along the wiper/primary channel and burp through the polysulfide at the weakest location (thinnest bondline or void location) in line with a vent slot.

This event has happened frequently. Two of the three gas paths observed on RSRM flight motors (11B and 20A) were in line with vent slots. Also, a review of all RSRM flight motors with multiple voids greater than 1.0-inch in the axial dimension has revealed that 8 out of 17 voids documented were in line with a vent slot. Considering that the void locations are generally recorded to the nearest 0.2-degree and if it is assumed vent slots do not have any affect on void location, then the probability of a void being located at a vent slot location is only 1 in 36.

4.5.6 RSRM-20 A & B Assembly Anomaly Scenarios

It is impossible to determine the exact type of air blockage that occurred during the RSRM-20 A & B nozzle installations because the configuration that formed the blockage occurred only during the assembly. However, information gathered during the postflight inspection can be used to develop probable scenarios for the gas path formations.

The vent slot fill profile for RSRM-20B, Table B-XI, shows a large portion of the joint circumference, from 223.2 deg to 295.2 deg, with no polysulfide in the vent slots. The gas path in this joint was located at 247 deg, centered within this arc. A portion of a joint with no vent slot fill generally signifies some kind of restricted air flow in that area, most likely caused by aft dome out of roundness. The gas path formation scenario for RSRM-20B would assume that an egg shaped aft dome resulted in metal to metal contact in the channel between the wiper and primary O-rings at approximately 220 deg and 300 deg. Air trapped between the polysulfide bead and the wiper O-ring in this arc would be prevented from flowing to the vent port located at 43.2 deg. Polysulfide would also be prevented from flowing aft and filling the vent slots. As pressure increased during the assembly due to the decreased volume in the joint, the trapped air blew through the polysulfide (path of least resistance), forming a gas path.

The gas path in RSRM-20A was located at 57.6 deg, which was in line with a vent slot. This would suggest a reverse venting scenario. The vent slot fill profile for RSRM-20A did not contain a large portion of the joint without any vent slot fill, Table B-XII. This could be due to the vent blockage occurring late in the assembly after most of the vent slots had already begun to fill with polysulfide. The shape of the gas path would also suggest that it was formed late in the assembly process, Figure B-1. This is evident by the bulge in the gas path just aft of the step, which would have been caused by a volume restriction at the joint step. Late in the assembly the bondline at the step region becomes thinner than the rest of the joint gap. The trapped air would have difficulty advancing forward over the joint step and appears to have began to bulge circumferentially before blowing through the step region.

It is not possible to identify the type of air vent blockage in RSRM-20A. Some type of blockage occurred to restrict the air flow to the vent port and caused it to blow through the polysulfide. It is recommended that further NJAD testing be performed to evaluate the different types of blockage in order to better understand the RSRM-20 A & B anomalies and to reduce the frequency of gas path formation.

4.5.7 Design Tolerance to Restricted Venting Scenario

After considering the possible scenarios for restricted air venting during the assembly process, it has been determined by the Gas Path Investigation Team that the present design of the joint has an inherent potential to form gas paths. The occurrence of gas path formation in flight motors to date has been 3 gas paths in 40 motors. Assuming that a complete redesign of the nozzle to case joint would not be feasible, some less drastic changes to the design could be made that could improve the probability for gas path free joints. It is recommended that the following design changes be evaluated: 1) Extending the aft end of the vent slots to the metal hardware. This change would allow venting earlier in the assembly process. 2) Adding more vent ports into the fixed housing. This would reduce the distance much of the trapped air would have to travel to be evacuated and lower the probability that a blockage in the channel between the wiper and primary O-rings would prevent air from venting. 3) Add a circumferential bleed path in the NBR at the aft end of the vent slots. This would allow another path in the case of metal to metal contact and it would eliminate concerns with NBR pinch-off.

TABLE B-XI

RSRM-20B ASSEMBLY ANOMALY SCENARIOS

Vent Slot Percent Fill:

Location	% Fill		Location	% Fill
0.0°	50		180.0°	100
7.2°	70		187.2°	100
14.4°	50		194.4°	95
21.6°	90		201.6°	95
28.8°	60		208.8°	70
36.0°	50		216.0°	50
43.2°	50		223.2°	50
50.4°	30		230.4°	70
57.6°	30 EFFECTED POLYSULFIDE *HEAT.*		237.6°	40
64.8°	20 (HEAT EFFECTED)		244.8°	70
72.0°	5 (HEAT EFFECTED)		252.0°	50
79.2°	2		259.2°	25
86.4°	0		266.4°	20
93.6°	2		273.6°	30
100.8°	2		280.8°	25
108.0°	25		288.0°	30
115.2°	20		295.2°	70
122.4°	40		302.4°	50
129.6°	10		309.6°	40
136.8°	15		316.8°	25
144.0°	50		324.0°	20
151.2°	70		331.2°	40
158.4°	80		338.4°	50
165.6°	95		345.6°	30
172.8°	100		352.8°	50

Overall Average Vent Slot Percent Fill: 46%

TABLE B-XII
RSRM-20A ASSEMBLY ANOMALY SCENARIOS

Vent Slot Percent Fill:

Location	% Fill		Location	% Fill
0.0°	30		180.0°	100
7.2°	50		187.2°	75
14.4°	40		194.4°	25
21.6°	40		201.6°	50
28.8°	40		208.8°	15
36.0°	60		216.0°	80
43.2°	20		223.2°	0
50.4°	40		230.4°	0
57.6°	60		237.6°	0
64.8°	25		244.8°	0
72.0°	50		252.0°	0
79.2°	100		259.2°	0
86.4°	80		266.4°	0
93.6°	90		273.6°	0
100.8°	90		280.8°	0
108.0°	70		288.0°	0
115.2°	20		295.2°	0
122.4°	20		302.4°	10
129.6°	10		309.6°	10
136.8°	50		316.8°	40
144.0°	50		324.0°	25
151.2°	30		331.2°	60
158.4°	30		338.4°	50
165.6°	100		345.6°	50
172.8°	100		352.8°	40

Overall Average Vent Slot Percent Fill: 40%

4.6 Thermal Analysis

Six analyses were performed, two with pressure to the primary O-ring and four with pressure just to the wiper O-ring. The first analysis was a matching of the results obtained with the PVM full scale static test motor. With the model validated, the 20A motor with blowby past the wiper allowing gas to the primary was simulated. Next, because the 20A motor only blewby for a short time, an analysis with pressure only to the wiper was performed to simulate the motor after the wiper had sealed. Simulation of the 20B motor involved pressure just to the wiper and was studied with three different analyses. The first simulating the reconstructed volume in the flight motor joint; the second, simulating the maximum possible volume if no polysulfide was present in the wiper O-ring groove; and the third, simulating the minimum volume assuming only 1 mil of gap exists between the wiper O-ring and the polysulfide in the groove.

4.6.1 Case One - PVM Simulation

Case one, or the PVM simulation, showed a maximum gas temperature of 4958°F exiting the insulation leak. The gas impinging on the primary O-ring reached maximum of 2065°F, resulting in 6 mils of primary O-ring erosion. This result matches the actual result of the test. The surface temperature of the exposed steel on the fixed housing in line with the flaw was predicted to be 814°F. The surface temperature of the steel in the gap just in front of the primary O-ring in line with the flaw was predicted to be 914°F. The fact that no steel melting or heat effect was predicted also matches the actual results from the test. The jet impingement erosion on the wiper O-ring was predicted to be 100 mils. This result also matches test results because the small diameter O-ring at the flaw location burned through.

4.6.2 Case Two - RSRM-20A Flow to the Primary Volume

The 20A flow to the primary volume, showed a maximum gas temperature of 5069°F exiting the insulation leak and a maximum gas temperature exiting the metal-to-metal gap in front of the primary O-ring of 2795°F, assuming the wiper did not seal. This resulted in 8.4 mils of primary O-ring erosion assuming the wiper O-ring had not sealed at 0.25 seconds. Before 0.25 seconds, the primary does not erode. The jet impingement erosion on the wiper O-ring was predicted to be 5 mils by 0.25 seconds and 72 mils if the wiper does not seal. The blowby erosion on the wiper O-ring was predicted to be 10 mils by 0.25 seconds and 46 mils if the wiper does not seal. The fact that 10 mils of blowby erosion can occur before the primary begins eroding seems to match flight motor results if you assume the smaller of the two eroded depths on the wiper is due to blowby erosion. The fact that the NBR in the wiper seal area does not seem to be eroded suggests blowby erosion did not occur. If that assumption is correct the model predicts the wiper must have sealed by 0.15 seconds to preclude blowby erosion.

4.6.3 Case Three - RSRM-20A Flow to the Wiper Volume

The 20A flow to the wiper case, showed a maximum gas temperature of 3342°F exiting the insulation leak. This resulted in 15 mils of wiper O-ring erosion. With the 5 mils of jet impingement erosion due to blowby of the wiper added to what occurred after the wiper sealed at 0.25 seconds,

C-2

the 20 mils of wiper erosion that occurred on the flight motor is matched assuming the blowby lasted until 0.25 seconds. Assuming the blowby only lasted 0.15 seconds, the code under predicts the erosion by 5 mils. This could be due to an inaccurate calculation of fill volume.

4.6.4 Case Four - RSRM-20B Nominal Volume

The 20B nominal volume case, showed a maximum gas temperature of 4009°F exiting the insulation leak. This resulted in 24 mils of wiper O-ring erosion. This result matches what occurred on the 20B flight motor.

4.6.5 Case Five - RSRM-20B Maximum Volume

The 20B maximum volume case, showed a maximum gas temperature of 4679°F exiting the insulation leak. This resulted in 150 mils of wiper O-ring erosion. This run illustrates the importance of filing the groove with polysulfide. The 150 mils of erosion would probably fail the wiper O-ring allowing gas to the primary O-ring regardless of whether blowby occurred or not.

4.6.6 Case Six - RSRM-20B Minimum Volume

The 20B minimum volume case was done to see if the no wiper erosion results of RESULTS-9, QM-6, and NJES 2-B could be matched by assuming the fill volume was extremely small in those tests due to good polysulfide fill. It showed a maximum gas temperature of 1970°F exiting the insulation leak. This resulted in 0.6 mils of wiper O-ring erosion. With conservatisms in the code this result could be interpreted as zero erosion answering the question.

4.6.7 Thermal Analysis Conclusion

In conclusion, it seems due to uncertainties in the manufacturing process, blowholes can happen and can cause wiper erosion if the wiper cavity is not filled sufficiently. The potential exists for primary O-ring erosion if the wiper O-ring blows by for more than 0.25 seconds. However, if primary erosion occurs, analysis and test data show that the amount of erosion will not compromise the sealing integrity of the joint.

APPENDIX C - QUALITY ASSESSMENT

1.0 INTRODUCTION

This section documents the findings of the Quality Assessment Team with respect to the Flight 20 Polysulfide Gas Path Investigation. The quality assessment team focused on process documentation reviews, looking for special conditions that could contribute to gas path formation. Reviews were conducted of material acceptance test plans; nozzle build logs; temperature and humidity conditions at assembly; time deltas between operations; tooling configuration; hardware configuration; assembly techniques; postflight hardware reviews; and nonconformances.

2.0 SUMMARY AND CONCLUSIONS

The physical review of the hardware, in conjunction with analysis of polysulfide rheology and acceptance test data, identified nozzle installation as the most probable occasion for the gas paths to form. From the data review, items 2.1 - 2.4 were determined to be contributing factors to the most probable cause. Other data reviewed did not reveal any noteworthy trends that could contribute to gas path formation. Item 2.5, while not a direct contributing factor, may indicate lack of necessary acceptance testing controls, and therefore be a secondary contributor. Item 2.6 summarizes the process and material change history which was provided to the NASA Polysulfide Investigation Team.

2.1 Polysulfide acceptance testing had one special cause variable. The Application Life Test (Figure C-1) identified a slow curing condition among the lots used on Flight 20 (Lots 36 and 37).

The Application Life Test (or Pot Life Test) evaluates polysulfide extrusion rate from a Semco gun a two hours after addition of the catalyst. The higher the extrusion rate, the higher the application life. The purpose of this test is to verify that the polysulfide cure rate meets requirements for the nozzle installation. A slow cure could contribute to the formation of gas paths during assembly. This gas path formation theory was proven empirically by testing performed on samples from lots with both high and low extrusion rates (See Appendix F.) High Application Life samples were more susceptible to gas path formation at equivalent pressures.

2.2 The 20B fixed housing encountered a high temperature within the region of the gas path (at 247°) (Figures C-2 and C-3).
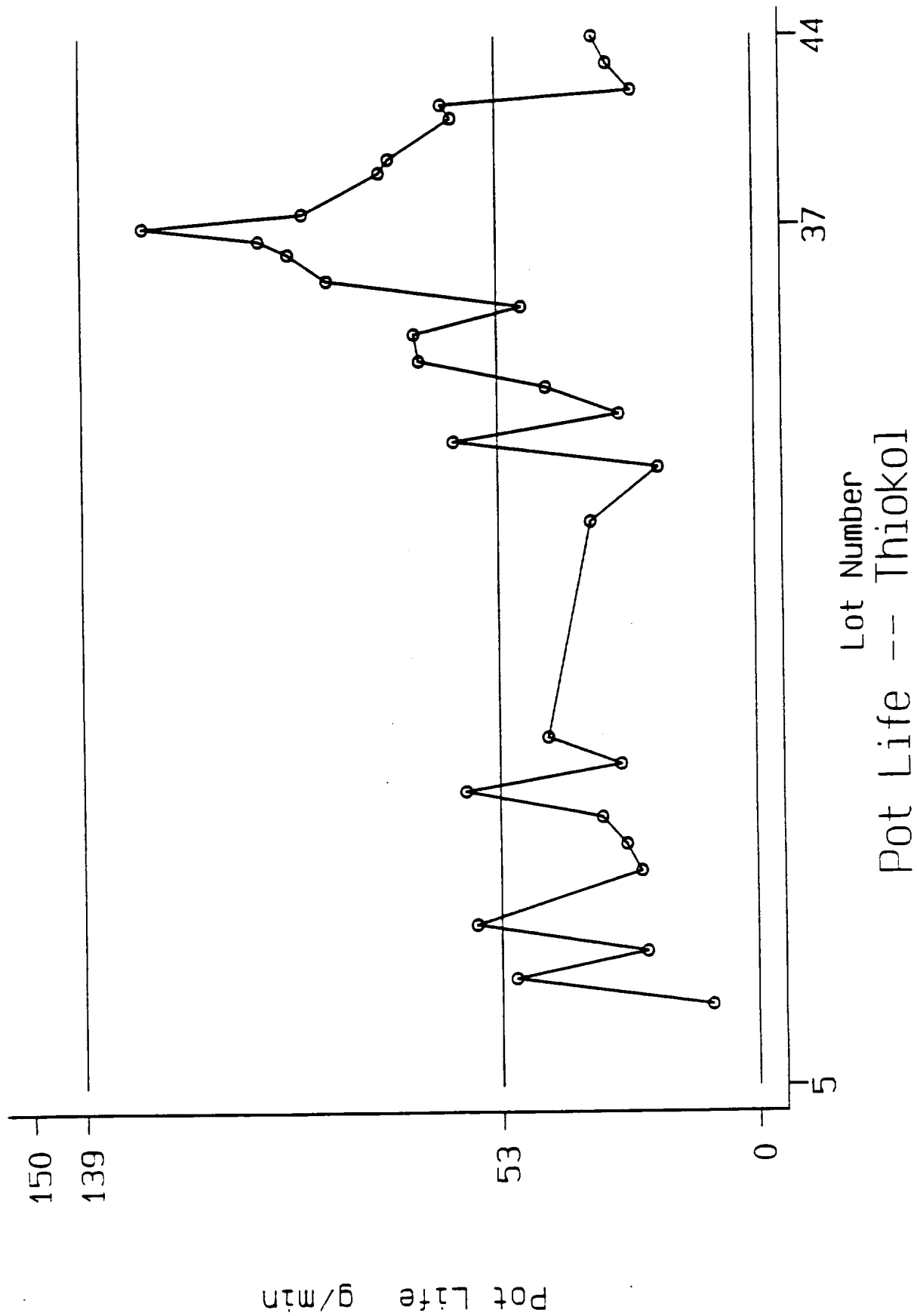
Figure C-1 Application Life Test
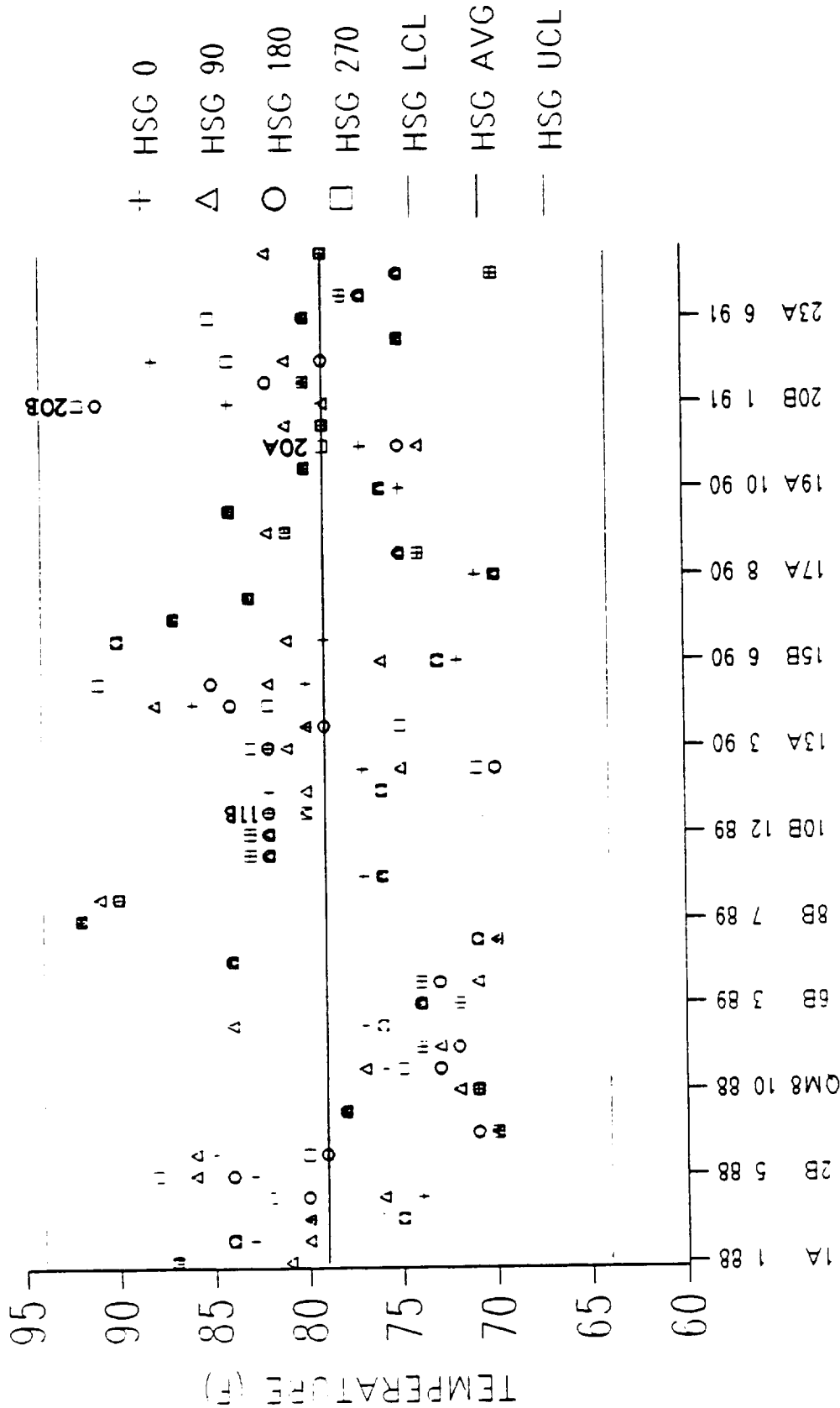
Figure C-2. Fixed Housing Temperature

DOME TEMPERATURE AT INSTALL NOZZLE
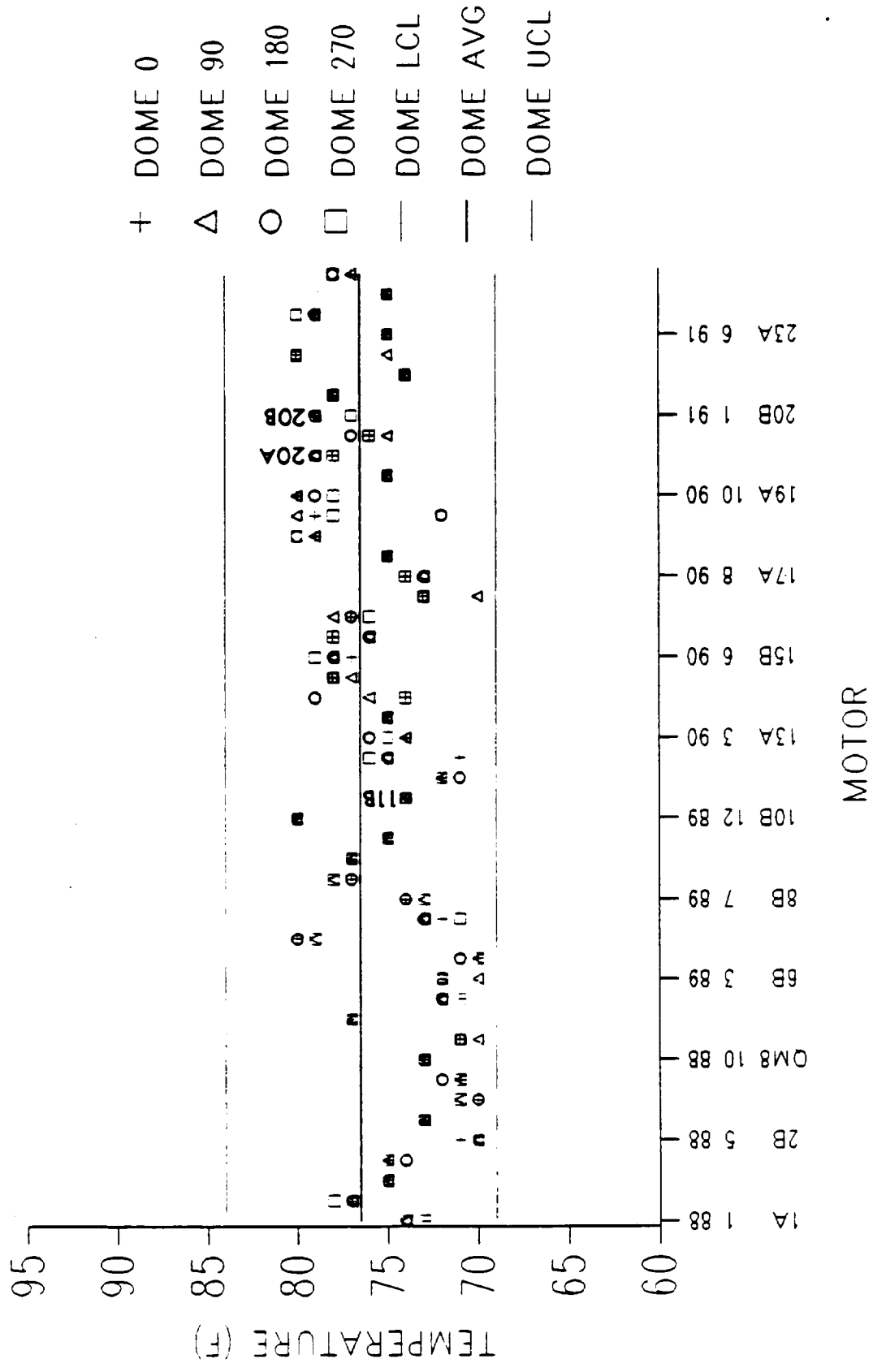
Figure C-3. Dome Temperature

94

Temperatures are monitored on both the aft dome and the fixed housing at four locations each prior to installation. The 208 fixed housing saw a high absolute temperature in circumferential locations between 180 and 270° as well as a large temperature delta around the hardware. Since an increase in temperature will reduce polysulfide viscosity for a short time, this could also contribute to gas path formation.

2.3 The potential exists for gas path formation due to variations in polysulfide application technique.

The method for application of the polysulfide is technique intensive. Operators have some potential for entrapping air while applying the polysulfide in front of the screed. The application technique varies somewhat between operators, which could contribute to the problem.

2.4 The current acceptance testing may not evaluate the necessary properties for adequate assurance that the material is acceptable for its intended use.

Review of properties that affect polysulfide profile showed that polysulfide thixotropy is involved. This is not currently tested in STW4-3311.

2.5 Investigation of the Acceptance Test data identified significant disparities between the vendor's and Thiokol's data. Although both tests showed that the material met specification, there was little correlation between the two sets of data. There are differences in environmental controls between the two facilities that may account for some variation, however, some of the data, particularly in Specific Gravity (Figures C-4 and C-5) and Application Life (Figures C-1 and C-6), showed special causes of variation. These trends were either long runs at the same y-axis value (i.e. no variation lot to lot) within the vendor data, or outlier data points that did not correlate (Thiokol Application Life was near three sigma at Lot 37, the vendor's was similarly high at Lot 41).

2.6 A review of specifications and planning changes and material nonconformances since RSRM-1 was performed to support the NASA Polysulfide Investigation Team. The nozzle installation planning was reviewed for changes to Inspection Points (IPs). Polysulfide, NBR rubber, and HD2 grease documentation was reviewed for materials specification changes and acceptance testing nonconformances. The results of this review identified a number of changes and nonconformances in all areas, however, the changes were either clarifications or added testing or storage requirements. Figures C-7 and C-8 are an example of the material specification changes for polysulfide. The only nonconformance related to material properties that affected flight hardware was a failed Tack Free Test on polysulfide Lots 034, 035, and 036. This was dispositioned "USE AS IS" and the specification was changed. The results of this review showed that there were no documented changes to materials, inspections, or specifications that affected the potential for gas path formation in the polysulfide.
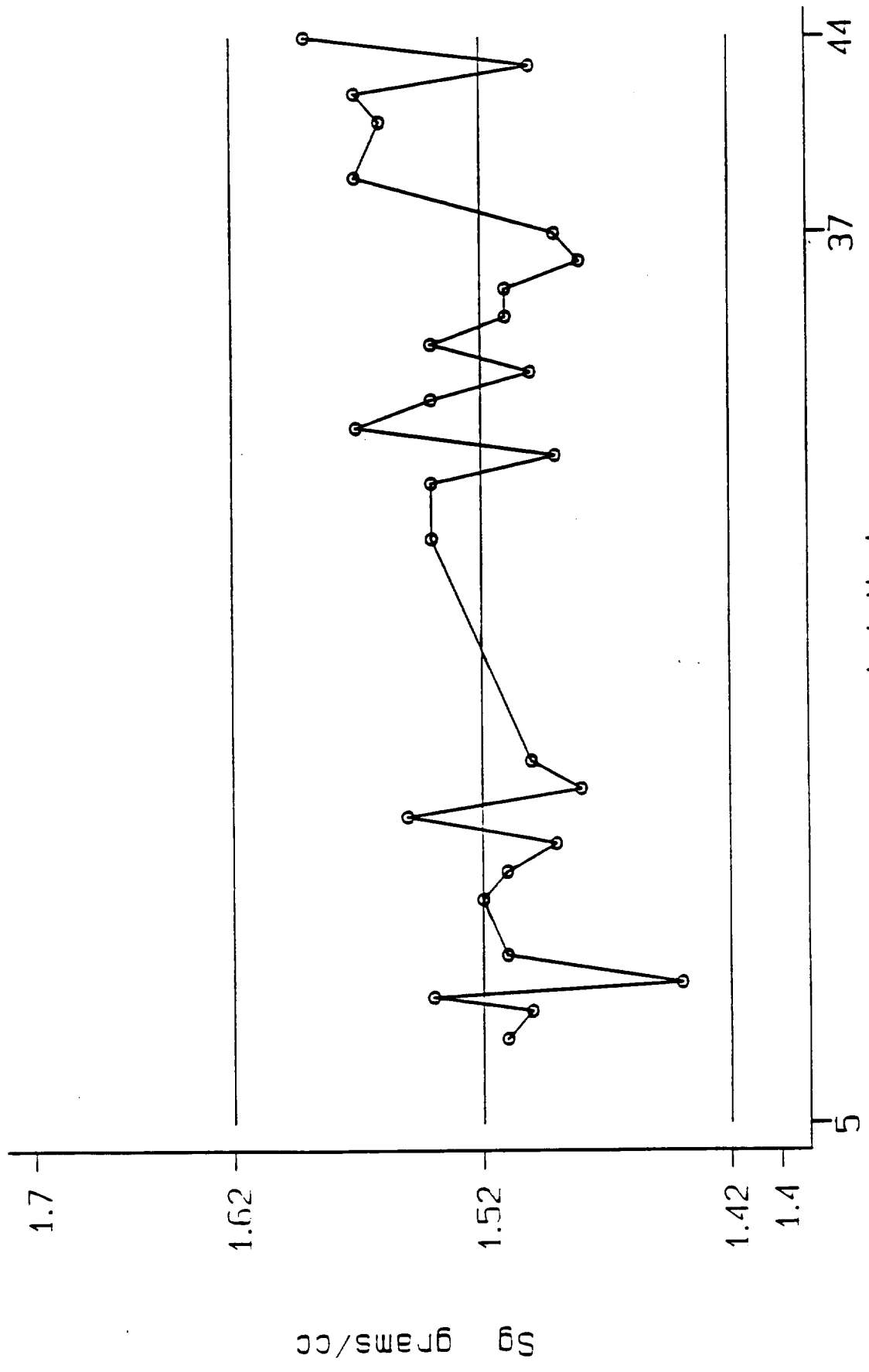
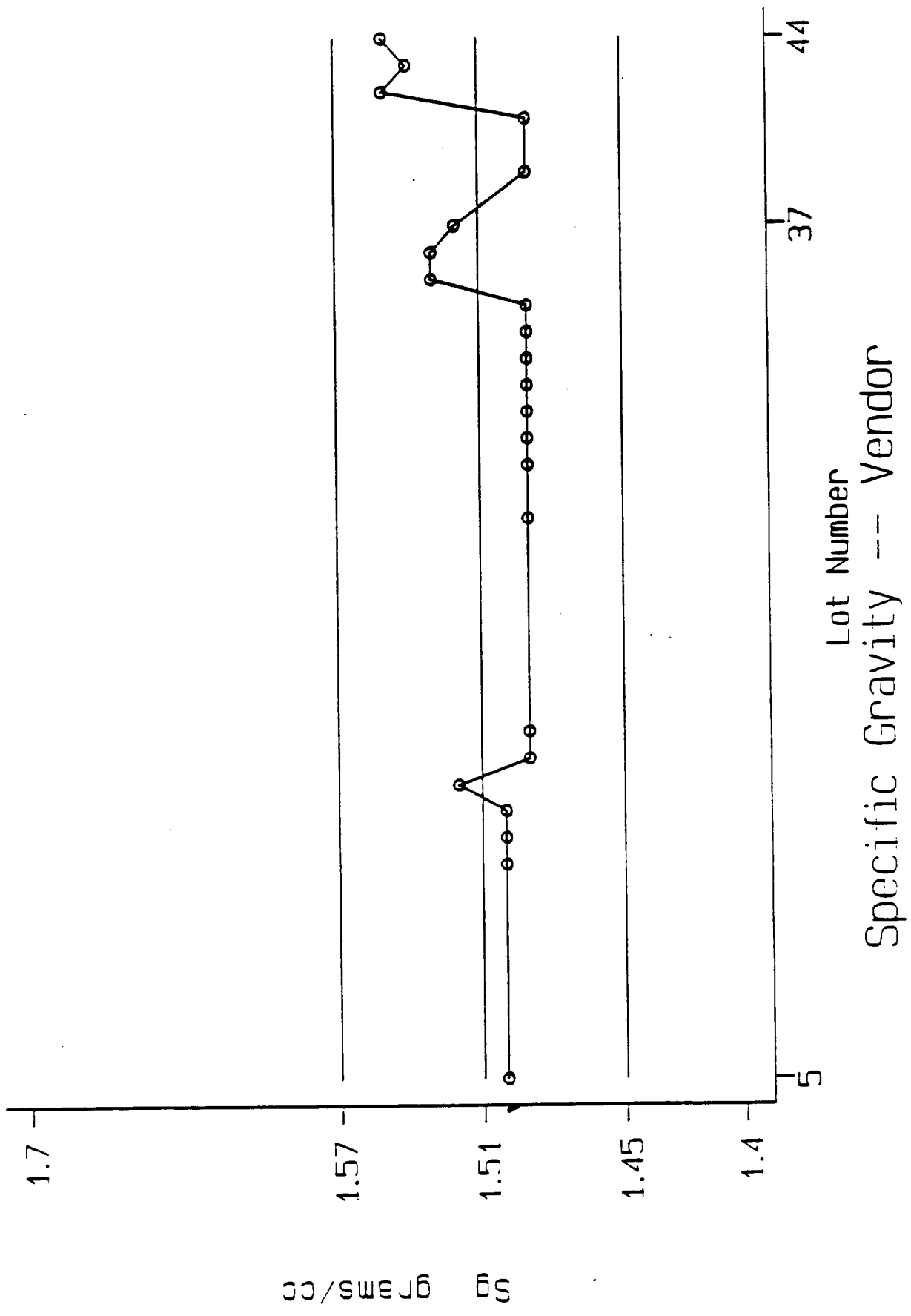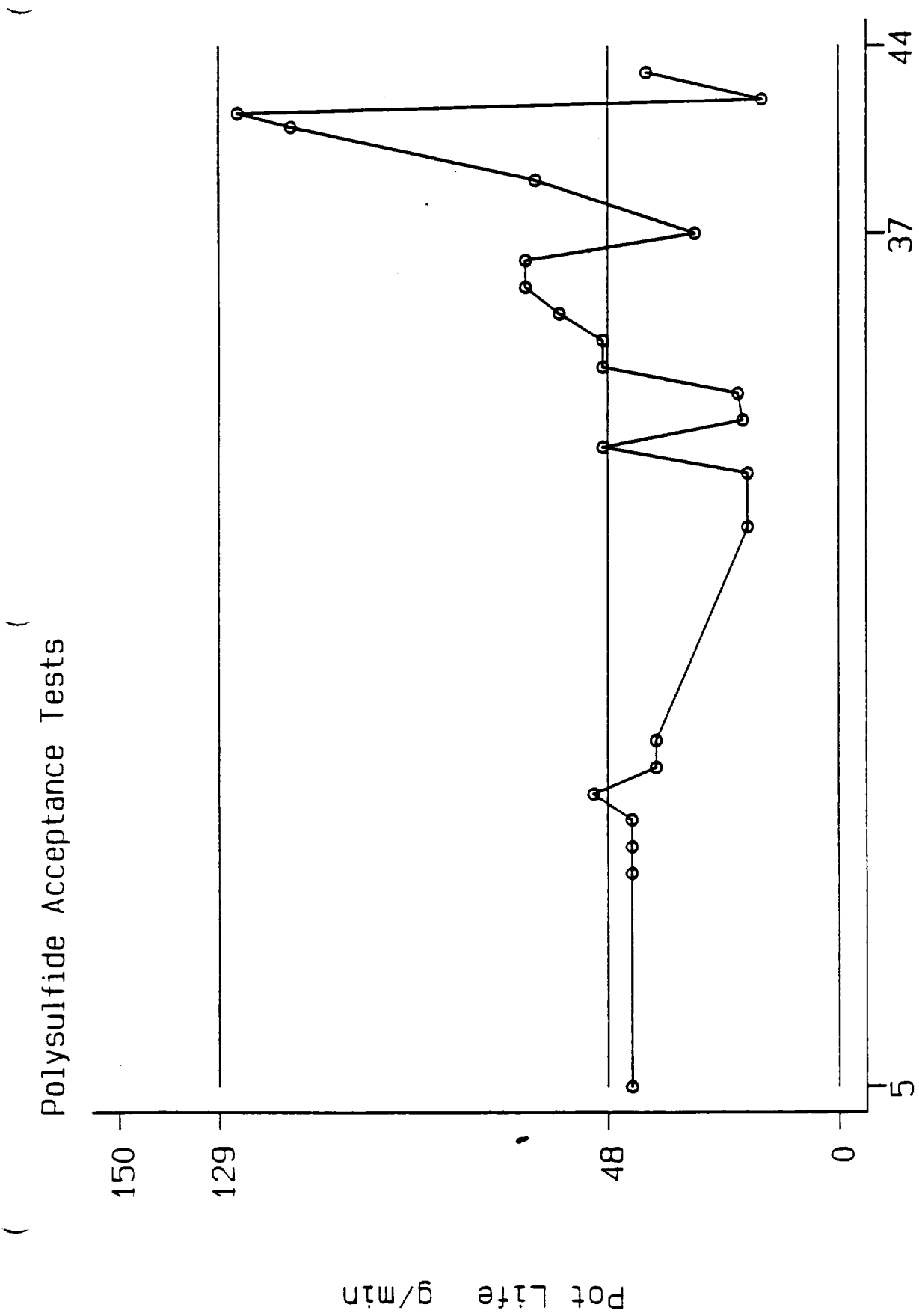Figure C-4. Specific Gravity

96

Polysulfide Acceptance Tests

Specific Gravity -- Vendor

Figure C-5. Specific Gravity

Figure C-6. Application Life Test

922023-3.3

Materials Specification Changes

- Polysulfide--STW4-3311, STK No. 4907

  - SCN 2 (9/3/89) Lot 24 and subsequent (pre-RSRM)

    - Implemented references to Type II and Type III adhesives
    - Changed storage from ambient to 33° to 45°F
    - Changed shelf life from 12 months to 6 months
    - Added 30-day maximum cumulative uncontrolled storage requirement
    - Eliminated storage life extension
    - Changed premix temperature conditioning from 3 hours to 8 hours
    - Added 16-hour tolerance to time requirement for lap shear
    - Changed peel strength test cure time at 120°F from 24.0 + 0.5, - 0.0 hours to 48.0 + 1.0, -0.0 hours

Figure C-7. Materials Specification

922023-3.2

Materials Specification Changes

- Polysulfide (cont)

  - SCN 3 (6/4/91) Lot 39, 40, 42, and subsequent, retest Lot 36 (22B)

    - Allowed retest to extend storage life to a maximum of 3 years in 6-month increments

  - SCN 4 (7/26/90) released before SCN 3, Lot 38 and subsequent (22A)

    - Doubled time (ex. from 24 to 48 hours for Type I) and added temperature and humidity requirements to tack-free time test

  - SCN 5 (6/8/90) released before SCN 3, 4, Lot 36 and subsequent (16A)

    - Added reference to NBR specification STW4-2621

Figure C-8. Materials Specification

3.0   RECOMMENDATIONS

3.1   SPC tracking of acceptance test variables should be implemented as part of the acceptance testing. Special cause data should be evaluated prior to acceptance.

3.2   Temperature controls should be implemented that limit temperature variation within a part as well as absolute temperature.

3.3   Polysulfide application operators should receive additional training and possibly certifications for the technique. Additional work should also be done to further limit variation within the application process (screed velocity, screed pressure, polysulfide application rate, finished profile requirements, void control, etc.).

3.4   Thiokol should gain an understanding of the cause of differences between vendor acceptance data and Thiokol acceptance data. Where possible, changes should be made to minimize this variation.

3.5   A flow test similar to that used in STW4-3829 should be used to evaluate effects due to thixotropy variations.

APPENDIX D - MANUFACTURING ASSESSMENT

1.0 INTRODUCTION

Appendix D documents the results of a comprehensive review of the manufacturing process related to RSRM -20A and -20B nozzle installation. All applicable records were obtained and reviewed. Emphasis of the review focused on processing variables related to individual component preparation, polysulfide application, and the actual nozzle installation and seating process. Variables such as time, temperature, installation rates, application techniques, etc. were compared to actual requirements and historical data. Validation of know requirements such as pertinent tooling dimensions was also accomplished.

2.0 SUMMARY AND CONCLUSIONS

2.1   The component preparation and nozzle installation process was accomplished per existing processing requirements.

2.2   There were no component discrepancies or process departures identified during processing.

2.3   Process data for the -20A nozzle installation was within the historical data base with the exception of the elapsed time from end of polysulfide mixing to the start of application, which was the fastest recorded time to date at the time of assembly. Faster processing times have the potential for reduced polysulfide viscosity based on normal cure curves.

2.4   Process data for the -20B nozzle installation was within the historical data base with the exception of the delta temperature between the four fixed housing measurements taken off the phenolic bonding surface prior to polysulfide application. In addition, the maximum temperature of 92° F on the phenolics at 270° was the hottest temperature to date. The actual temperature at time of assembly is not available, and was probably lower due to nozzle movement through ambient outside air, which was 30° F at time of assembly.

2.5   The polysulfide was properly weighed up and mixed.

2.6   The polysulfide application process is variable and can cause small voids within the polysulfide which could possibly result in gas paths when exposed during motor operation.

2.7   The location of the beginning and end of polysulfide application was not in the location of the gas path on the -20B segment. In addition, it is probable that it was not in the location of the gas path on the -20A segment either.

2.8   The Manufacturing and Inspection personnel involved in the component preparation and nozzle installation process were experienced and knowledgeable of the existing processing requirements.

2.9   All tooling used during the -20A and -20B nozzle installation process met blue print requirements.

2.10   The absolute humidity at the plant during nozzle installation for both the -20A and -20B was low which could have resulted in a lower polysulfide viscosity at time of assembly.

3.0   RECOMMENDATIONS

3.1   The polysulfide application process should be improved to reduce the variability of the final polysulfide profile. Application rates based on known viscosities should be established. In addition, the operator performing the polysulfide application should receive formal training and certification.

3.2   The polysulfide screed should be redesigned to incorporate features which will minimize the effects of operator techniques.

3.3   The polysulfide application screed should be transferred to a controlled tool drawing and periodically inspected for compliance to blue print requirements.

3.4   Limits should be established for the volume of air expected to be evacuated through the vent port. In addition, the volume of air evacuated should be quantified and verified to be within the established limits.

3.5   The conditioning of the fixed housing and aft dome should be better controlled to improve uniformity of the component.

3.6   Limits should be established for the absolute humidity at time of polysulfide application.

3.7   End of mix viscosity limits should be established for the polysulfide.

4.0   DISCUSSION

        The RSRM -20A nozzle was installed on 11-29-90 in casting pit #8, Polysulfide lot 0036 was used for this assembly. The RSRM -20B nozzle was installed on 30 January 1991 in casting pit #1. Polysulfide lot 0037 was used for this assembly. To adequately investigate the potential cause of the gas paths in the polysulfide, a number of shop travelers were obtained and reviewed. The records included the installation records for both the -20A and -20B nozzles, in addition to all of the available records for every nozzle installation of the redesigned nozzle to case joint, beginning with DM-9. An overview of the installation process and requirements is included in Table D-1. Individual pieces of data were evaluated against the historical mean and experience base. The summary of each evaluation will be discussed.

NOZZLE-TO-CASE JOINT ASSEMBLY PROCESS

- PREPARE SEGMENT AND NOZZLE

    - CLEAN AND INSPECT METAL SURFACES
    - INSTALL RADIAL BOLT HOLE PLUGS
    - CLEAN AND INSPECT INSULATION AND PHENOLIC SURFACES
    - ABRADE BONDING SURFACES USING 180 GRIT ABRASIVE PAPER
    - COVER NON BONDING SURFACES
    - INSTALL O-RINGS

- MEASURE COMPONENT TEMPERATURES JUST PRIOR TO POLYSULFIDE APPLICATION

    - AVERAGE DOME INSULATION - 70° - 80° F
    - AVERAGE NOZZLE PHENOLIC - 70° - 100° F

- APPLY POLYSULFIDE

    - MIXED PER BATCHCARD REQUIREMENTS
    - HAND APPLIED WITH 2 EACH SEMCO GUNS AND SCREEDS

- FINALIZE AFT BOSS

    - REMOVE TAPE AND CHECK RADIAL HOLE FILLER PLUGS
    - CLEAN METAL SURFACES AND APPLY GREASE
    - INSTALL GUIDE PINS

- LIFT THE NOZZLE AND CENTER OVER SEGMENT. LOWER UNTIL FIXED HOUSING ENGAGES LONG GUIDE PINS

    - CONTINUE TO LOWER UNTIL GAP IS NOT LESS THAN 3" BETWEEN MATING SURFACES
    - ENGAGE LEVELING PINS WITH THREADED RODS

- LOWER NOZZLE IN .1" INCREMENTS, FROM 3" TO .8"

    - LEVELNESS OF .2"
    - NO TIMED DELAYS

- STOP LOWERING NOZZLE AT .8"

    - LOWER NOZZLE FROM .8" TO SEATING, AT A RATE OF .050" EVERY 60 SEC
    - LEVELNESS OF .1"
    - VERIFY AIR FLOW FROM THE JOINT 5 TIMES MINIMUM
    - REMOVE SECONDARY O-RING CLIPS AT .1" - .050"
    - SEAT THE NOZZLE BY RELEASING HYDRASET PRESSURE

- REMOVE LIFTING ARRANGEMENT AND INSTALL AXIAL AND RADIAL BOLTS

4.1   SHOP TRAVELER REVIEW

The actual Shop Travelers used to manufacture both the RSRM - 20A and 20B nozzle to case joints were obtained and reviewed. Emphasis was placed on identification of discrepancies, process departures and changes to the process. There were no discrepancies or process departures identified. Changes from previous assemblies were identified (see Table D-II). Nothing of significance was identified.

A comprehensive review was also accomplished on all available Shop Travelers from the first installation of the redesigned nozzle to case joint (DM-9) to the -20A and -20B assemblies. The only significant identified changes determined to have any influence on the actual assembly process and possible formation of gas paths were implemented prior to the RSRM -1A and -1B reinstallation. It should be noted that these changes were specifically made as corrective actions following the discovery of unplanned gas paths found during DM-9 disassembly (post test) and disassembly prior to flight of RSRM -1A and -1B due to nozzle change out.

4.2   VIDEO REVIEW

Comprehensive video coverage of the RSRM -20B nozzle installation process from the start of polysulfide application to final seating was available for review. The video was made due to the fact that the -20B assembly process was the last assembly which would use the existing installation fixture. Subsequent assemblies, starting with RSRM -21B used the new installation fixture. A review of the video verified that the assembly process was completed per existing requirements.

4.3   PROCESS VARIABLES

All recorded process variables were reviewed for compliance to requirements (if established) with comparison to the historical mean and the calculated control limits. The variables included:

- Start to end of polysulfide mixing.
- End of polysulfide mixing to start of application.
- Start to end of polysulfide application.
- End of polysulfide application to final seating.
- Start of polysulfide mixing to final seating.
- Absolute humidity at time of installation.
- Average fixed housing surface temperature prior to polysulfide application.
- Average aft dome insulation surface temperature prior to polysulfide application.
- The delta between the average aft dome insulation surface temperature and the fixed housing phenolic surface temperature prior to polysulfide application.

20 B TYPE II & III OCR CHANGES

OCR #	TYPE	DESCRIPTION	JUSTIFICATION
L001194	II	Changed the surface preparation of the aft dome to fixed housing interface, for the weather seal application.	Analysis of test data showed better peel strength of 5.29 PLI versus 2.995 PLI. Documented in interoffice memo L840-FY91-039A
Q003374	III	Added step to inspect nozzle guide pin threads with a GO-NO-GO gauge.	Required inspection of tooling interfacing with component hardware.
LE00225	III	Perform supplement "A" regreased aft boss, shipped segment to storage delayed because the nozzle was not available.	Regreasing metal surfaces and shipping segments are standard practices.
L003171	III	Added an alternate air filter for the nozzle conditioning enclosure.	The furnace filter which was called out was 2" wide. 2 ea. 1" wide filters were used which provided equivalent capabilities.
L003155	III	Changed the serial number of the nozzle and fixed housing being used.	Planning error - wrong serial numbers were recorded.

20 B TYPE II & III OCR CHANGES - (CONTD)

OCR #	TYPE	DESCRIPTION	JUSTIFICATION
L003263	III	Added a data line in IP for recording excursion time remaining on polysulfide (9829) sealant. Deleted IP-1270	Materials require excursion times be recorded. Wrong IP called out.
Q003525	III	Changed the data recording in IP 1010 of SL to, SA & SP.	Planning error - IP was incorrect.
L002797	III	Changed End Item Part No. from -08 to -09.	Planning error.

20 A TYPE II & III OCR CHANGES

OCR #	TYPE	DESCRIPTION	JUSTIFICATION
NONE	II		
L002707	III	Oper 055 changed STW7-2744 Revision from M-0038 to N-0045	Update Engineering to latest revision
L002764	III	Re-Abraded the aft dome insulation surfaces.	Surfaces were inspected by M.E. & D.E. and found to be unacceptable. Decision was made to reperform steps.
L002784	III	Perform Supplement "B" Reperform calibration of transducers on leak test fixture.	Recalibration of transducers for high pressure deadhead was necessary due to equipment problems.

The total polysulfide mix time for the RSRM -20A and -20B segments were 14 and 13 minutes respectively. Both mix times were below the mean of 17 minutes, but well within the historical data base (See Figure D-1).

The elapsed time from end of polysulfide mixing to the start of application was 18 minutes for the -20A segment and 30 minutes for the -20B segment. This time frame represents the time necessary to vacuum load the SEMCO cartridges, transport the cartridges from the mix room to the casting pits, and to begin application. Both times are below the mean of 30.5 minutes. While the elapsed time for the -20B is very close to the mean, the -20A segment time was the fastest recorded time to date at time assembly. Since that time, only the -24A segment has had a faster processing timeline for this particular parameter (See Figure D-2). Faster processing times have the potential for reduced polysulfide viscosity at time of assembly, based on normal polysulfide cure curves.

The elapsed time from start of polysulfide application to end of application was 23 minutes for both the -20A and -20B segments. This is slightly above the mean of 18.5 minutes, but well within the historical data base (See Figure D-3).

The elapsed time from the end of polysulfide application to final seating was 75 minutes for the -20A segment and 68 minutes for the -20B segment. This time frame represents the time necessary to prepare the aft boss following polysulfide application, install the guide pins and incrementally lower the nozzle into the segment until the fixed housing flange seats against the aft boss. Both times are above the mean of 67.4 minutes, but well within the historical data base (See Figure D-4).

The combined times from start of polysulfide mixing to final seating was 130 minutes for the -20A segment and 134 minutes for the -20B segment. This is just slightly below the mean of 134.7 minutes, but well within the historical data base (See Figure D-5). The maximum time allowed per the specification is 180 minutes.

The absolute humidity at the plant during the nozzle installation process was .0019 lbs of water per lb of dry air for the -20A segment and .0014 lbs of water per lb of dry air for the -20B segment. Both readings are below mean of .00446 lbs of water per lb of dry air, but within the historical data base (See Figure D-6). Lower absolute humidity has the potential for reduced polysulfide viscosity since moisture is a cure accelerator. The current polysulfide application specification does not have absolute humidity requirements, however, the new specification does.

The average of four fixed housing temperature measurements taken off the phenolic bonding surface prior to polysulfide application was 76°F for the -20A nozzle and 86.5°F. for the -20B nozzle. The -20A nozzle was slightly below the mean of 79.0°F. while the -20B nozzle was 7.5°F. above the mean. However, both are within the historical data base (See Figure D-7). The average temperature per the specification is 70 - 100° F. It should be noted that the temperature measurements are taken
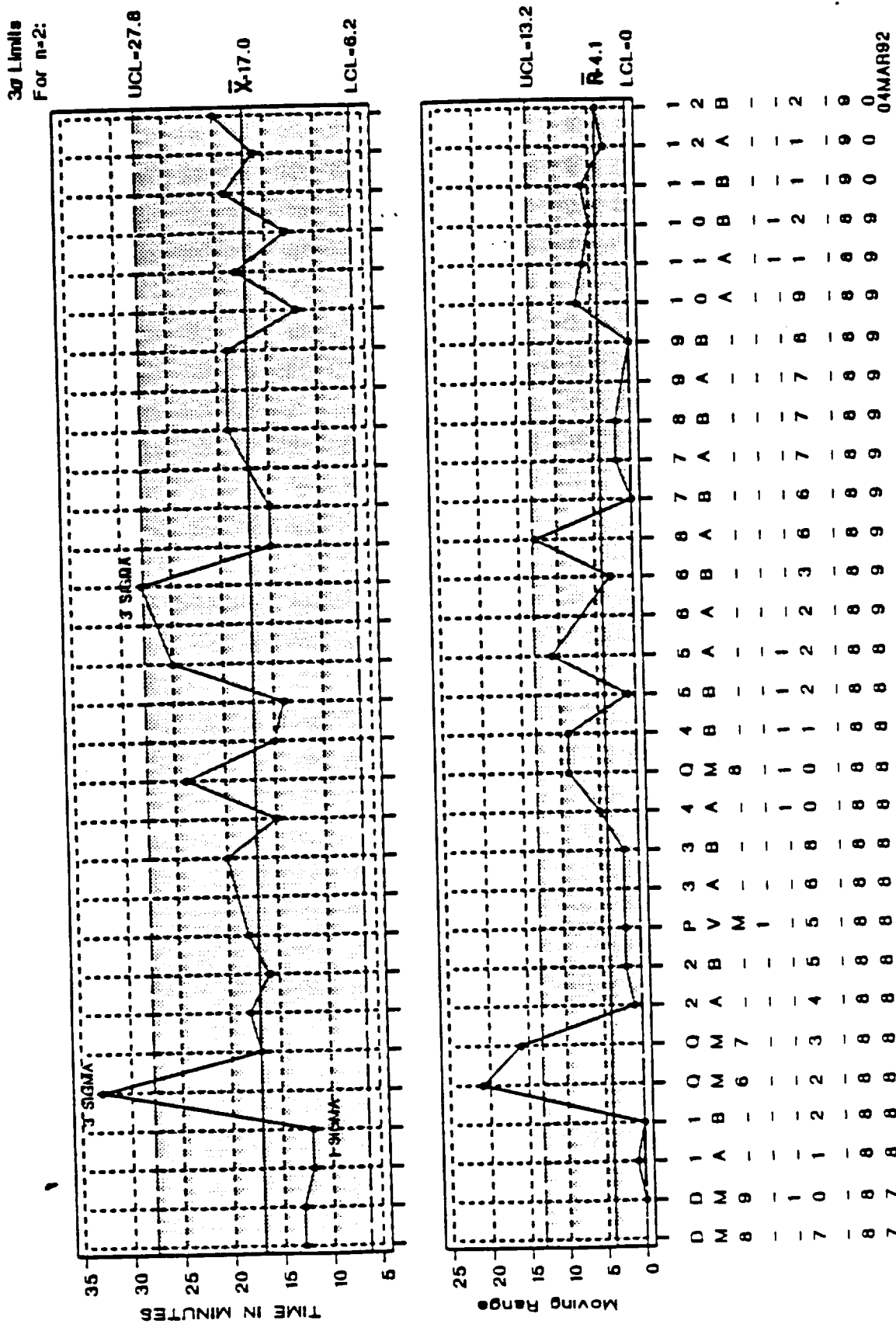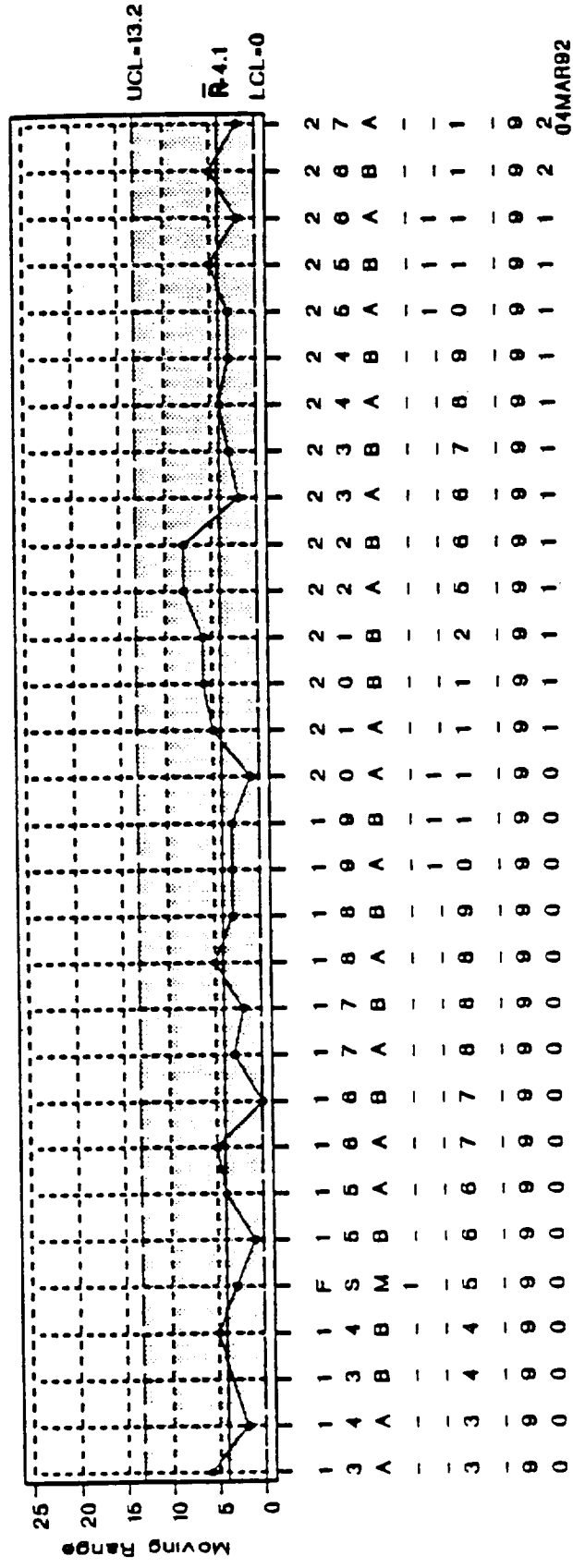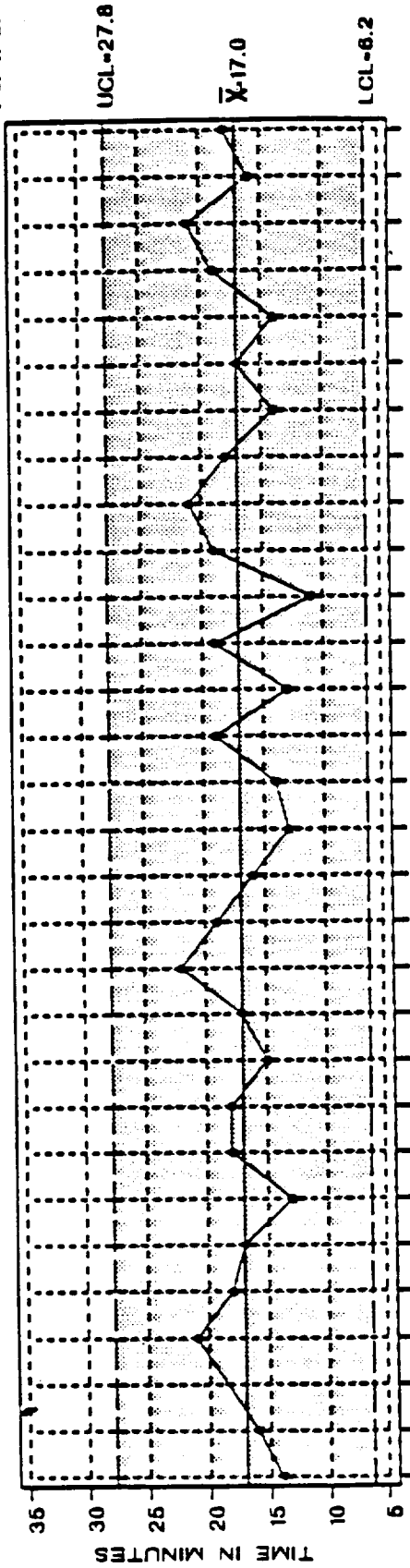
Figure D-1. Polysulfide Mix Times

Figure D-1. The Catalide Mix Times (CONT)

TIME FROM END OF MIX TO START OF APPLY

X̄=30.6

LCL=2.0

TIME IN MINUTES — 60, 40, 20, 0

UCL=36.1

R̄=10.7

LCL=0

Moving Range — 40, 30, 20, 10, 0

MOTOR AND DATE

04MAR92

Figure D-2. Polysulfide Transportation Times

Figure D-2. Polysulfide Transportation Times (CONT)

113

Figure D-5. Polysulfide Application Times

114
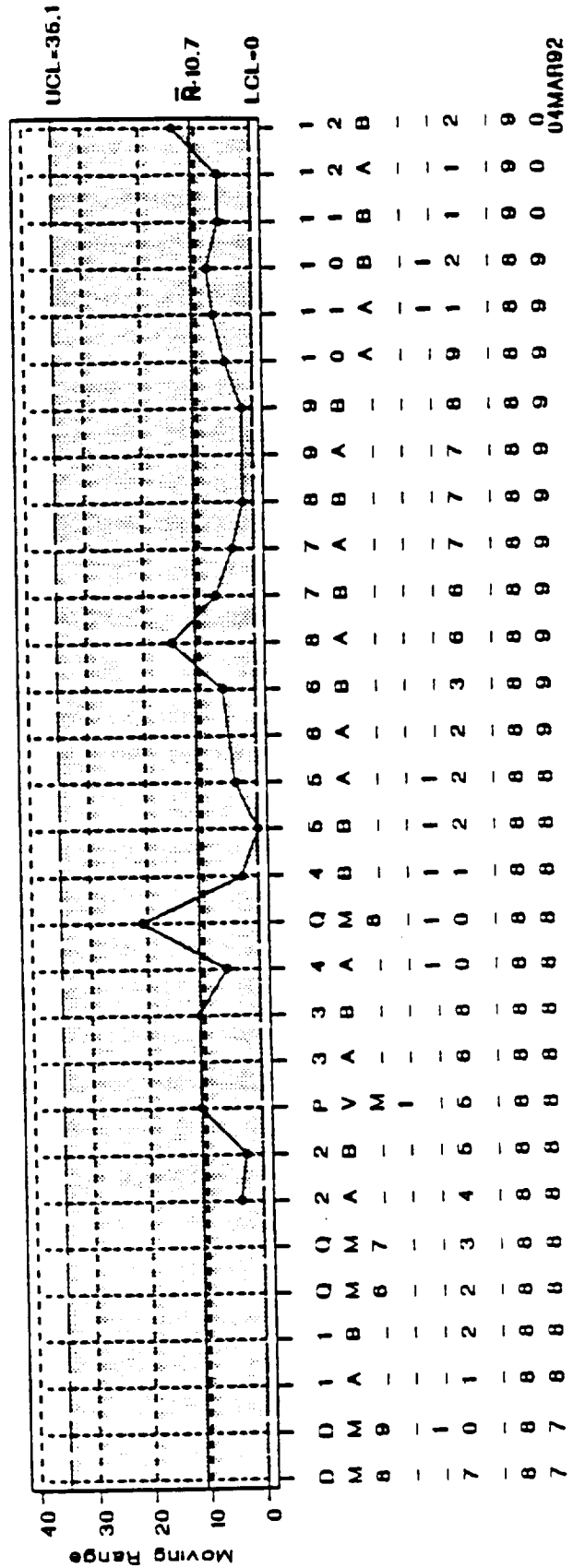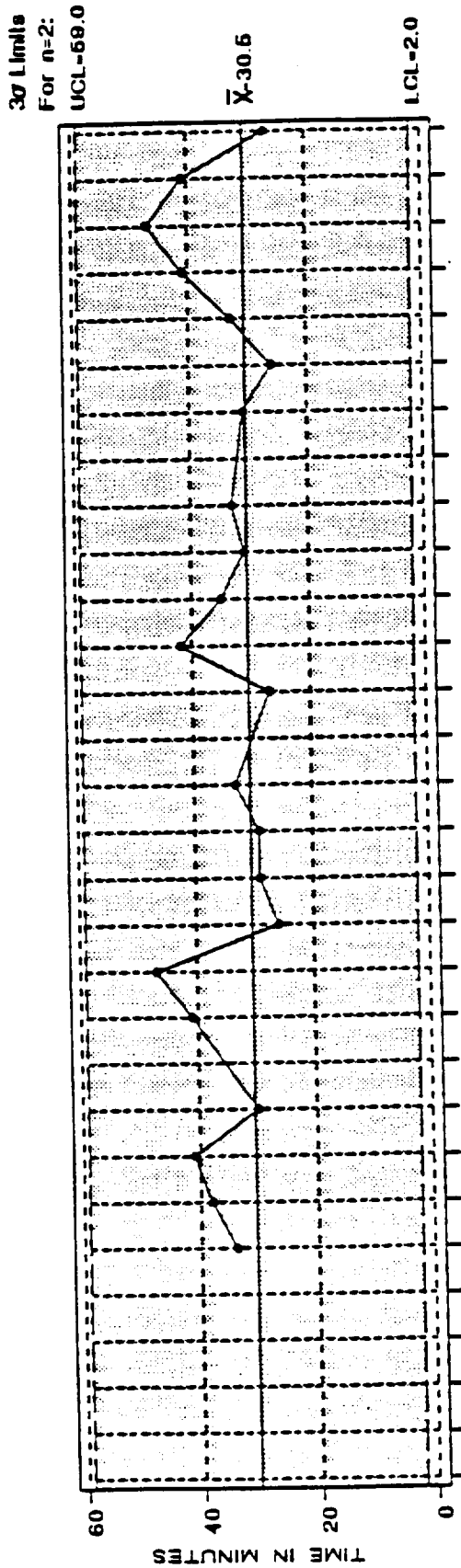
TIME FROM START TO END OF APPLY
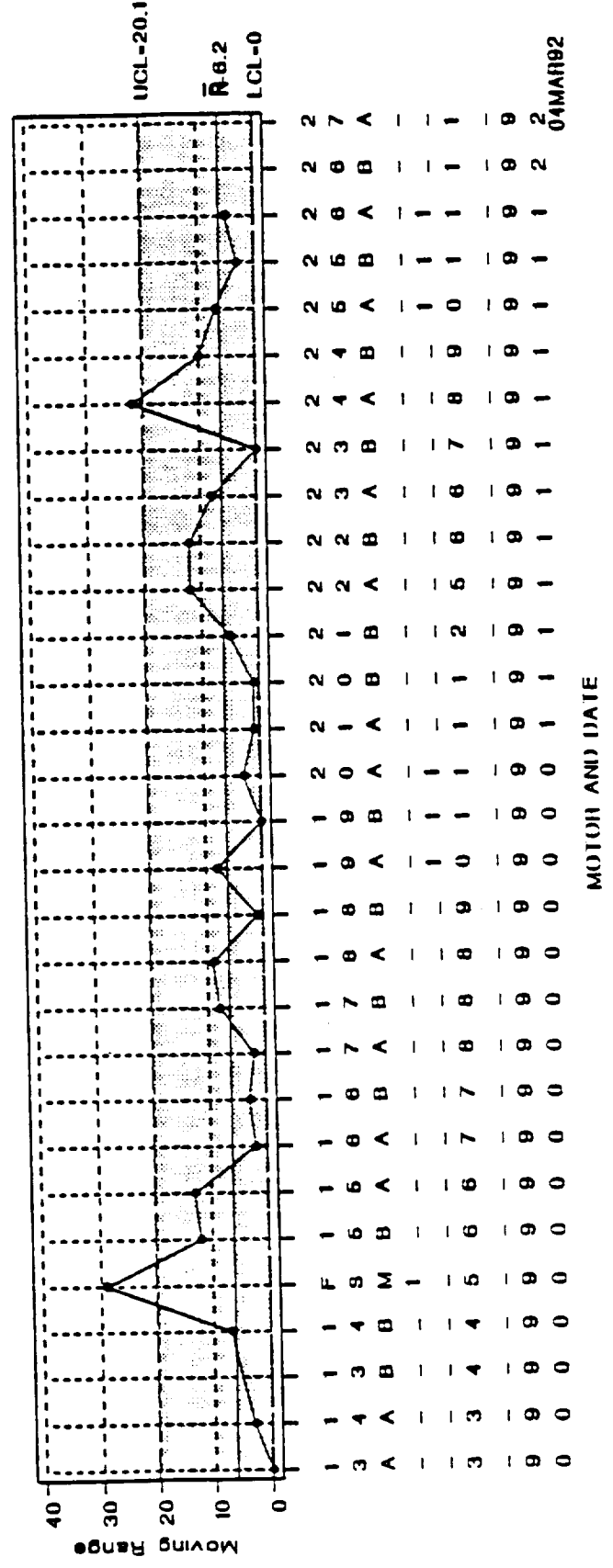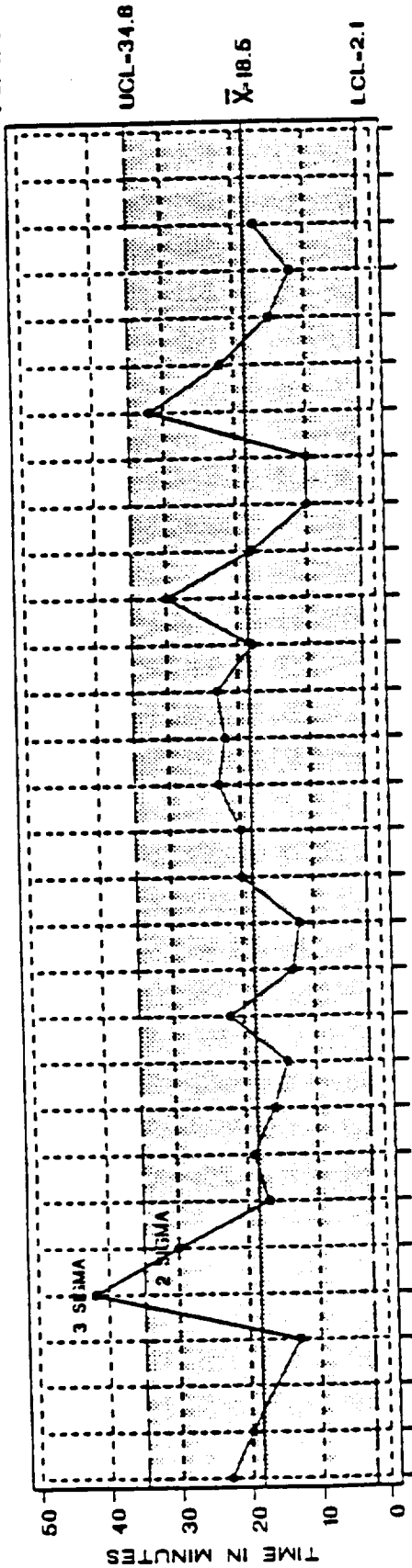
Figure D-3. Polysulfide Application Times (CONT)

115

TIME FROM END OF APPLY TO SEAT

Figure D-4. Nozzle Seating Times

116

TIME FROM END OF APPLY TO SEAT

Figure D-4. Nozzle Seating Times (CONT)

117

TIME FROM START OF MIX TO SEAT

Figure D-4. Total Process Time

TIME FROM START OF MIX TO SEAT
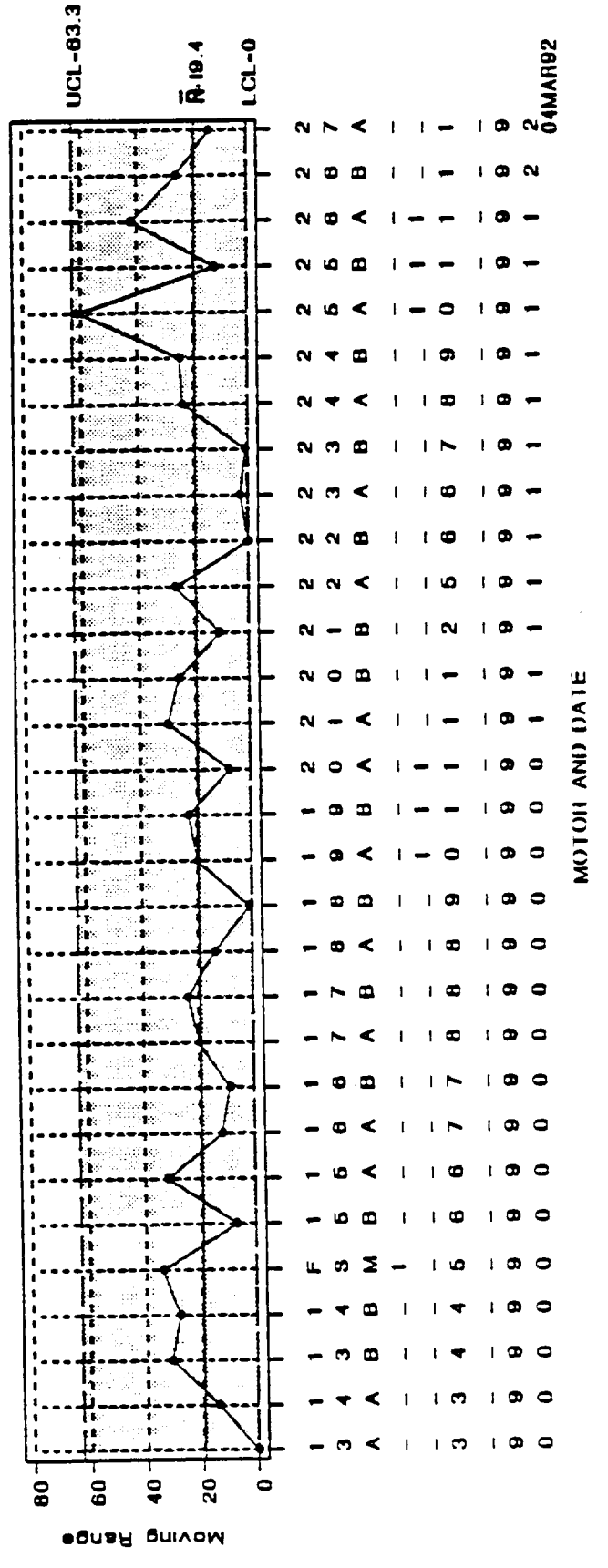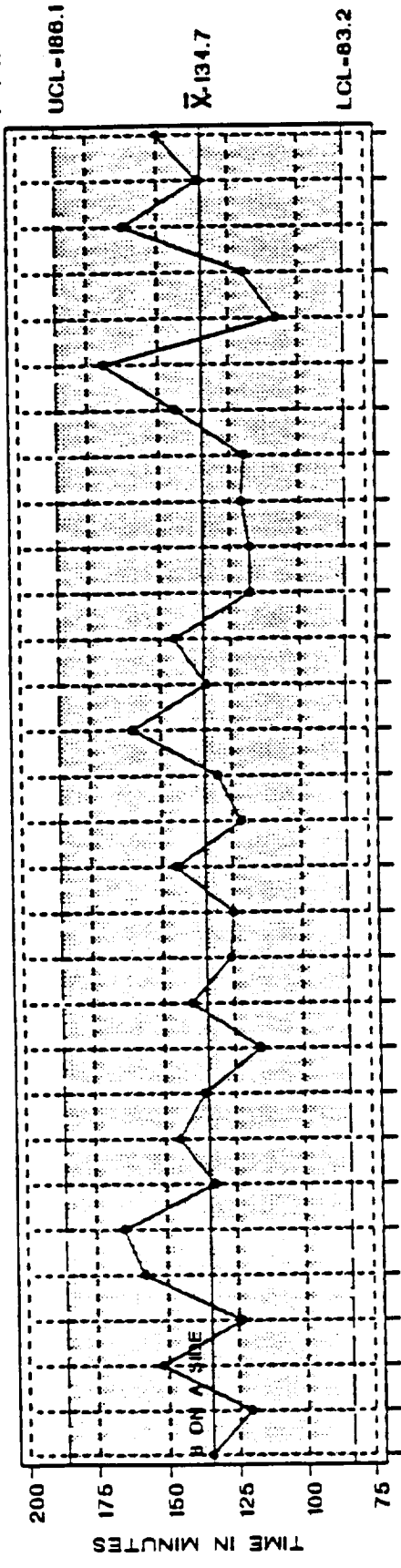
Figure D-7. Total Process Time (CONT)

119

Figure 2-6. Absolute Humidity
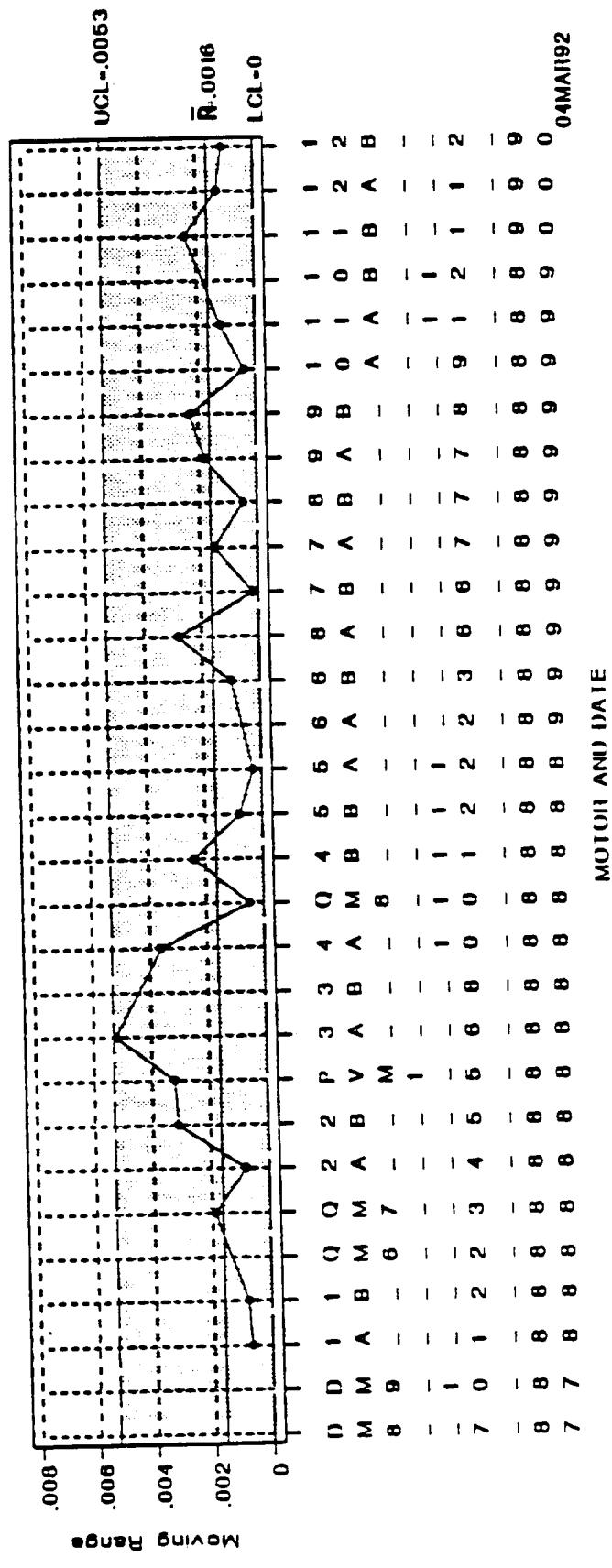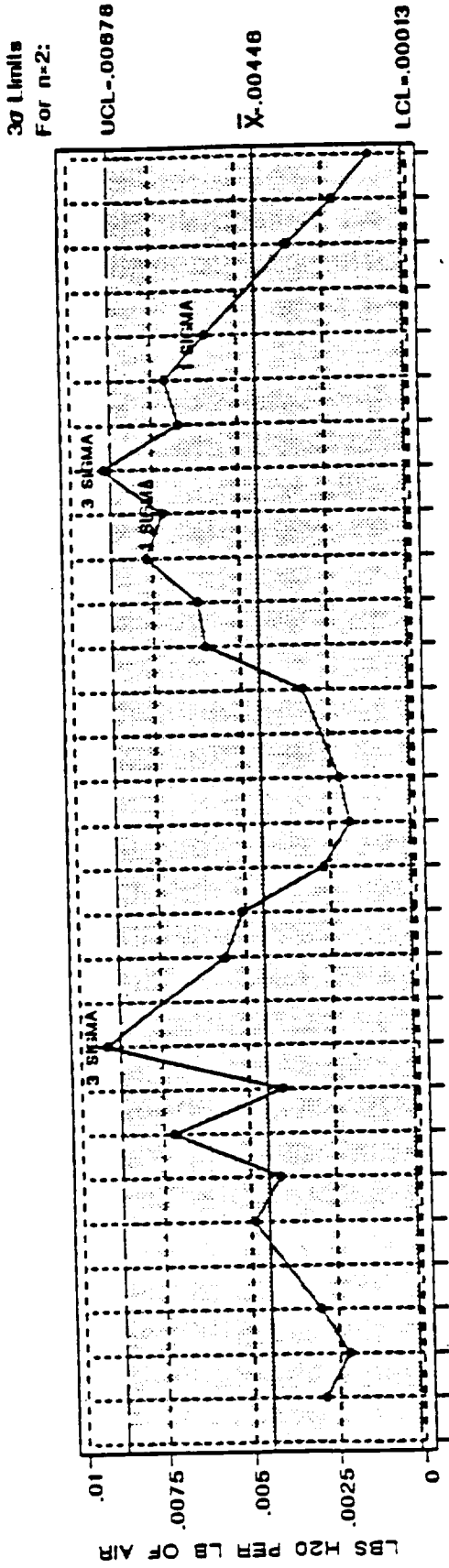
Figure 5-6. Absolute humidity (CONT)

121

HOUSING TEMPERATURE AT INSTALL NOZZLE

Figure D-7. Average Fixed Housing Temperatures

122

Figure B-7. Average Fixed Housing Temperature (CONT)

123
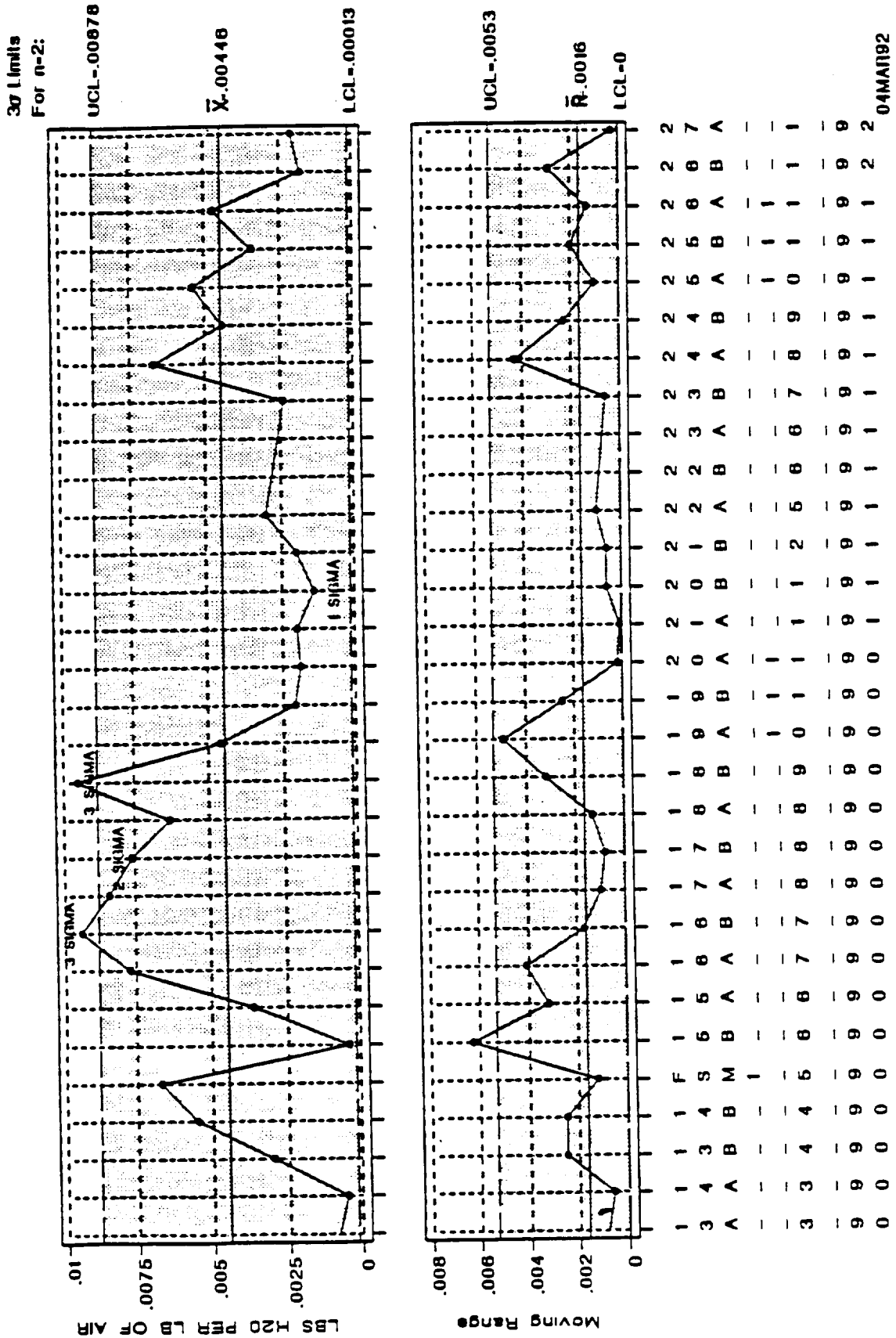
prior to polysulfide application in an enclosure adjacent to the casting pit. The actual temperature at the time of assembly was most likely somewhat less do to its movement through the ambient air which at the time of assembly was 30°F at the plant for both assemblies.

The temperature range between the four fixed housing temperature measurements taken off of the phenolic bonding surface prior to polysulfide application was 5° F. for the -20A nozzle and 13° F. for the -20B nozzle. Both are above the mean of 3° F, with the -20B having the largest temperature range of any segments processed to date (See Figure D-8). In addition, the high of 92° F. on the -20B nozzle is the highest temperature recorded to date (See Figure D-9). Higher temperature has the potential for reducing the polysulfide viscosity at time of assembly.

The average of four aft dome temperature measurements taken off of the insulation bonding surface prior to polysulfide application was 78.5° F. for both the -20A and -20B segments. This is slightly above the mean of 77.1° F., but well within the historical data base (See Figure D-10). The average temperature per the specification is 70 - 80° F.

The temperature range between the four aft dome temperature measurements taken off of the insulation bonding surface prior to polysulfide application was 1° F. for the -20A segment and 2° F. for the -20B. The -20A was slightly below the mean of 1.65° F. while the -20B was slightly above the mean. However, both were within the historical data base (See Figure D-11). In addition, the high of 79° F. for each of the segments was on the high side but within the historical data base (See Figure D-12).

The Delta between the average fixed housing phenolic bonding surface temperature and the average aft dome insulation bonding surface temperature prior to polysulfide application was a positive 2.3° F. for the -20A assembly and a negative 8° F. for the -20B assembly. The -20A was 4.3° F. above the mean of negative 2.0° F. while the -20B was 6.0° F. below. However, both were within the historical data base (see Figure D-13).

4.4   PERSONNEL

The manufacturing and inspection personnel involved in the assembly process were identified . The RSRM -20A nozzle was installed on day shift by "B" shift in Casting Pit #8. Tim Heyder, Badge #16905 was the Leadperson. The RSRM -20B nozzle was installed on graveyard by "B" shift in Casting Pit #1. Ronnie Hansen, Badge #17055 was the Leadperson. Both the Manufacturing crews and the Inspection Personnel have been involved in numerous assemblies. Lack of experience did not influence these assemblies.

4.5   TOOLING

All tooling determined to have a potential influence on the installation process was inspected for compliance to drawing requirements. This included the 4U127097 polysulfide application

Figure D-8. Fixed Housing Temperature Range

125

Figure D-8. Fixed Housing Temperature Range ((CONT)

Figure D-9. Fixed Housing Temperatures

127

DOME TEMPERATURE AT INSTALL NOZZLE

3σ Limits
For n=2:
UCL=84.7

$\bar{X}$=77.1

LCL=69.4

UCL=9.42

$\bar{R}$=2.88

LCL=0

TEMPERATURE IN DEG F

95
90
85
80
75
70
65

Moving Range

10
7.5
5
2.5
0

SIGMA

2 SIGMA

2 SIGMA

1 SIGMA

1 SIGMA

2 SIGMA

MEAN VALUE

MOTOR AND DATE

04MAR92

Figure D-10. Average Aft Boss Temperatures

DOME TEMPERATURE AT INSTALL NOZZLE

Figure D-10. Average Aft-boss Temperatures (CONT)

129

DOME TEMP RANGE AT INSTALL NOZZLE
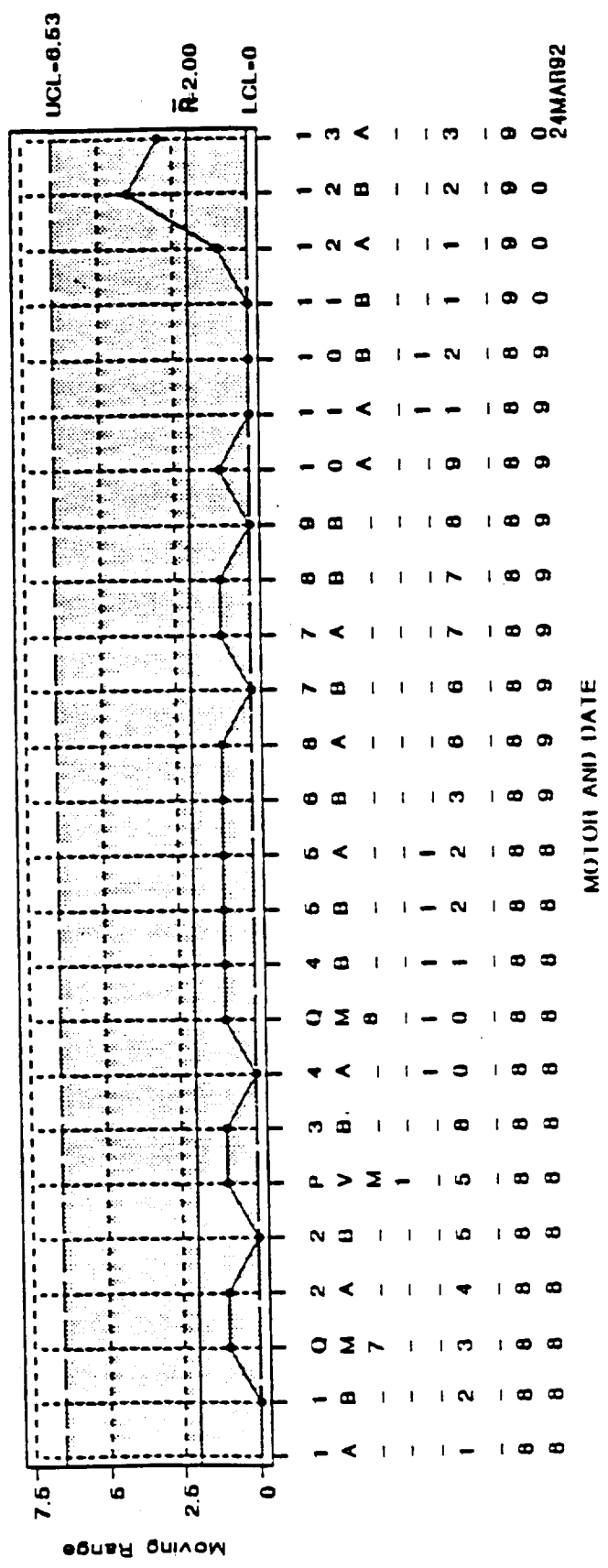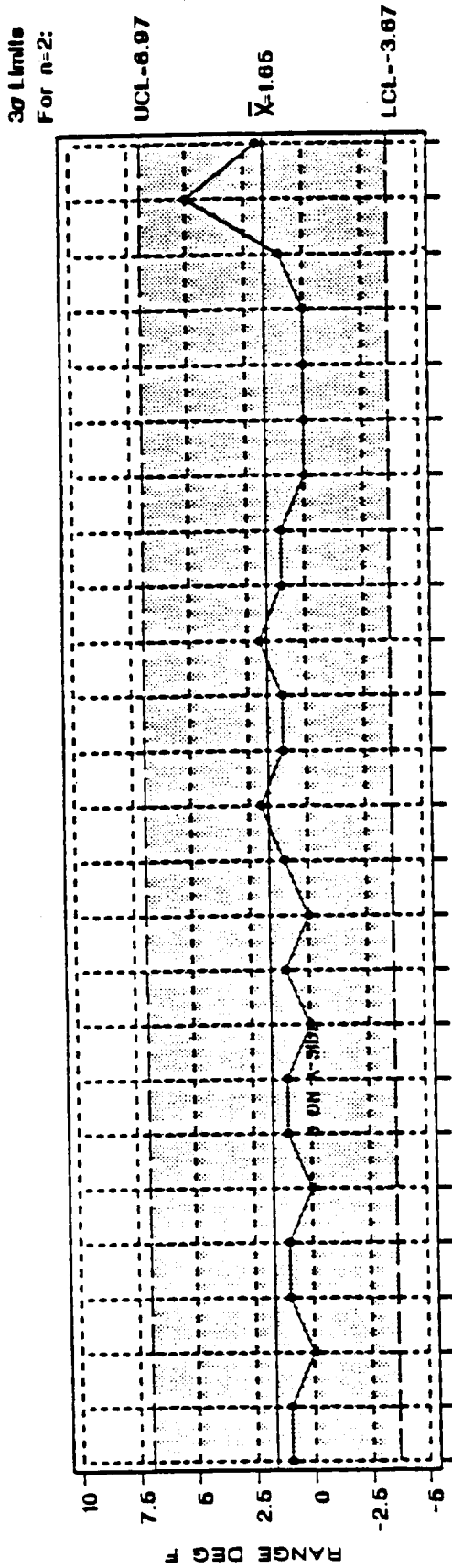
Figure D-11. Arc Ross Temperature Range

DOME TEMP RANGE AT INSTALL NOZZLE

Figure D-11. Aft Boss Temperature Range (CONT)

Figure D-12   Aft Boss Temperatures

Figure D-13. Aft boss to Nozzle Delta Temperature

133

Figure D-13. Aft Boss to Nozzle Delta Temperature (CONT)
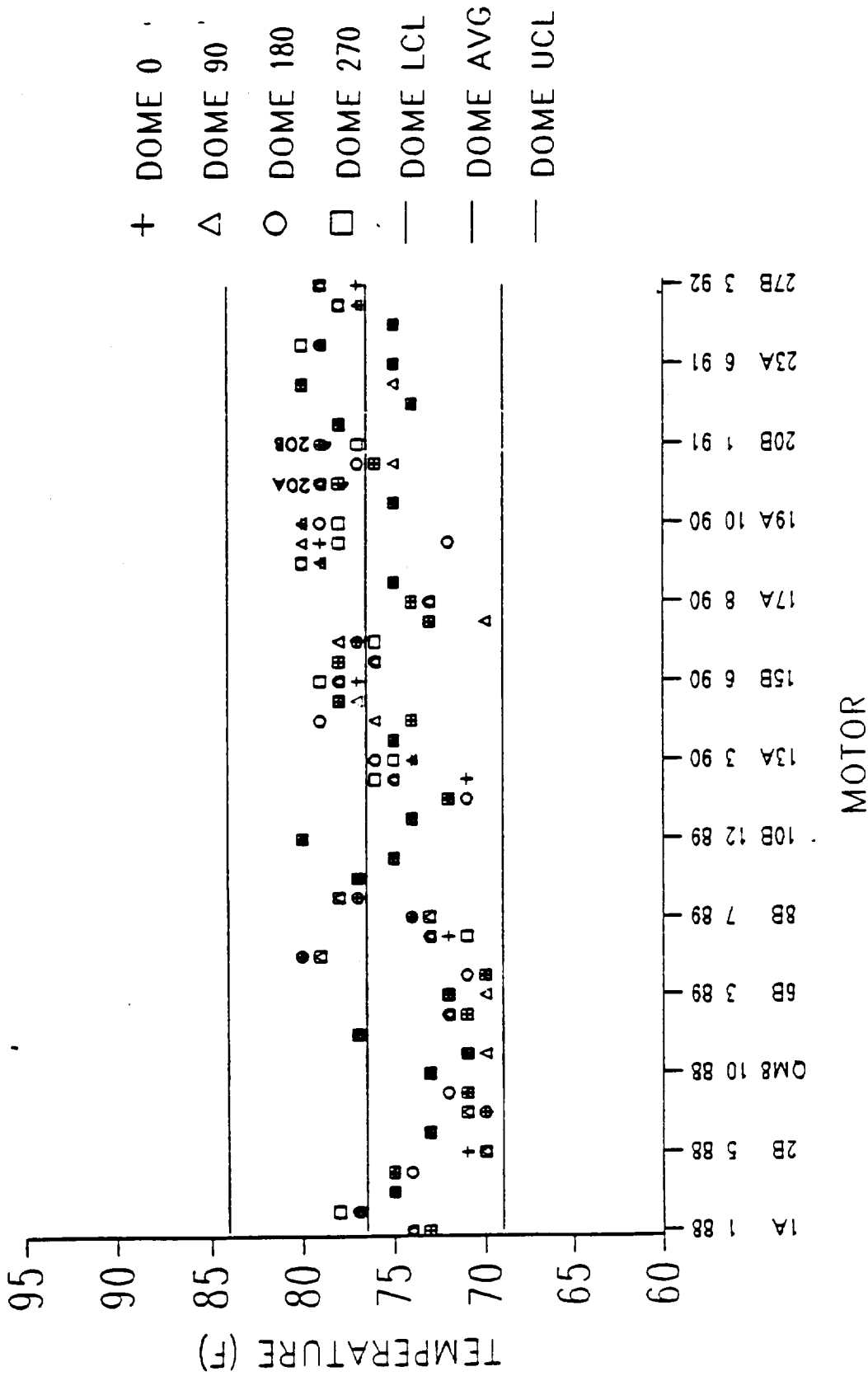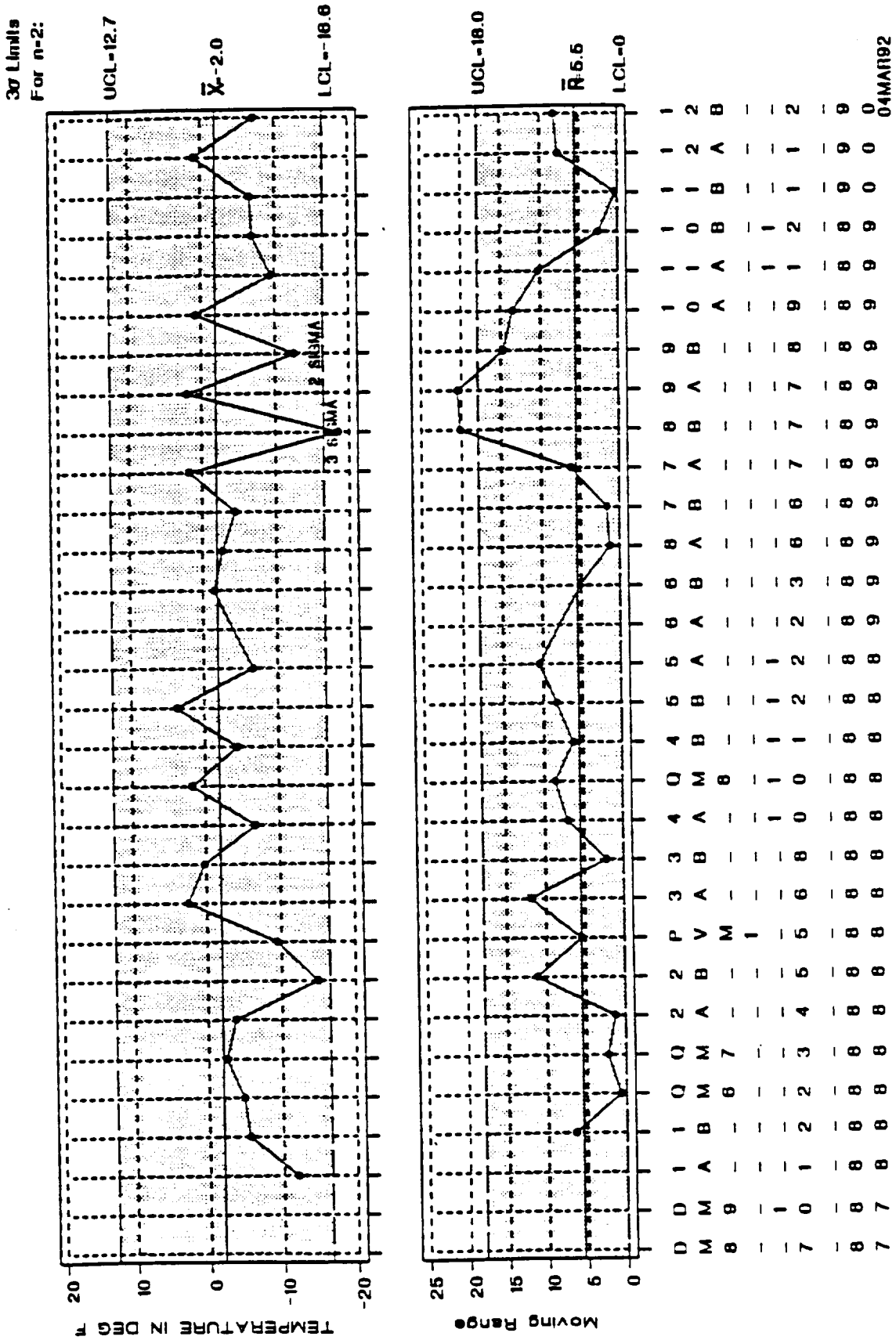
screeds and the various 2U65378 guide pins. The results indicated the all critical dimensions were within blue print requirements.

4.6   POLYSULFIDE MIXING

Review of the mix sheets used to produce the polysulfide per batchcard STW4-3811-2182 indicated that the polysulfide was properly weighed up and mixed. No anomalies were identified. The total mix times, which includes two each three minute vacuum mix cycles, interrupted by a blade scrape down were 14 and 13 minutes respectively. As stated previously, both mix times were below the mean of 17 minutes but well within the historical data base. Physical indications of proper mixing at end of mix was not available as there are currently no requirements for end of mix viscosity.

The shore "A" hardness of the three cure samples taken from each mix used for each installation was evaluated. Hardness after the cure is another indication of proper weigh up and mixing. The average hardness of three samples is taken immediately following cure. An average shore "A" hardness of 37 was obtained on the -20A segment while an average shore "A" hardness of 30 was obtained on the -20B segment. Both average measurements are near the mean of 35.7 and were within the historical data base (See Figure D-14).

4.7   POLYSULFIDE APPLICATION METHOD

Following receipt of the polysulfide at the casting pits from the M-52 mix room, the application process begins. A total of four operators are required to complete the application. Beginning at unspecified degree locations approximately 180° apart, the application is accomplished with one operator applying the polysulfide bead from the SEMCO cartridge in front of the 4U127097 screed, positioned and moved by the other operator. A typical application process has both teams rotating clockwise until both halves are covered. At this point, one screed will be removed and the other may continue around the boss until the appearance of the polysulfide bead appears to be correct. The last screed is then removed when the last team is satisfied that the application is adequate. The acceptance criteria is subjective.

Review of the video of the -20B polysulfide application process indicated that the application began at 0 and 180°. The removal of the screed did not affect the gas path location at 247°. Based on interview with the manufacturing crews, it is believed that the removal of the screed did not affect the gas path on the -20A segment, located at 57.6°.

Review of all available videos, observations by various engineering organizations and discussions with manufacturing crews established the fact that the application technique can generate small voids. In addition, the speed of the screed and bead application has an effect on the final profile of the bead.

The weight of the polysulfide applied to the aft dome insulation was 11.54 lbs for the -20A and 11.74 lbs for the -20B. This is within the

Figure D-14 Polysulfide Hardness

136

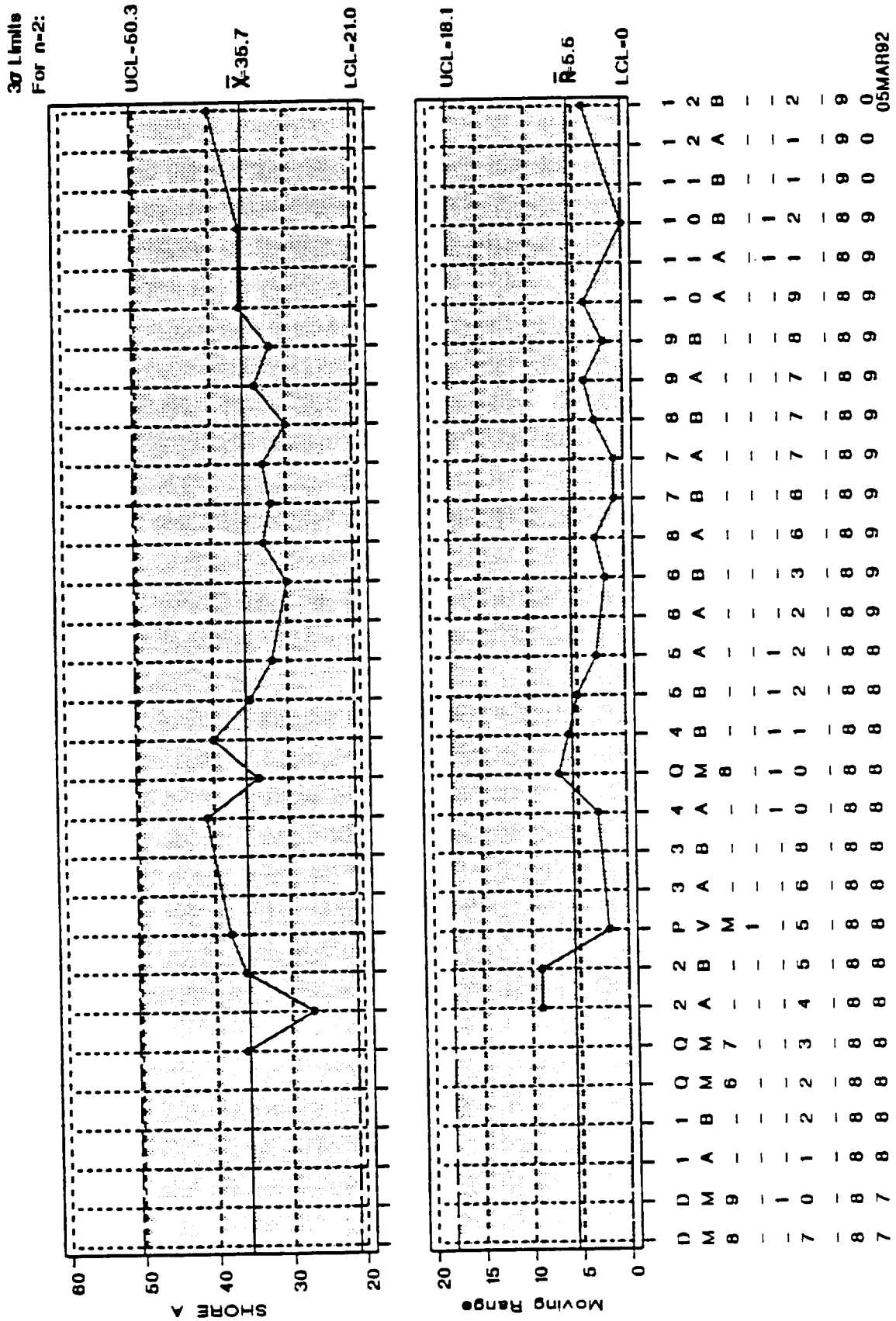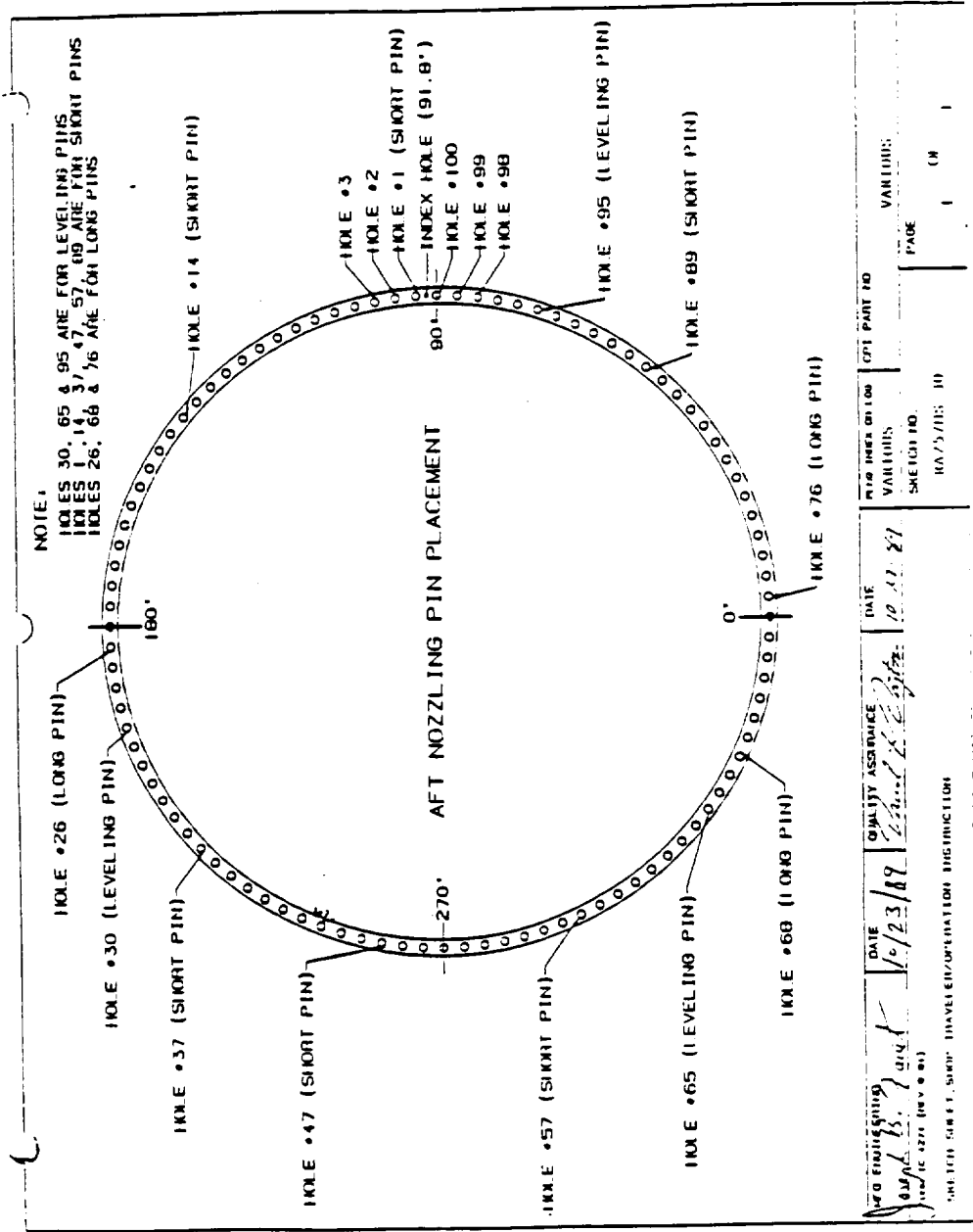# POLYSULFIDE HARDNESS AFTER CURE

Figure D-14. Polysulfide Hardness (CONT)

137

historical data base. However, the data does not represent what is actually in the joint. Material loss due to application variables and extrusion during assembly affect the final weight in the joint.

4.8   CONCENTRICITY

The influence of out of round conditions on the assembly was evaluated. Concentricity is controlled during assembly by the use of three each long tapered guide pins (36-inches long) and six each short tapered guide pins (8.5-inches long) which are positioned in the axial bolt holes on the aft boss. The guide pins are installed at various locations to force the fixed housing and aft boss to conform to each others shape (see Figure D-15). The long guide pins begin the initial "rounding" with the final shape accomplished by both the long and short guide pins at 5-inches from seating. The clearance between the fixed housing through holes and the guide pins is .020 to .032 inches. The maximum condition of .032 inches is the controlling factor until approximately 3 inches from seating when the wiper O-ring on the fixed housing enters the aft boss. At this point, the guide pins are no longer controlling the assembly. The metal tolerances of the fixed housing and aft boss are tighter than the guide pin to fixed housing through holes and the components now control the assembly clearances. The long guide pins begin the "rounding" with the final shape accomplished by both the long and short guide pins at 5 inches from seating.

NOZZLE-TO-CASE JOINT ASSEMBLY

Figure D-15. Guide Pin Positions

APPENDIX E - MATERIALS ASSESSMENT

Polysulfide Assessment

During the course of the investigation into the cause of gas paths in the 20A and 20B nozzle-to-case joint, the review of the manufacturing records indicated Lots 036 and 037 polysulfide (Stock Number 4907) were used. The review of the raw material lot acceptance results showed Lots 036 and 037 to have out-of-history application life (extrusion through a Semco tube at a given time, temperature, and pressure). Figure E-1 shows the out-of-history condition. All other lot acceptance test results were within historical bounds. The lot acceptance test results prompted the question whether the lot acceptance results were correct or not and what they meant. It was decided to locate all available 4907 polysulfide lots. Efforts to locate material found Lots 043, 042, 041, and five kits (quarts) of scrap Lot 037. Later, remnants of Lot 039 were also found in the M-52 mixing room.

An informal test plan was agreed upon to test the available lots for flow (per ASTM D2202), Brookfield viscosity (HBTD, spindle TD, 5 rpm), application life (per STW4-3311) and slump (on a subscale ring with correct axial profile per ETP-0876). Kits from Lots 043, 042, 041, 039, and 037 were obtained for testing and comparison. One mix of each lot of polysulfide was made with the noted tests run concurrently on each mix. Testing involved running the flow, viscosity, and application life tests over time at 70-75°F to generate profiles for subsequent comparison and analysis. The test environment was in Building M-43 where temperature was controlled to 70-75°F and relative humidity was under 10 percent. Figures E-2, E-3, and E-4 are plots of the results. Slump on the subscale ring model was very close to the same for all lots. The actual slump profiles are documented in the Engineering Assessment (Appendix B). A review of previous test reports found TWR-16599 to contain some of the above noted tests which were run previously on Lots 037 and 041 in February 1991 and which closely correspond with results from the later testing. A review of available reports with viscosity profiles also found Lots 042 and 043 to be more representative of typical materials. Also learned from the report review is the effect of high humidity on cure time. Higher humidity decreases cure tack-free time.

The following things were learned from this initial phase of testing:

1. Lot 037 viscosity build is significantly slower than the other four lots tested

2. Lot 037 flow down a vertically-oriented, graduated aluminum bar was the lowest of the five lots tested

3. Lot 037 application life as measured by Semco tube extrusion was the highest of the lots tested (120 gms/min) and confirmed the original lot acceptance test results (127 gms/min)
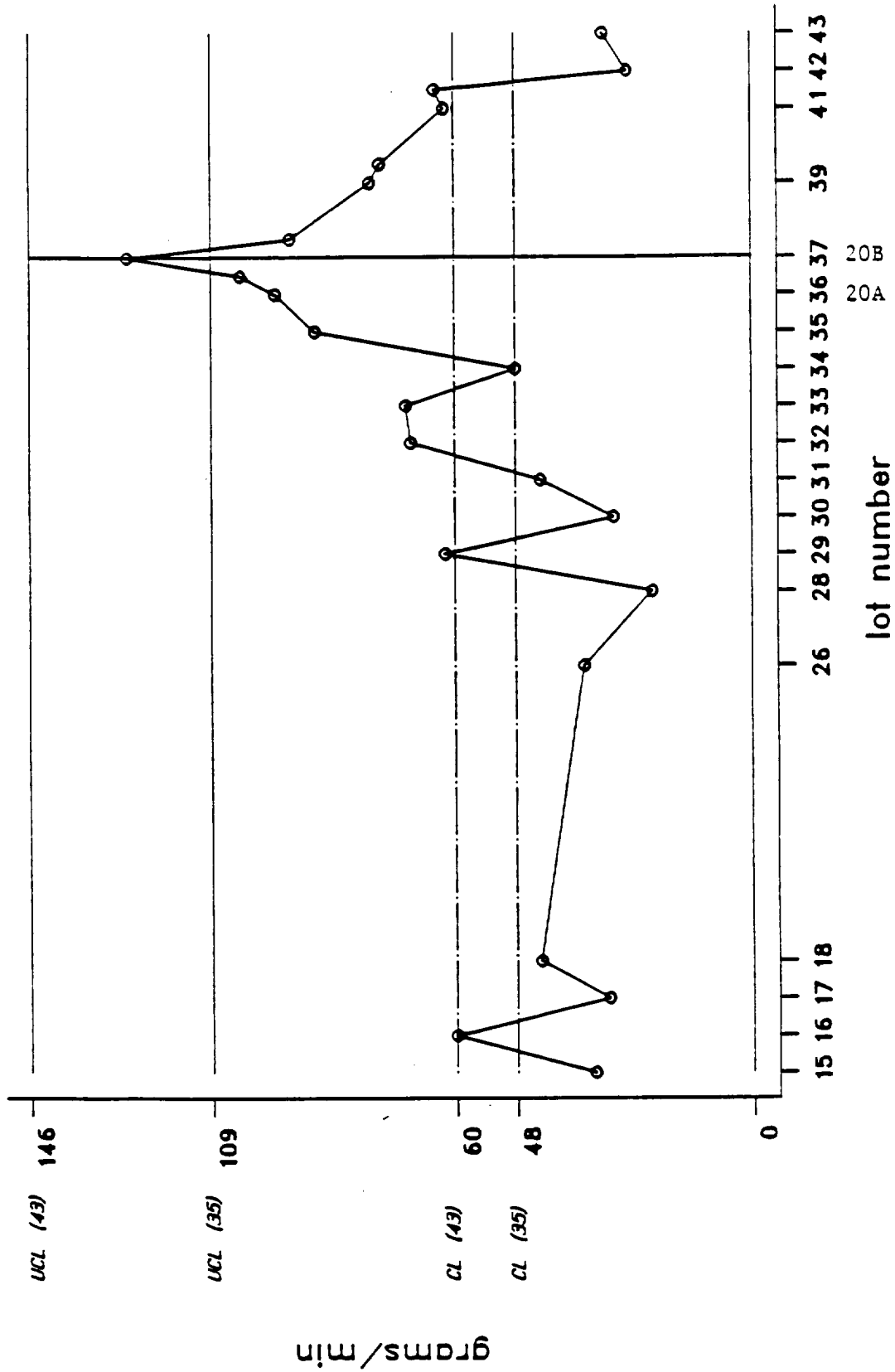
Figure E-1. Application Life (Extrusion) Acceptance History for 4907 Polysulfide

fs'1   3-25-72

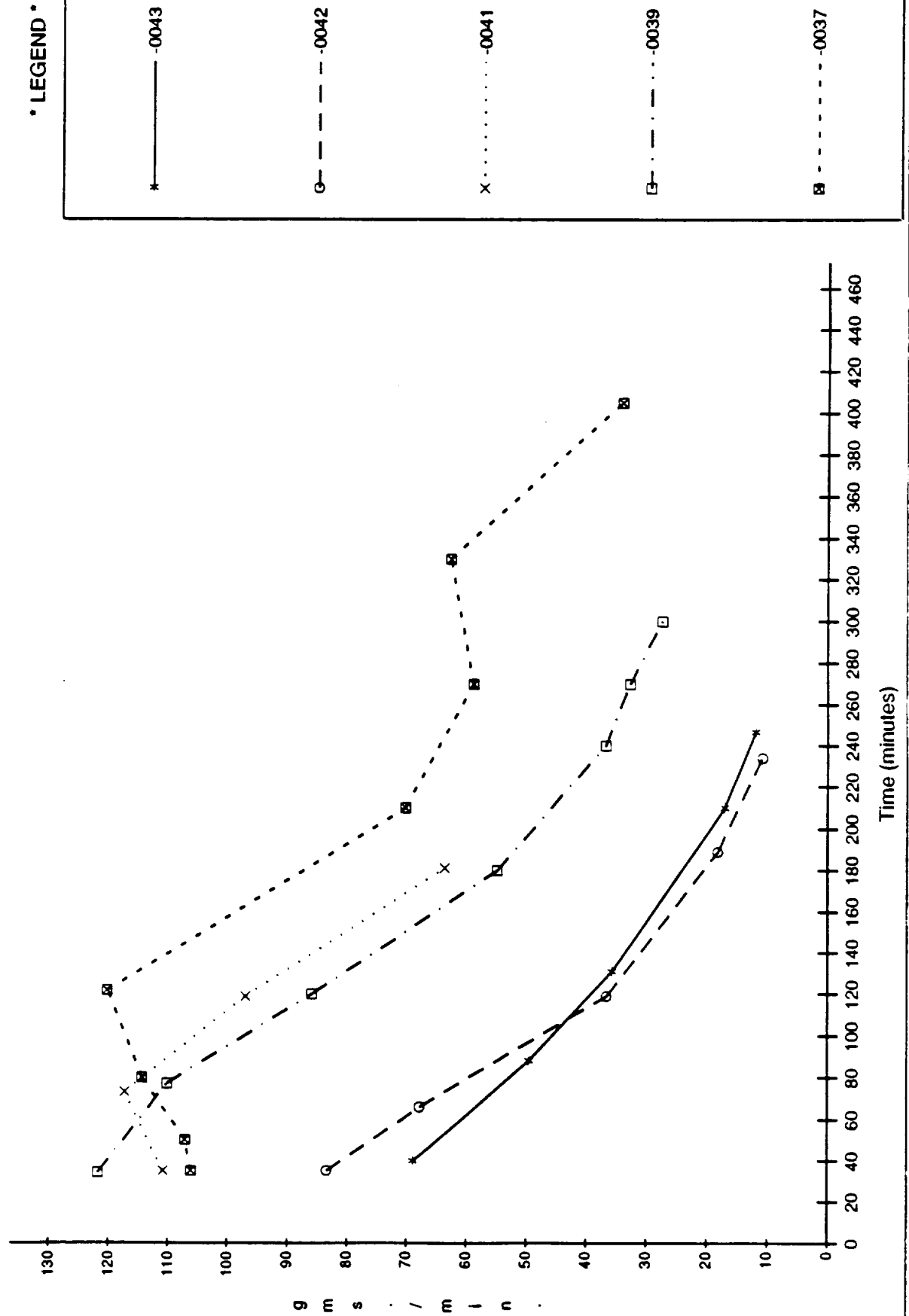4907 POLYSULFIDE APPLICATION LIFE (EXTRUSION) @ 70-75 F

LEGEND

-0043
-0042
-0041
-0039
-0037

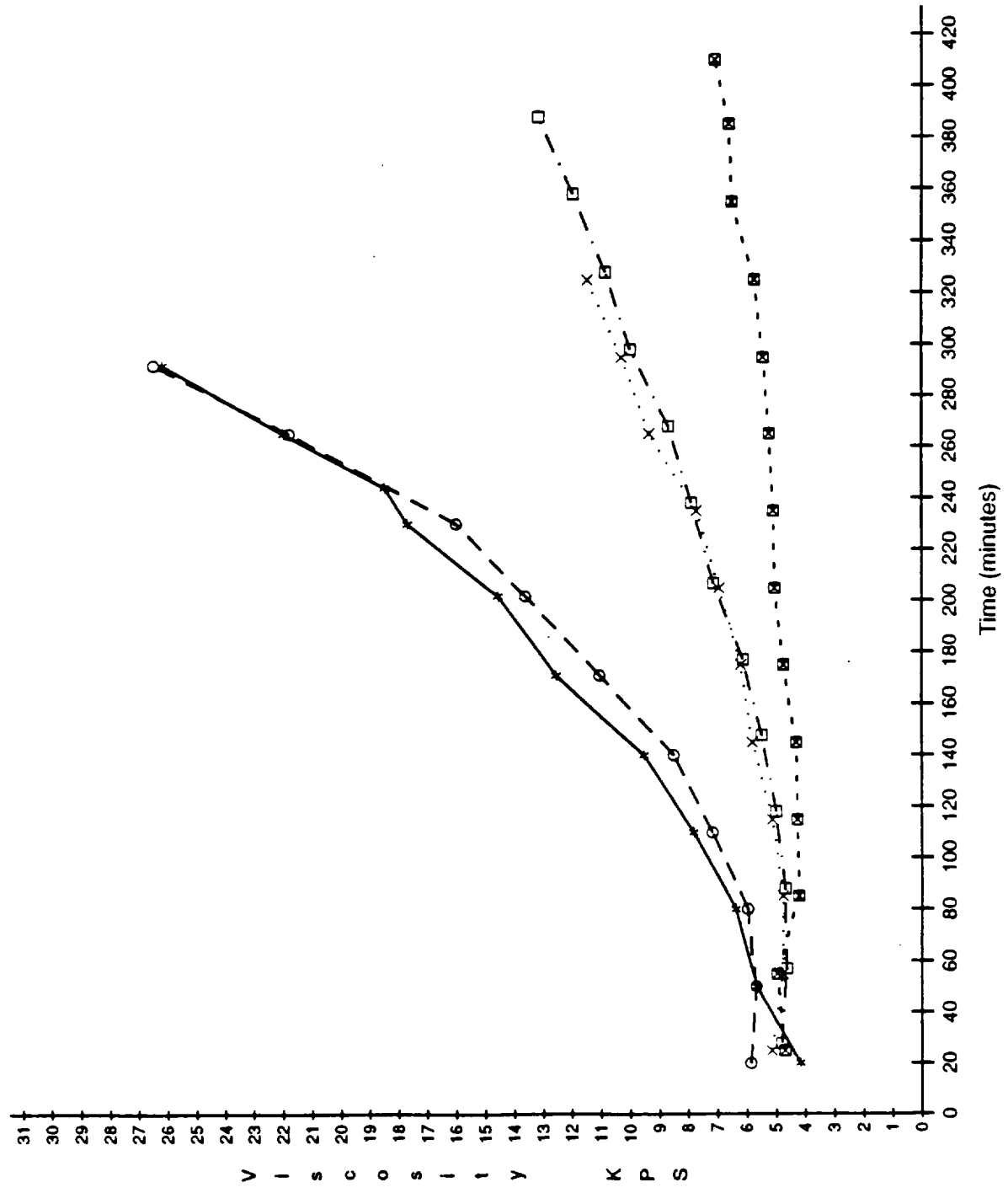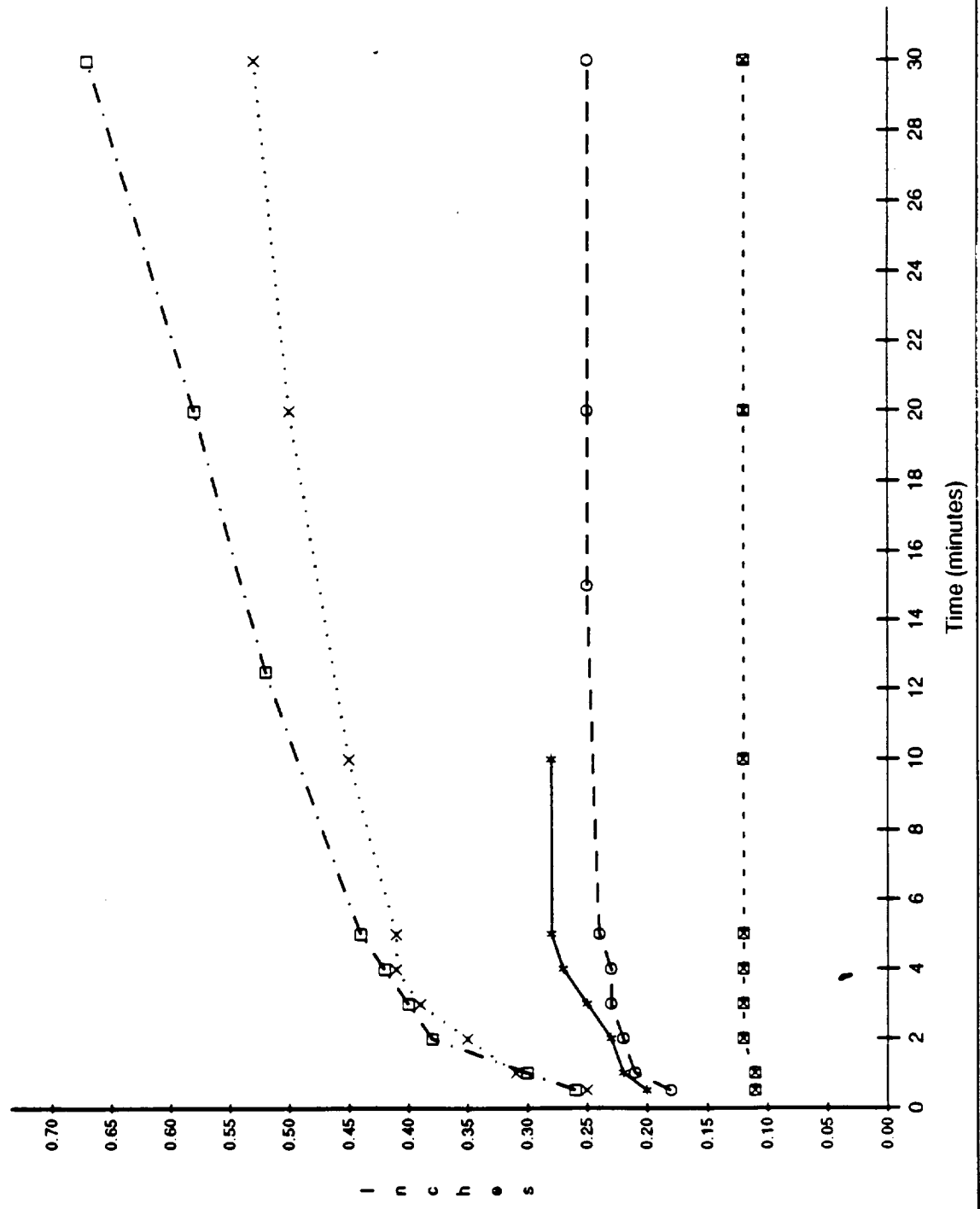Time (minutes)

Figure E-2   Polysulfide Application Life Testing In M-73

142

Figure F-3. Polysulfide Viscosity (Brookfield) Testing in M-43

4907 POLYSULFIDE FLOW @ 70-75 F

Vertical Graduated Aluminum Bar

Time (minutes)

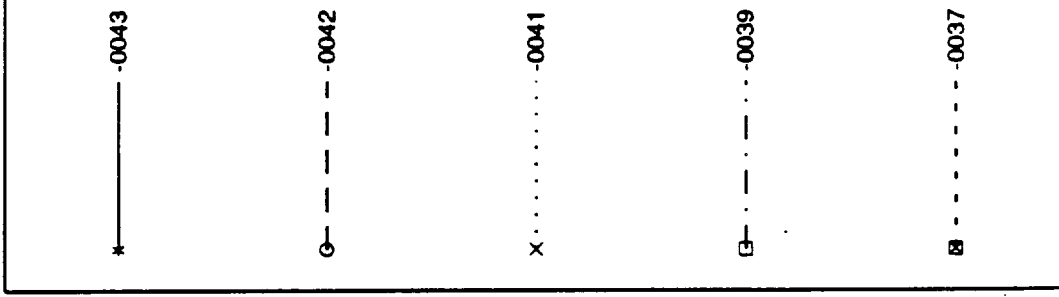LEGEND

-0043
-0042
-0041
-0039
-0037

PSI   3-23-92

144

4. Flow per ASTM D2202 (down a vertically-oriented, graduated aluminum bar) and viscosity at the noted shear rate did not correlate indicating flow may be a function of another property (i.e., thixotropy)

5. Slump on the subscale joint ring and viscosity do not correlate. Flow and slump are probably different measures of the same properties

6. Application life (extrusion) and viscosity do correlate (See Figure E-5) indicating that extrusion is a function of viscosity

7. There is significant variability in the material lots of polysulfide tested

The knowledge that Lot 037 (20B) polysulfide was found to be slow to build viscosity over time and flowed the least of the lots tested, prompted the next question. Could the atypical viscosity build influence the air pressure required to form a gas path during assembly? CAD analysis indicated 1.15 psi could be generated based on a predicted volume between the aft dome and fixed housing from the time the fixed housing phenolic engaged the polysulfide until the wiper O-ring vented through the vent slots.

It was learned that a set-up existed to test polysulfide for response to air pressure. The set-up consisted of two plexiglass plates shimmed apart and bolted together with a port in the center of one of the plates from which to draw vacuum. Polysulfide was screeded in a uniform circle (6-inch I.D.) using the port in the plexiglass plate as the center of the circle (screed was indexed from the port). The plexiglass plates were then placed together with the appropriate shims between the plates and clamped together. The screeded polysulfide ring would effectively seal between the plates. A mercury (Hg) manometer and a bleed valve in line to a vacuum source allowed the air pressure to be varied between the I.D. and the O.D. of the polysulfide ring (ambient air pressure). The test set-up is shown in Figure E-6 with uncatalyzed base polysulfide. Vacuum was applied starting with 1-inch Hg and being increased by increments of 1-inch Hg at 1-minute intervals (i.e., at time = 0: 1-inch Hg, at time=1 minute: 3 inch-Hg, etc.) until the polysulfide ring failed by formation of a gas path. A stopwatch was used to measure the time from start of vacuum to failure.

The above test rate was selected based on the actual seating process of the full scale nozzle. The full scale nozzle is lowered in increments at one minute intervals. The actual time at failure and the vacuum (inches-Hg) along with calculated air pressure differential are shown in Tables 1 and 2. The viscosity values shown in Table 2 were taken when the air pressure experiment (Table 1) was performed.

Typical gas path shapes are shown in Figures E-7, E-8, and E-9. The shapes are similar to the failure gas paths on the 20A N/C joint. The polysulfide failures in the plexiglass plate model would occur after some level of vacuum (air pressure) caused the polysulfide to move and an oval-shaped bubble would form and begin to move through the polysulfide ring until a gas path had breached the ring width. Most of the testing was with a 1.2-inch wide screed and 0.085-inch thick shims (See Figure E-10). Some variations in screed widths and shim thickness were made to understand polysulfide response to the individual model parameters (See Figures E-11
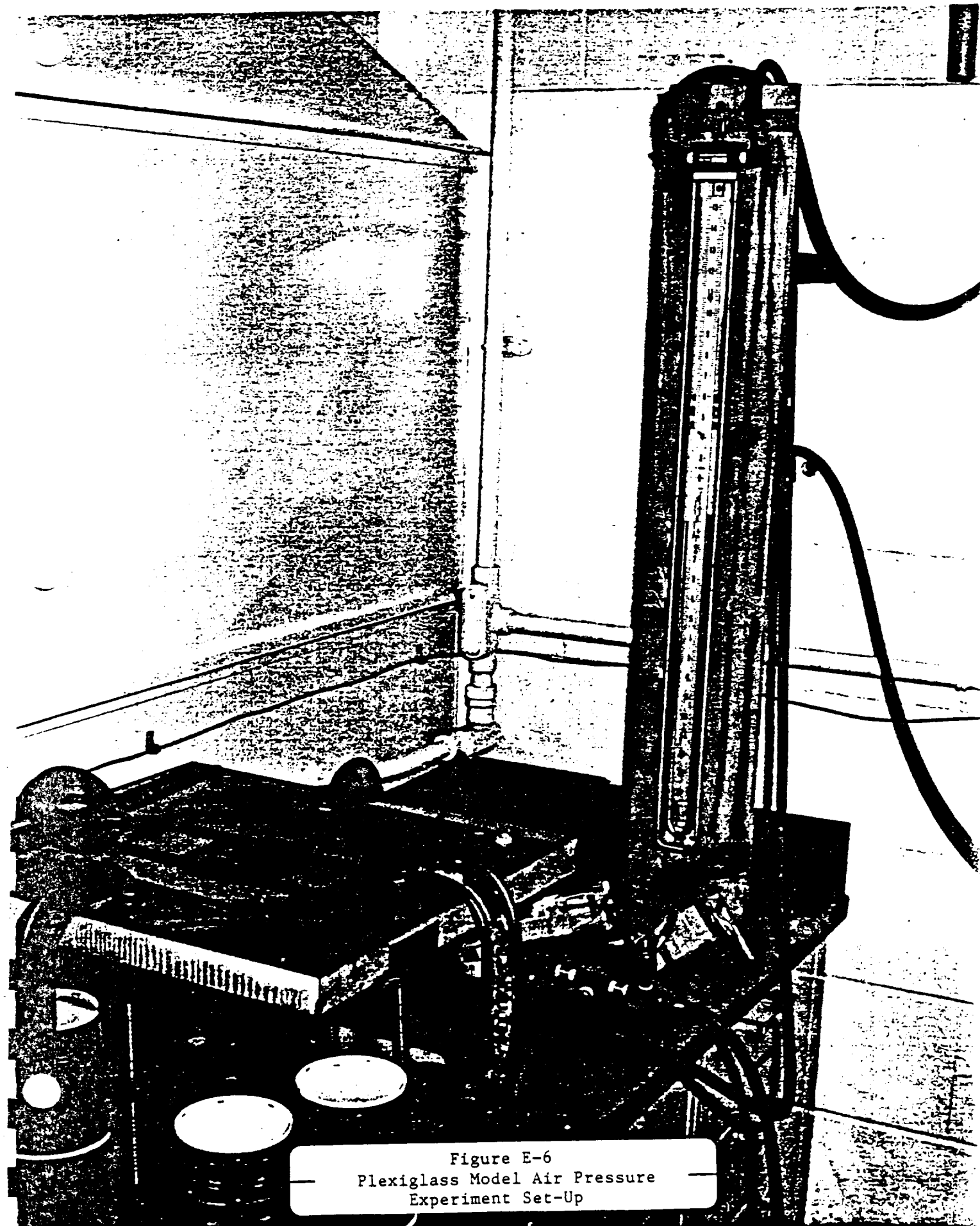
4907 POLYSULFIDE FOR NOZZLE-TO-CASE JOINT

Viscosity vs. Application Life (Extrusion) @ 70-75 F

* LEGEND *

*	-0043
O	-0042
×	-0041
☐	-0039
⊠	-0037

Application Life (gms./min.)

Polysulfide Viscosity versus Application Life Correlation

Figure E-6
Plexiglass Model Air Pressure
Experiment Set-Up

TABLE I. AIR PRESSURE EXPERIMENTS

<u>Air Pressure Model Parameters (Unless Otherwise Noted)</u>
  1.2" Wide PS Ring, 0.085" Thickness, Temp 70-75 Deg. F

4907 Mat'l Lot	Start Vac To Failure (Min:Sec)	Vacuum In-Hg @ Failure	PSI @ Failure	Test Date	Start of Mix to Test (Min)
-0043 Base Only	2:24	3.0	1.5	2/23/92	N/A
-0043	2:37	3.0	1.5	2/24/92	48
-0043	3:55	4.0	2.0	2/24/92	91
-0043	3:43	4.0	2.0	2/24/92	139
-0043	4:20	5.0	2.5	2/24/92	208
-0043	4:50	5.0	2.5	2/24/92	258
-0043	5:50	6.0	3.0	2/24/92	297
-0041 Base Only	2:35	3.0	1.5	2/24/92	N/A
-0041	3:38	4.0	2.0	2/26/92	48
-0041	3:19	4.0	2.0	2/26/92	97
-0041	3:49	4.0	2.0	2/26/92	159
-0041	3:59	4.0	2.0	2/26/92	219
-0041	5:10	6.0	3.0	2/26/92	281
-0041	5:16	6.0	3.0	2/26/92	339
-0037 Base Only	2:39	3.0	1.5	2/27/92	N/A
-0037	3:25	4.0	2.0	2/27/92	39
-0037	4:15	5.0	2.5	2/27/92	108
-0037 (90.°F)	3:59*	2.0	1.0	2/27/92	130
-0037	3:57	4.0	2.0	2/27/92	170
-0037	4:26	5.0	2.5	2/27/92	270
-0037	3:30	4.0	2.0	2/27/92	361
-0037	4:28	5.0	2.5	2/27/92	453
-0037	4:47	5.0	2.5	2/27/92	542
-0037	5:37	6.0	3.0	2/27/92	634
-0037 .5" Wide	1:59	1.0	0.5	2/27/92	72

TABLE I. AIR PRESSURE EXPERIMENTS

Air Pressure Model Parameters (Unless Otherwise Noted)
1.2" Wide PS Ring, 0.085" Thickness, Temp 70-75 Deg. F

4907 Mat'l Lot	Start Vac To Failure (Min:Sec)	Vacuum In-Hg @ Failure	PSI @ Failiure	Test Date	Start of Mix to Test (Min)
-0037 .5" Wide	3:18	2.0	1.0	2/27/92	184
-0037 .5" Wide	3:32	2.0	1.0	2/27/92	326
-0037 .75" Wide	4:53	2.5	1.25	2/27/92	84
-0037 .75" Wide	4:43	2.5	1.25	2/27/92	197
-0037 .75" Wide	5:42	3.0	1.50	2/27/92	343
-0042 Base Only	5:59*	3.0	1.5	3/3/92	N/A
-0042 Base Only	4:45*	2.5	1.25	3/3/92	N/A
-0042 Base Only 0.328 Shims	1:15*	1.0	0.5	3/3/92	N/A
-0042 Base Only 0.145 Shims	3:35*	2.0	1.0	3/4/92	N/A
-0042 Base Only 0.145 Shims	3:32*	2.0	1.0	3/4/92	N/A
-0042 Base Only 0.204 Shims	2:12*	1.0	0.5	3/4/92	N/A
*NOTE: In-Hg started @ 0.5 and increased 0.5 in-hg each minute until failure.					

TABLE I. AIR PRESSURE EXPERIMENTS

Air Pressure Model Parameters (Unless Otherwise Noted)
1.2" Wide PS Ring, 0.085" Thickness, Temp 70-75 Deg. F

4907 Mat'l Lot	Start Vac To Failure (Min:Sec)	Vacuum In-Hg @ Failure	PSI @ Failure	Test Date	Start of Mix to Test (Min)
-0039	3:28	4.0	2.0	3/19/92	54 Min
-0039 HD-2	3:17	4.0	2.0	3/19/92	105 Min
-0039 TCA	3:22	4.0	2.0	3/19/92	135 Min
-0039	4:20	5.0	2.5	3/19/92	228 Min
-0039	5:06	6.0	3.0	3/19/92	287 Min
-0039	5:08	6.0	3.0	3/19/92	386 Min

TABLE II. VISCOSITY DURING POLYSULFIDE AIR PRESSURE EXPERIMENTS

4907 Material Lots	Test Date	SOM to Test (Min)	Viscosity @ 70-75°F Kps
-0043	2/24/92	29	5.37
		59	5.56
		95	6.64
		123	7.15
		153	8.11
		183	9.14
		215	10.83
		240	12.20
		276	14.24
		312	16.57
-0041	2/26/92	34	6.68 (62 Deg. F)
		64	6.10 (67 Deg. F)
		79	5.45 (69 Deg. F)
		94	5.16 (70 Deg. F)
		124	5.31 (71 Deg. F)
		155	5.52
		184	5.76
		215	6.38
		244	6.97
		275	7.75
		305	8.55
		326	9.05
		352	9.59

TABLE II. VISCOSITY DURING POLYSULFIDE AIR PRESSURE EXPERIMENTS

4907 Material Lots	Test Date	SOM to Test (Min)	Viscosity @ 70-75°F Kps
-0037	2/27/92	31	4.08
		61	4.17
		91	4.17
		121	4.13
		151	4.63
		211	4.75
		241	4.95
		272	5.08
		301	5.31
		331	5.35
		363	5.54
		392	5.72
		421	5.93
		456	6.38
		481	6.46
		511	7.00
		546	7.43
		571	7.85
		601	8.13
		639	9.22

TABLE II.   VISCOSITY DURING POLYSULFIDE AIR PRESSURE EXPERIMENTS

4907 Material Lot	Test Date	SOM to Test (Min)	Viscosity @ 70-75°F Kps
-0039	3/19/92	28	4.80
		57	4.64
		88	4.69
		118	4.99
		148	5.48
		177	6.12
		207	7.13
		238	7.90
		268	8.68
		298	9.99
		328	10.85
		358	11.97
		388	13.16
		409	14.04

Figure E-7
Polysulfide Gas Path Formation
in Plexiglass Model   154

Figure E-8
Polysulfide Gas Path
in Plexiglass Model

155

Figure E-9
Beginning of Polysulfide Gas Path
Formation in Plexiglass Model 156

Figure E-10
Screeded Polysulfide Ring
Between Plexiglass Plates

157

and E-12). All the testing was performed at 70-75°F with humidity under 10 percent RH except one data point was taken at 100°F.

During testing of Lot 039 material, two contaminants were tested for their affect on gas path formation. The first contaminant tested was Conoco HD-2 grease. It was tested by smearing a half-inch wide grease path on one of the plexiglass plate halves to see if the contamination would facilitate a gas path through the polysulfide ring. The failure (gas path) did not occur at the greased location. The second contaminant tested was methylchloroform. A circle of polysulfide was screeded on the plexiglass model with methylchloroform liberally poured across a two-inch portion of the screeded ring. The failure (gas path) did not fail at the methylchloroform-treated portion of the screeded polysulfide ring. Figure E-16 shows the contamination test results. Plots of the other test results are shown in Figures E-13 through E-19 (Photo Negative #127384).

Figure E-19 suggests that perhaps another variable, thixotropy, also influences air pressure required to form a gas path. Lot 043 initially required lower air pressure to form a gas path than Lot 037. Efforts to understand the rheological response of the polysulfide better began with additional viscosity tests on Lots 037 and 043 at three different shear rates using a Contraves Rheomate 135 rheometer (cup and bob size 125), which measures steady tangential annular flow. The results indicated that the polysulfide exhibits non-Newtonian behavior and was identified as a shear thinning (pseudoplastic) material. The results are shown in figures E-20 and E-21. Differences between materials were better illustrated by plotting the log shear stress vs the log shear rate (See Figures E-22 and E-23). The slopes substantiate that the material is non-Newtonian, the slope of a Newtonian fluid = 1.0 while slopes <1.0 are shear thinning. The extent by which slopes are less than 1.0 indicates more flow/lower viscosity with increases in shear rate. Lot 043 had a lower slope (0.50) than Lot 037 initially, but achieved a shear thinning minimum 60 minutes from end of mix. Lot 037 started at a higher slope initially (0.55), but stayed there longer requiring 200 minutes to achieve the same shear thinning minimum (slope of 0.64). The higher shear thinning of Lot 037 material probably made it less resistant to gas paths as substantiated by the plexiglass model results. The air pressure experiment responses noted in Figure E-19 where Lot 043 initially required only 1.5 psi to create a gas path and Lot 037 required 2.0 psi and remained at 2.0 psi for quite some time correlate with the noted shear thinning slopes. When these results are considered in conjunction with the start of mix time to N/C joint seating times for 20A and B, it puts the difference in material response in the proper perspective. The seating times were 130 and 134 minutes, respectively, from start of mix. The results indicate that the Lot 037 material was less shear resistant than Lot 043 and therefore probably less gas path resistant than other lots. Gas path resistance appears to be driven by both viscosity and thixotropy (or factors which contribute to thixotropy, i.e., molecular chain size or shape).

Some chemical analysis was also performed on different lots of polysulfide. Fourier-transform infrared (FTIR) analysis was run on cured and uncured samples of Lots 037, 042, and 043. The uncured samples of base and accelerator were run and compared. FTIR scans are not included but can be obtained from the author or the R&D Laboratory (see Attachment I and LWR-668454).

Inherent weaknesses in the plexiglass plate testing are the configuration of the plates (flat rather than to the actual profile

4907-0037 POLYSULFIDE AIR PRESSURE EXPERIMENT @ 70-75 F
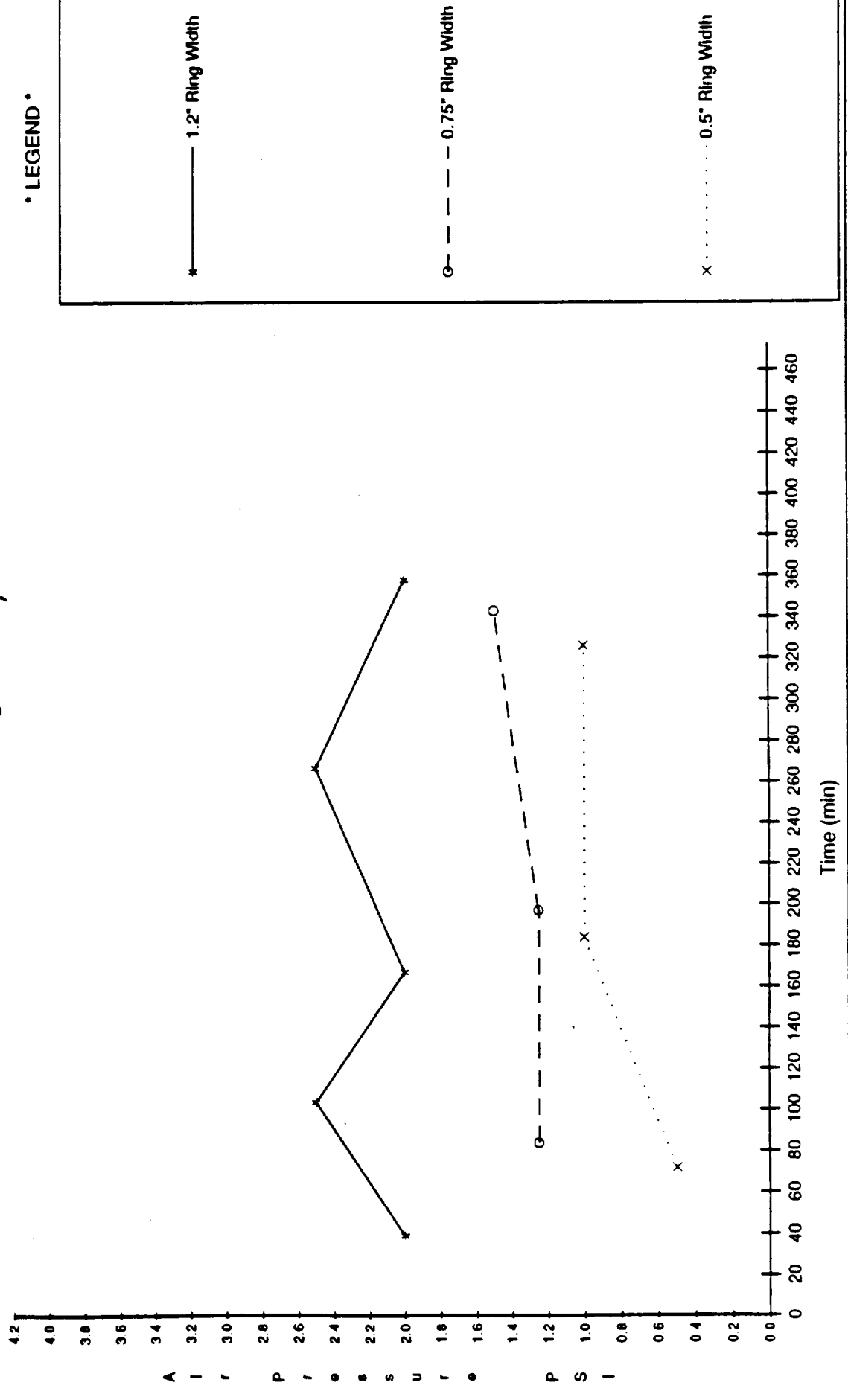
Testing 2-27-92 , .085" Thickness

* LEGEND *

——————*—————— 1.2" Ring Width

— — —O— — — 0.75" Ring Width

·······×······· 0.5" Ring Width

Time (min)

Figure F-11.   Screeded Polysulfide Ring Width Effect on Required Air Pressure
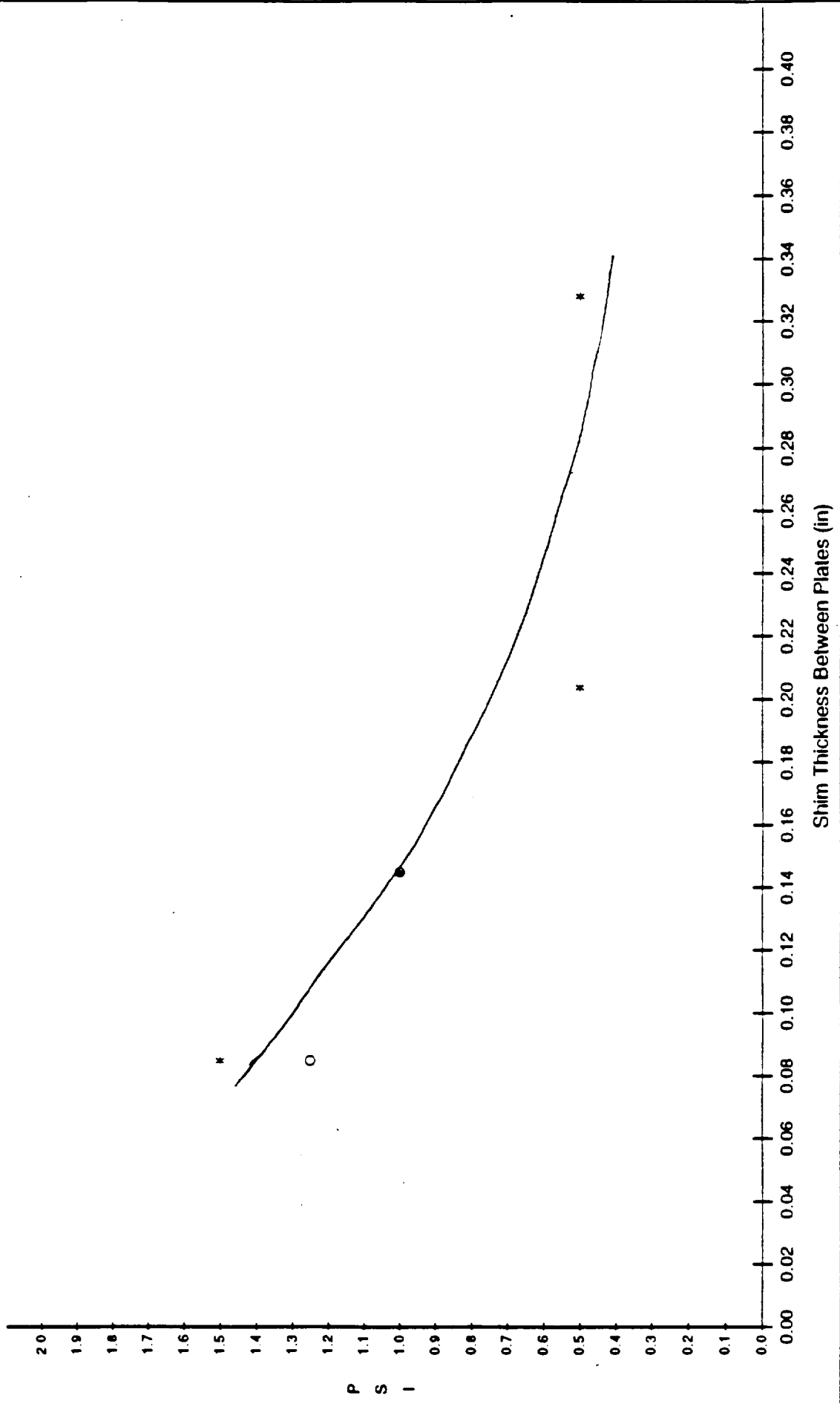
Figure E-12.   Screeded Polysulfide Ring Thickness Effect on Required Air Pressure

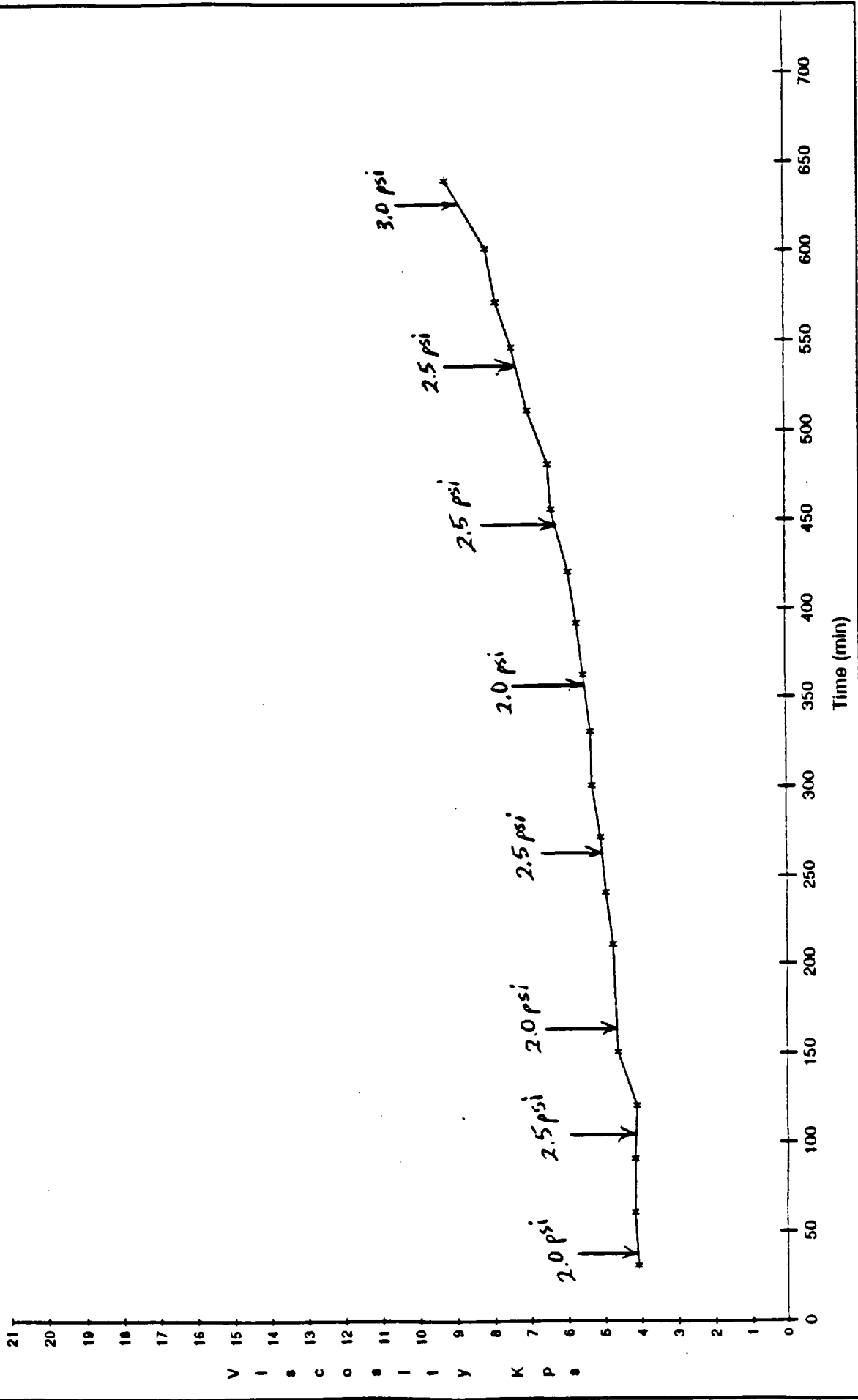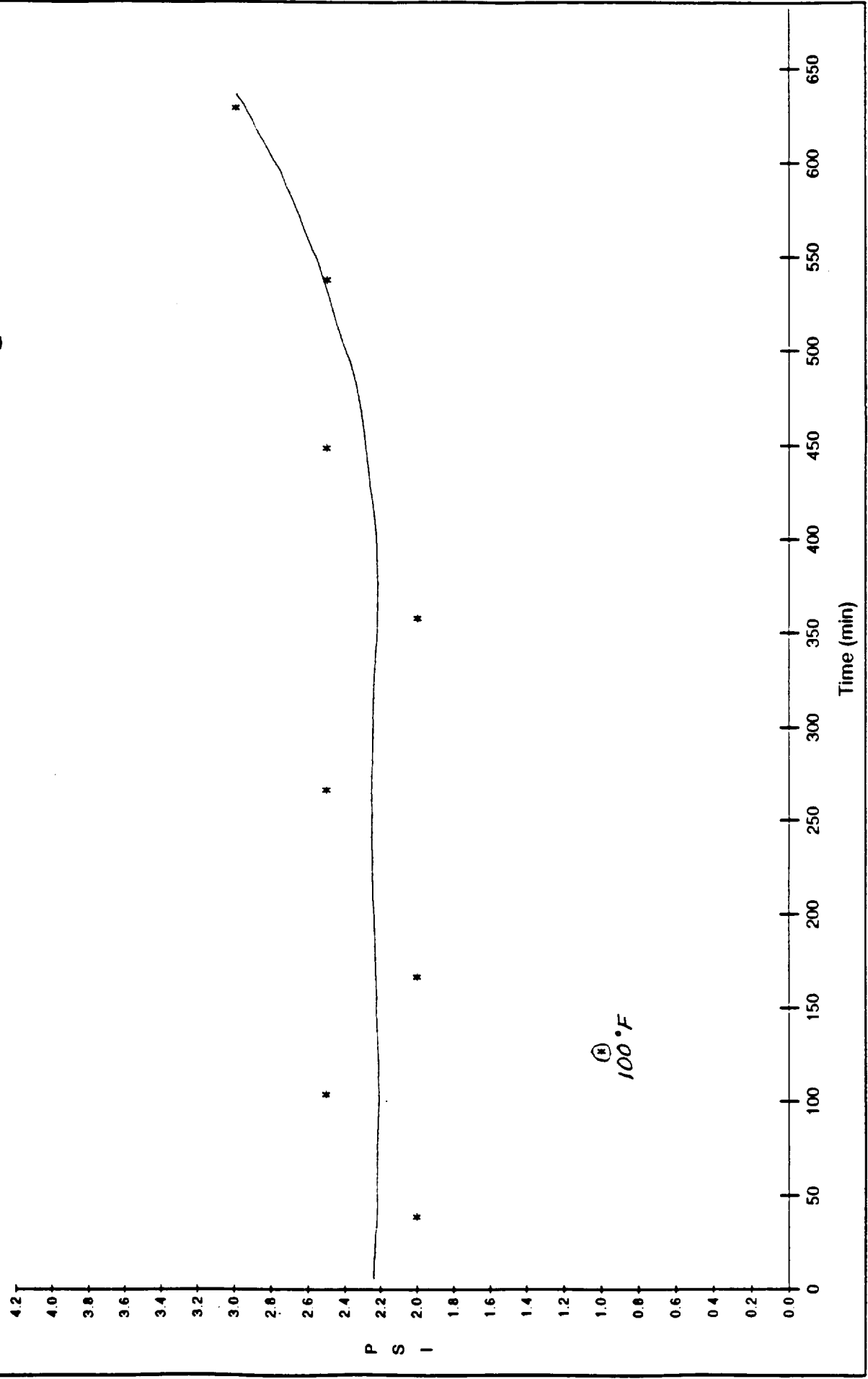Figure E-13. Air Pressure Required to Form Gas Path During Viscosity Build of Lot-0043

4907-0043 POLYSULFIDE AIR PRESSURE EXPERIMENT

Air Pressure vs. Viscosity, 70-75 F
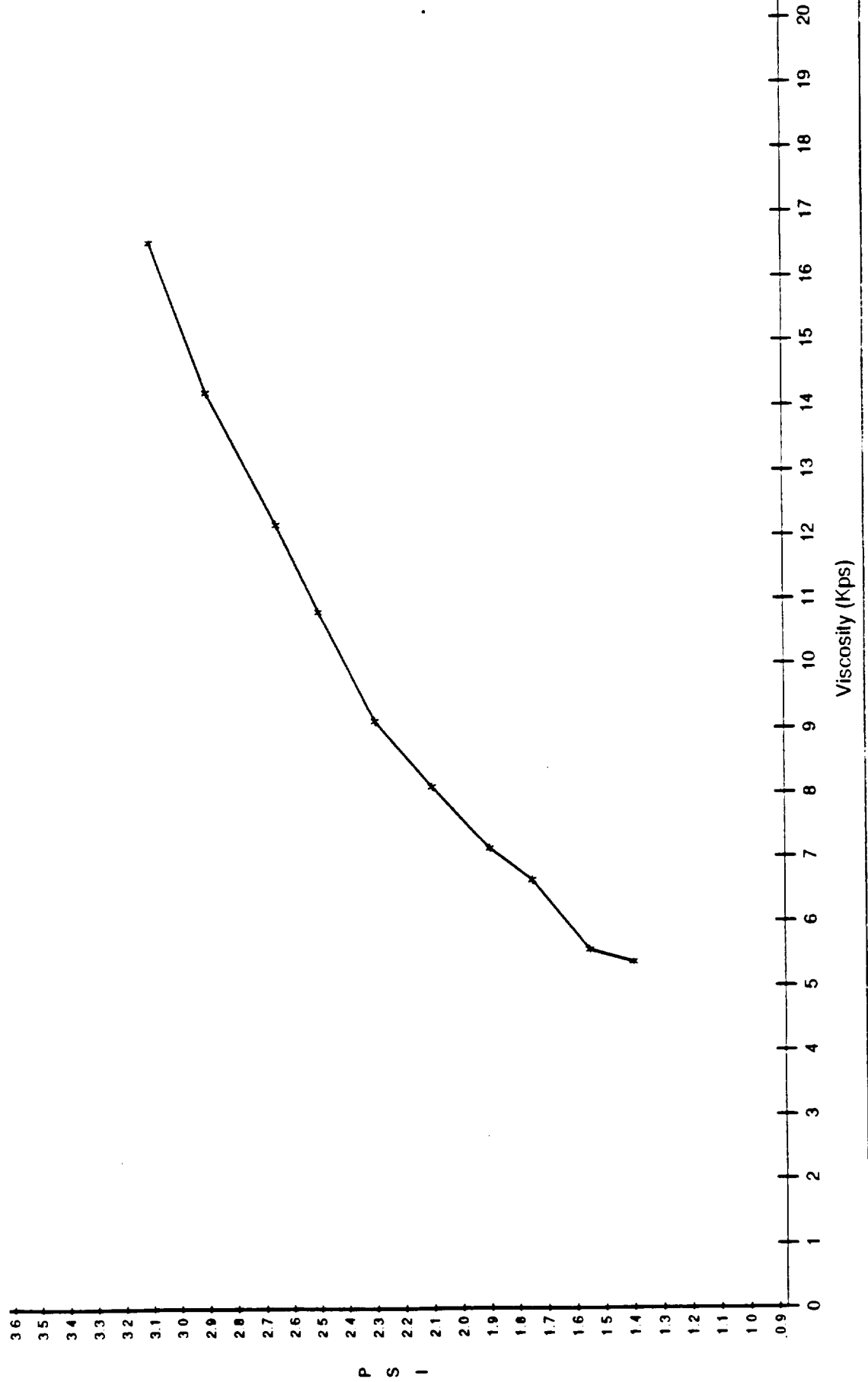
Viscosity (Kps)

Figure F-14. Air Pressure Required to Form Gas Path During Viscosity Build of Lot-0043
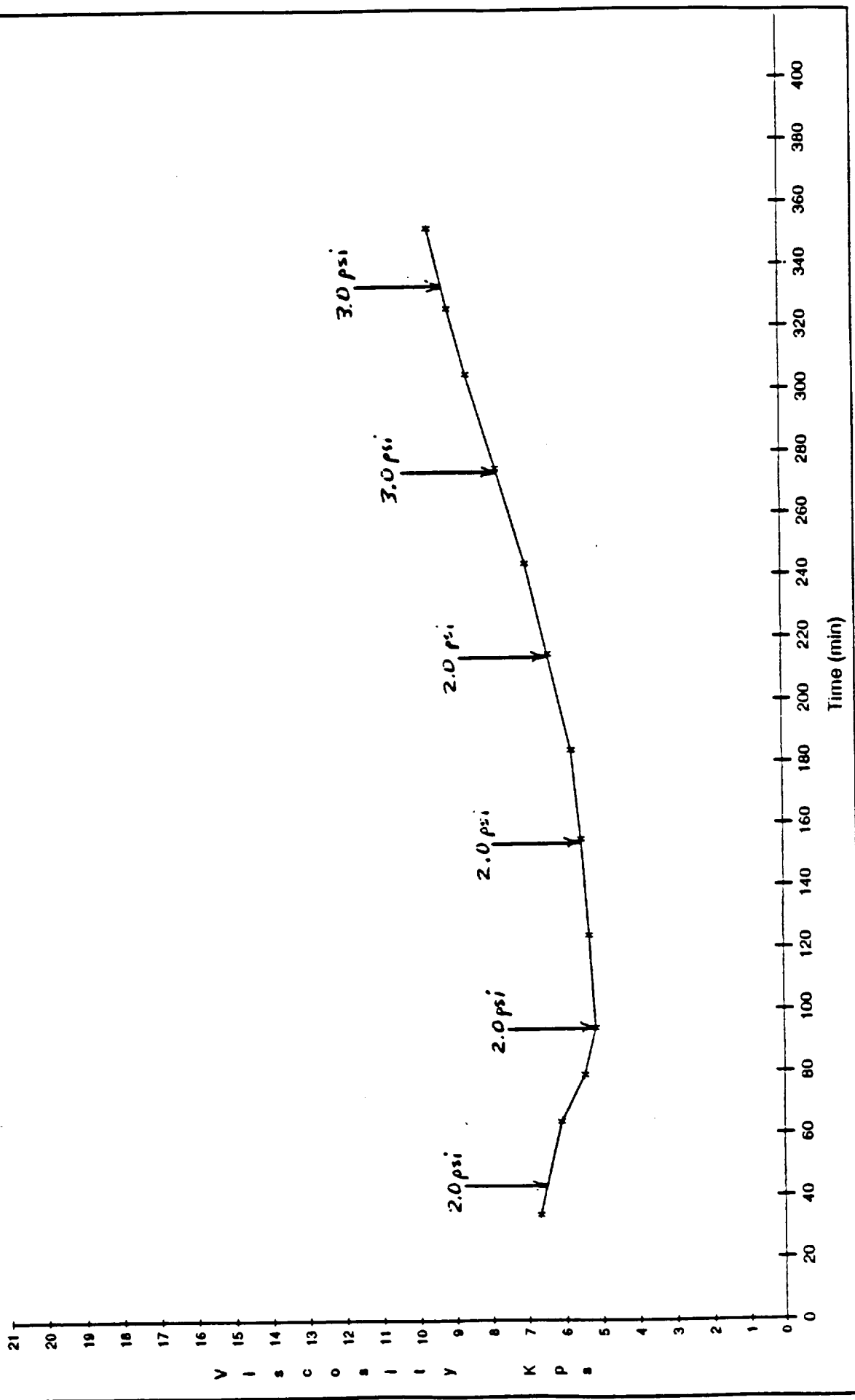
Figure E-15. Air Pressure Required to Form Gas Path During Viscosity Build of Lot-0041

4907-0039 POLYSULFIDE VISCOSITY @ 70-75 F
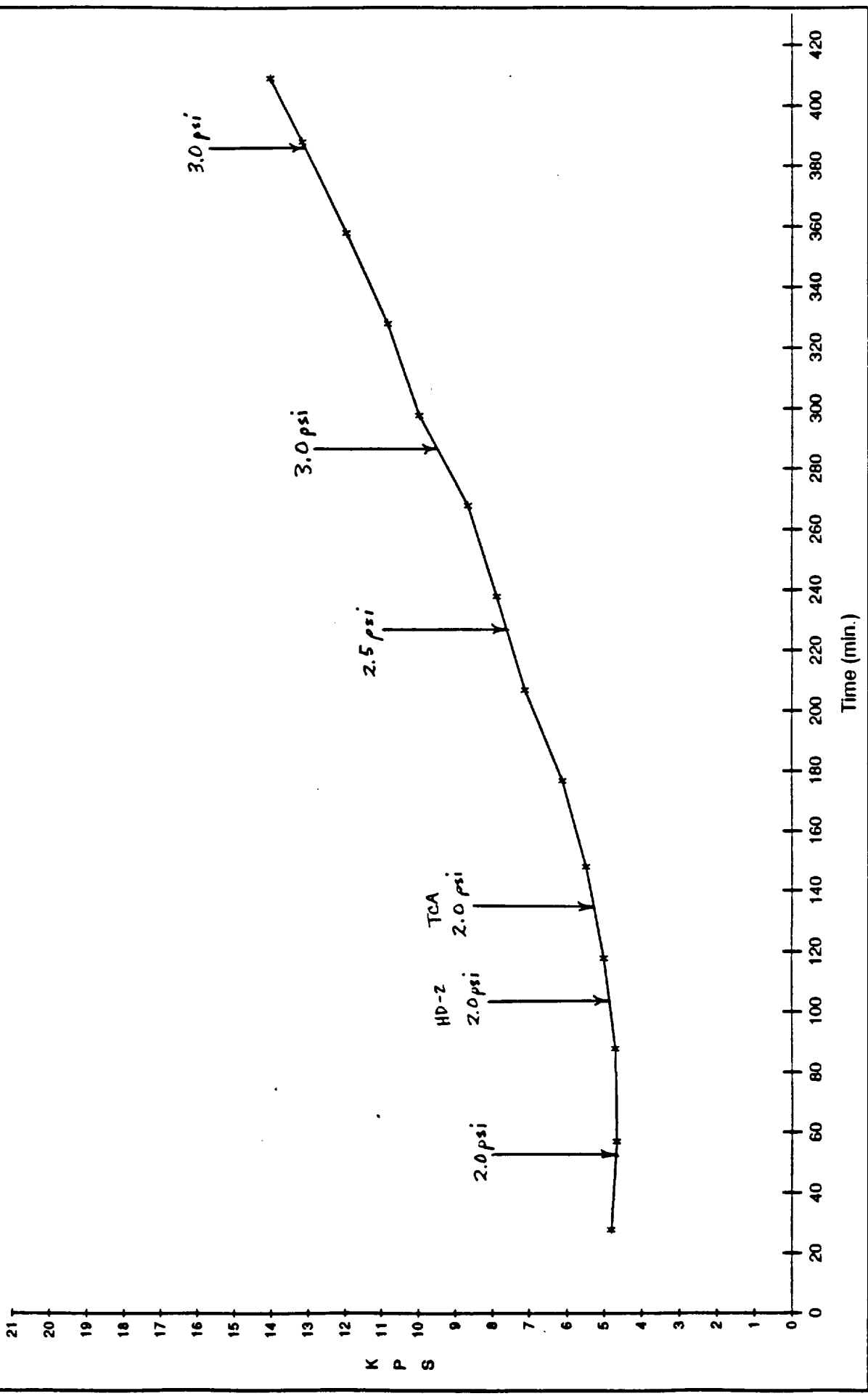
Figure E-16. Air Pressure Required to Form Gas Path During Viscosity Build of Lot-0039

4907-0037 POLYSULFIDE VISCOSITY @ 70-75 F

Figure E-17. Air Pressure Required to Form Gas Path During Viscosity Build of Lot-0037
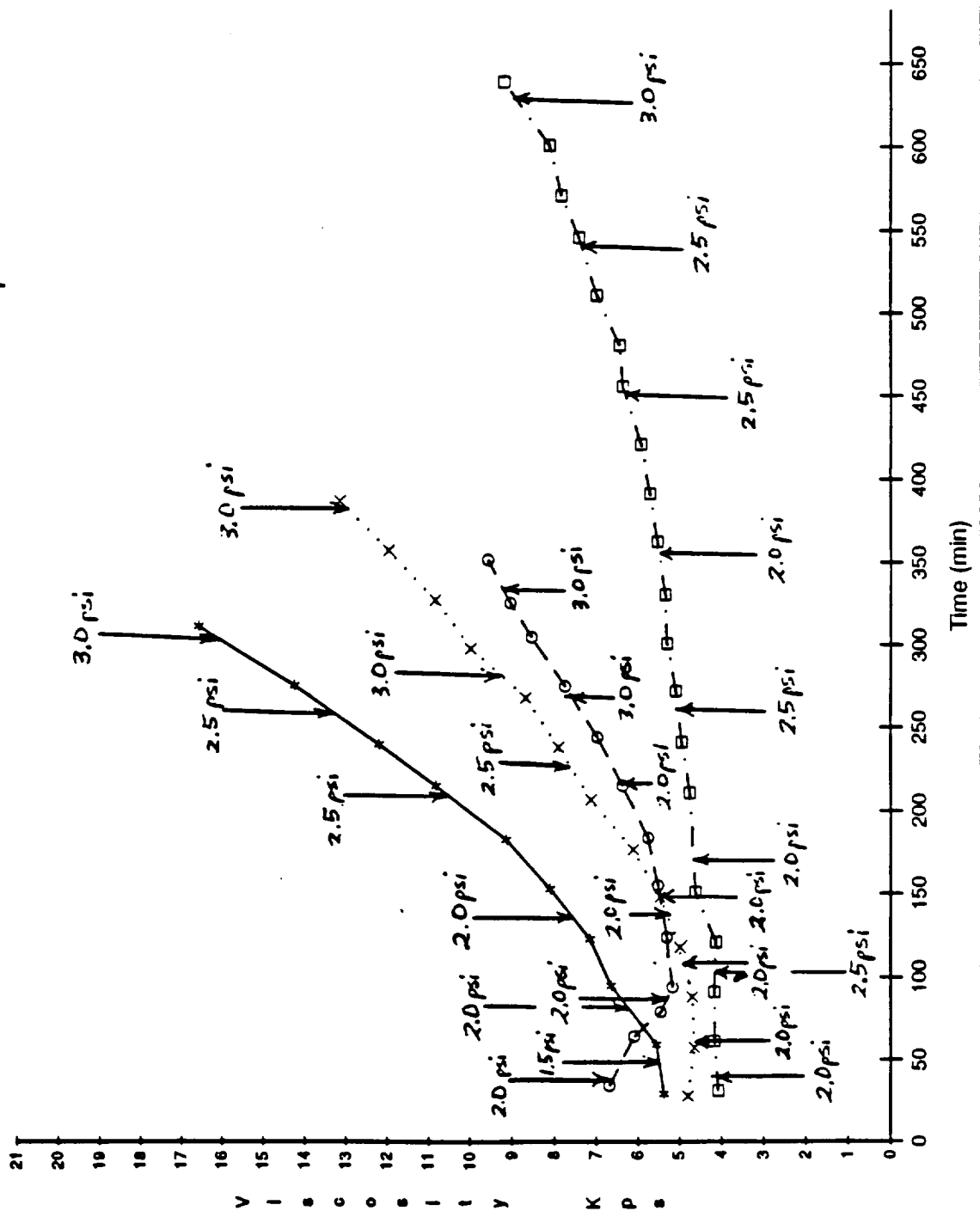
Figure E-18. Temperature Effect on Plexiglass Model Air Pressure

Figure E-19. Comparison of Plexiglass Model Air Pressure by Lots During Viscosity Build

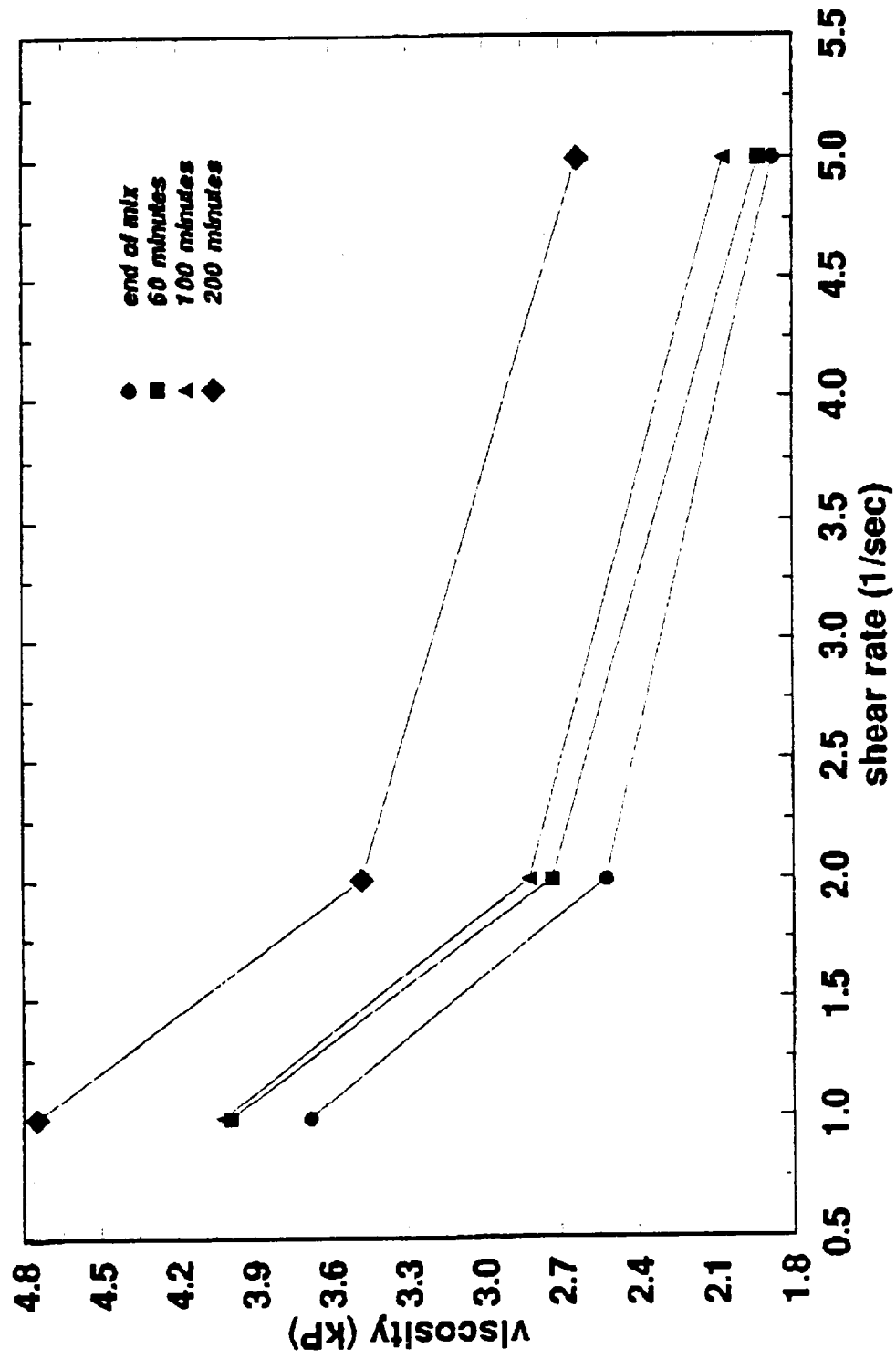## Lot 37
Polysulfide

Figure E-20.   Concentric Cylinder Viscosity at Three Different Shear Rates – Lot–0037

Lot 43
Polysulfide
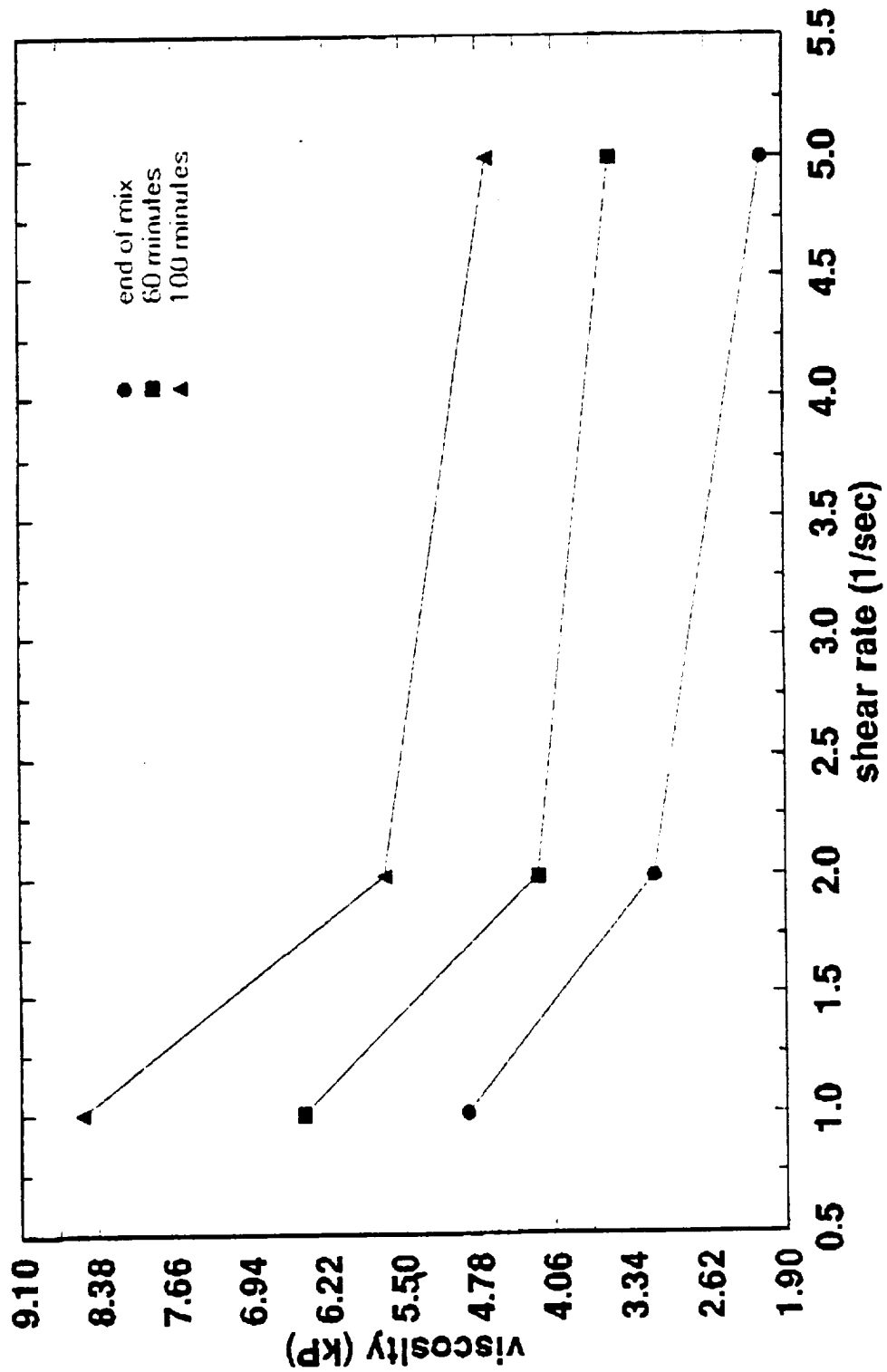

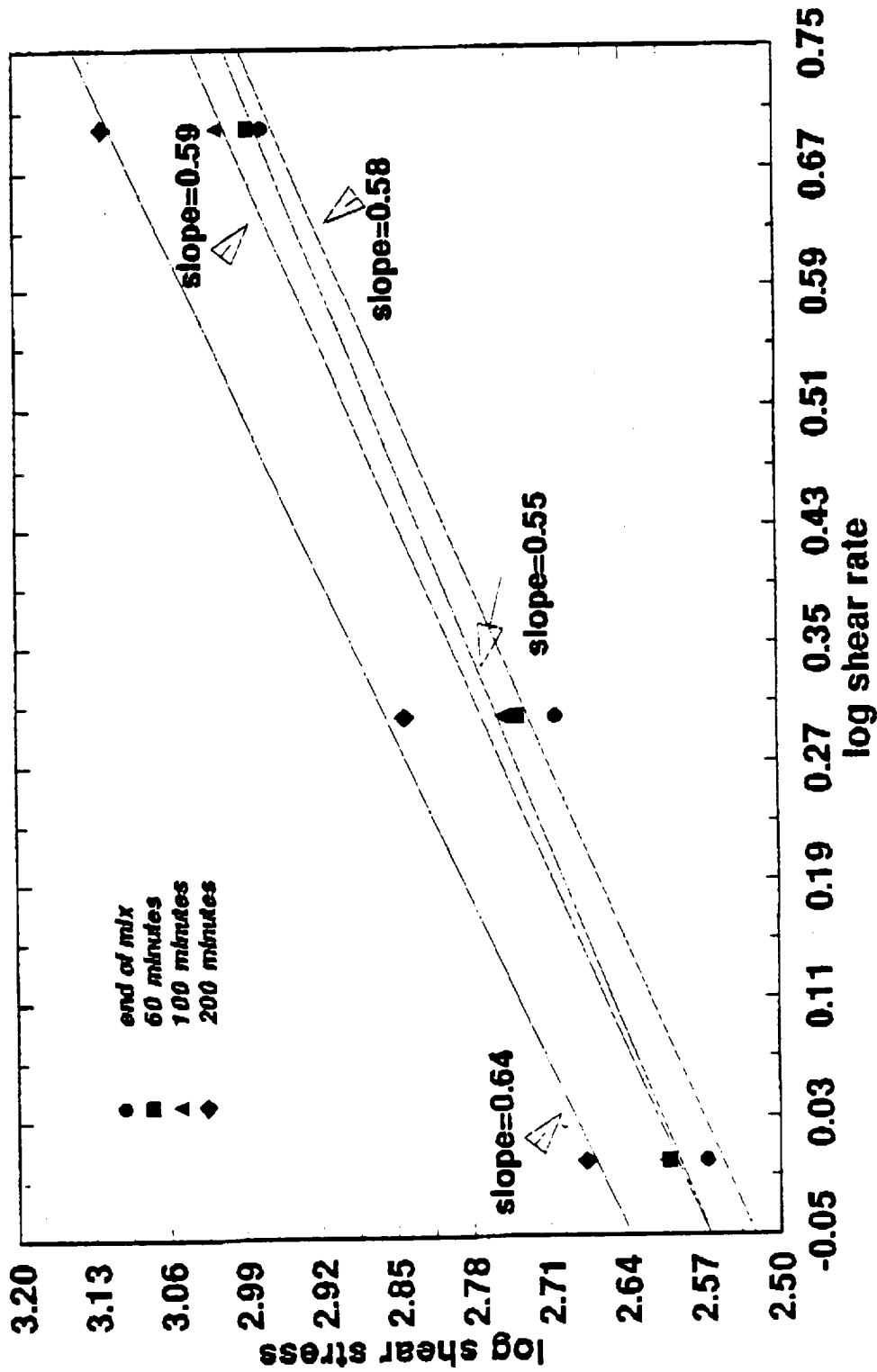Figure E-21. Concentric Cylinder Viscosity at Three Different Shear Rates – Lot-0043

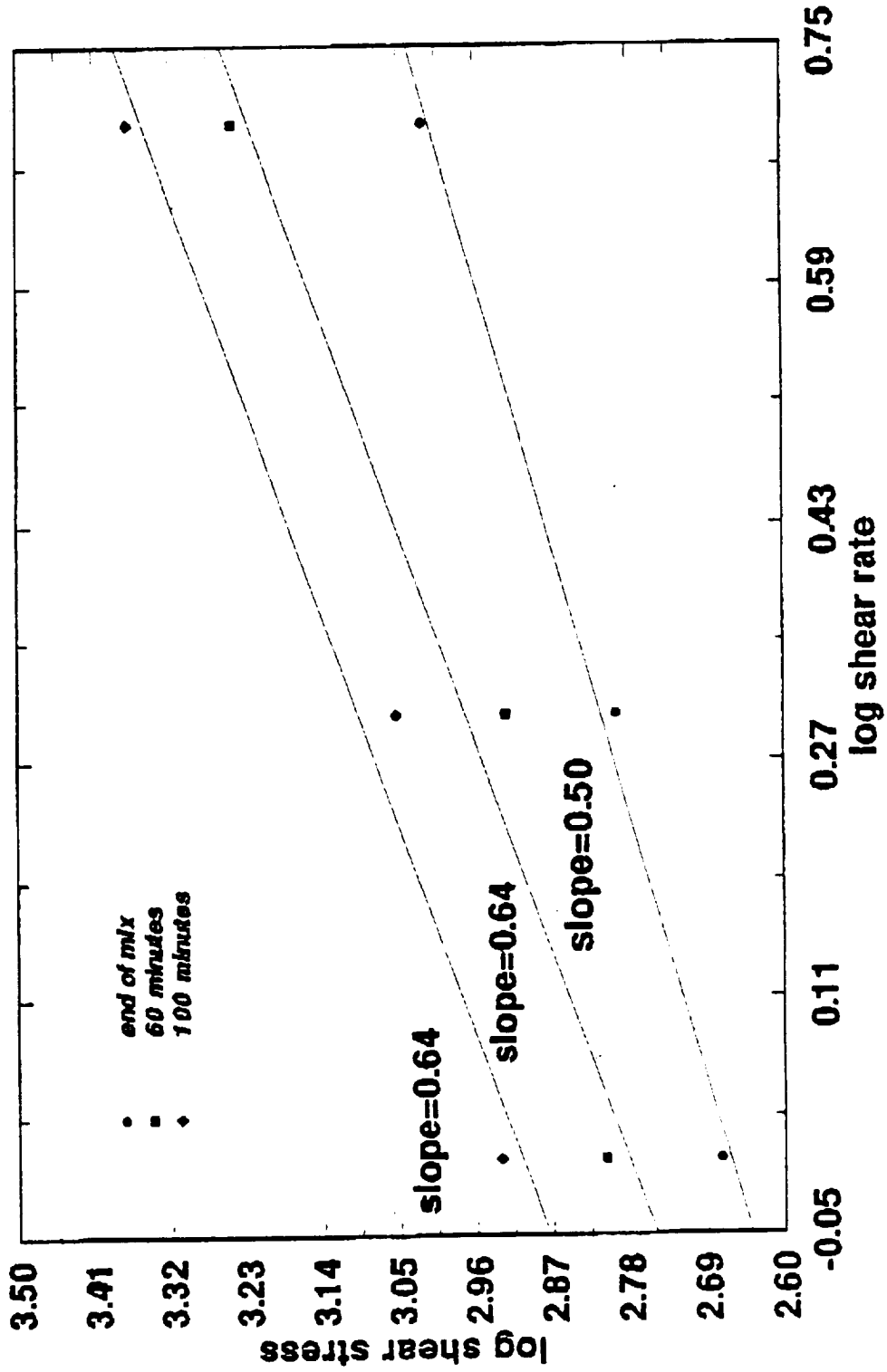Figure E-22. Log Shear Stress versus Log Shear Rate for Lot-0037

Figure E-23. Log Shear Stress versus Log Shear Rate for Lot-0043

ADVANCED TECHNOLOGY
LABORATORY SERVICES

LABORATORY REPORT

12 Mar 1992

Originator: R. Haddock
       Ext. 6437, M/S E80

Request: LWR 668454
  Lab. Log # 03-02-92-48239

Subject: FTIR Analysis of Polysulfide Rubber Samples

     Three lots of cured polysulfide and their raw materials were submitted for comparison analysis. The lots analyzed were 4907-0037, 4907-0042 and 4907-0043. Each sample was analyzed using ATR/FTIR analysis. FTIR looks at the organic base of each material but not the inorganic fillers. It was concluded on examination of the spectra, that there were no differences in the materials.

     Copies of the FTIR spectra are attached.

R. C. Raisor, Spectrochemical Analysis
LAB92075
B1352

dimensions), static test conditions rather than dynamic conditions in actual nozzle-to-case joint (variable and changing polysulfide widths and thicknesses during lowering, out-of-round parts, part temperature variations, variable air pressure based on air volumes, polysulfide shearing rate variations attributed to seating lowering rate and volume changes, etc.). The static condition of the polysulfide in the plexiglass plate model is conservative and air pressure required to form a gas path while the material is being sheared during nozzle lowering would probably be significantly lower. Even with the noted inherent conditions, the air pressures tested in the model are in close approximation to the predicted air pressure (based on CAD analysis) which can be generated as the joint closes.

In summary, the test results suggest that viscosity is an important variable in the formation of gas paths in the nozzle-to-case joint polysulfide The viscosity variable may be as important in gas path formation as the variables which create the air pressure source. Polysulfide viscosity may be significant enough to overcome the variables which influence air pressure creation in the joint (i.e., vent slot dimensions, volume differences due to out-of-roundness and tolerance stack-ups, etc.) except for total plugging of the vent port. The low humidity during the assembly of 20A and B may also have contributed to gas path formation.

The following conclusions were drawn from the testing:

1. The results indicate that air pressure required to form a gas path increases as viscosity increases.

2. Thickness and width of the polysulfide influences air pressure required to form a gas path.

3. Increasing temperature decreases air pressure required to form a gas path probably because it lowers viscosity in the short term.

4. Polysulfide is a pseudoplastic (shear thinning) fluid where by definition "resistance to flow decreases as shear rate increases." Increased shear rate appears to lower gas path resistance.

5. Lot 037 shear thins more than Lot 043 at the time frame of 20A and 20B nozzle seating.

6. Gas path formation does not appear to be sensitive to methylchloroform and Conoco HD-2 grease contaminants.

Based on the conclusions, the following recommendations are made:

1. The polysulfide applied to the aft dome be allowed to build viscosity to some level (10-12 kilopoise range suggested) prior to seating the nozzle to make the polysulfide more resistant to gas path formation.

2. The nozzle-to-case seating rate be decreased to reduce shear thinning, which will improve gas path resistance.

3. The application life (extrusion) lot acceptance test be upgraded to test extrusion through a Semco tube at more than one time interval to generate a "viscosity" profile for SPC tracking.

4. The replacement polysulfide be tested for amount of shear thinning and compared to results contained herein. Shear thinning should be equal to or less than that of 4907-0043 material.

NBR Assessment

A significant portion of the aft dome profile consists of nitrile butadiene rubber (NBR). A review of the process records raised the question whether or not the 180-grit sanding and methylchloroform (TCA) cleaning caused the NBR to swell thus changing the configuration of the aft dome profile. A couple of simple experiments were conducted to determine the effect of TCA on NBR. Several samples of 1-inch square by 0.5-inch thick NBR were prepared. Sanding was performed on the samples using 180-grit sand paper. Two NBR samples were cleaned thoroughly with rymplecloth liberally soaked in TCA. After a minute or two to allow the TCA to flash-off, measurements indicated a 0.001-inch thick increase in the samples. Two NBR samples were then placed in small beakers of TCA and allowed to soak for five minutes. The samples were removed, allowed to flash-off, and measured. The samples increased in thickness 0.007-inches and 0.009-inches, respectively. Samples decreased over half of the noted thickness increase in the first 30 minutes in the ambient environment (73°F and <10 percent R.H.). It is unlikely that the sanding and TCA cleaning of the NBR aft dome mating surface caused significant swelling and should not be considered as a contributor to polysulfide gas path formation in the nozzle-to-case joint.